The tectonic evolution of the Friuli Alps (NE Italy) in the context of the Alpine-Dinaridic orogenic system

MSc Thesis
By Anissa A. Smits

Supervisors
Drs. Inge van Gelder
Dr. Ernst Willingshofer
and Dr. Liviu Matenco

Department of Earth Sciences
Utrecht University
3474755

January 2016

The tectonic evolution of the Friuli Alps (NE Italy) in the context of the Alpine-Dinaridic orogenic system

Anissa A. Smits

Abstract

The Friuli Alps in NE Italy are located directly at the intersection of the south west vergent Dinarides and the south vergent Alps and is therefore a key area to study interference tectonics caused by the two mountain ranges. In order to understand the structural and paleo-geographical evolution of the geologically complex area, a clear separation of Dinaridic and Alpine structures had to be made. For this purpose field kinematic data have been collected, which serve together with the geological map to construct a NNE-SSW trending cross-section. This cross-section provides important insights into the subsurface structure of the area and is used to estimate the amount of shortening that affected the Friuli Alps since the beginning of the Paleocene, utilizing balancing software *MOVE*. The stratigraphic formations occurring in the area are an alternation of soft evaporates and basinal deposits and rigid platform carbonates; this alternation most likely influences the tectonic style of the area.

The field data and balanced cross section define four stages of deformation: (D1) N-S extension, creating E-W striking normal faults, that have been dated as Late Cretaceous or older. (D2) NNE-SSW shortening, characterized by (S)SW vergent thrust faults and NW or SE plunging fold axes, related to the Dinaridic orogeny (60 - 30 Ma). The D2 phase caused typical ramp-flat structures in the subsurface, which accommodated thin-skinned tectonics along the "soft" Bellerophon and Raibl formations. (D3) N-S shortening, related to the Alpine phase (23 Ma), which is defined by north and south vergent folds and faults. The large fault offsets suggest thick-skinned tectonics. (4) Dextral E-W to ENE-WSW oriented transpression due to NW-SE reactivation of pre-existing thrusts, starting at 8 Ma. The youngest two phases (D3 and D4) are still active, as they showed recent seismic activity.

The D2 thin-skinned thrusting had the biggest influence on the total amount of shortening in the Friuli Alps; it facilitated 57 km of the overall shortening. The subsequent D3 thick-skinned thrusts that displaced the D2 faults, added an additional amount of 11 km to this shortening, resulting in a total 68 km of shortening. However, the amount of D2 shortening is considered to be a minimal amount, due to the lack of shortening constraints on this phase at the surface. More shortening was expected, which could for example be obtained by introducing more shallow ramps or longer décollements into the balanced cross-section. The latter would require a substantial amount of subduction of the Adriatic plate underneath the European plate, which favours the subduction polarity switch theory in this area.

Table of contents

1. Introduction

The Friuli Alps, located in North-East Italy (fig. 1; indicated in red) are part of the Southern Alps and entails a complex geological history. The study area, located within the rectangle in figure 2, dominantly exposes Mesozoic rocks and has been involved in both the Dinaridic and Alpine orogeny (Schönborn, 1999; Nussbaum, 2002, Schmid, 2008). The Paleogene Dinaridic orogeny has a dominant south-west direction of shortening, whilst the Neogene Alpine orogeny is characterized by a southward direction of shortening (Doglioni and Bosellini, 1987; Schönborn, 1999; Doglioni and Carminati, 2008). The Friuli Alps are located directly at the intersection of these Dinaridic and Alpine structures and is therefore a key area to study the influence of the inherited structures of the Dinaridic orogeny on the younger "Alpine" phase of deformation and vice versa.
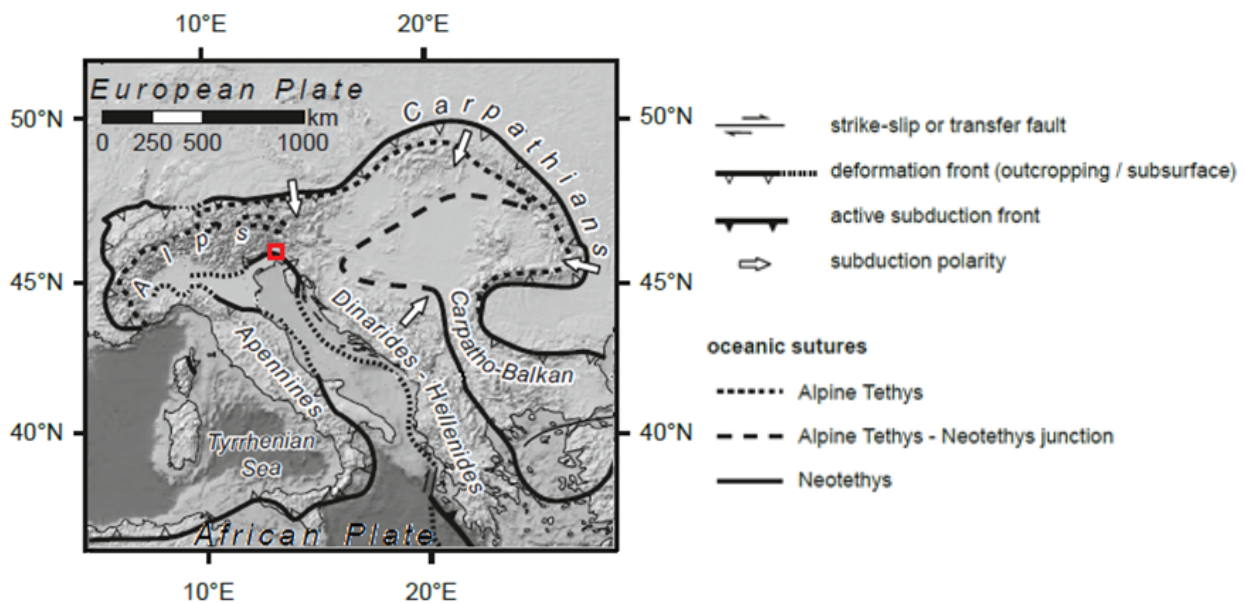
Figure 1. Overview of the present-day deformation and subduction fronts that influence the project area (Ustaszewski et al., 2008). The Friuli Alps are located in NE-Italy, within the red rectangle, where the Southern Alps and Dinarides intersect each other; note the change in strike between the two mountain ranges. The white arrows indicate the subduction polarity for the Alps-Carpathian-Dinarides region (or AlCaDi-system, after Schmidt et al., 2008).

Previous research in the Friuli Alps has focussed mainly on the sedimentology (e.g. Stefani et al., 2007) and palaeontology of this area, but tectonic interpretations are few. The general tectonics of the Southern Alps have been studied intensively by, for example, Schmid et al. (2004) and Castellarin and Cantelli (2010). More detailed studies have been conducted in the Dolomites by Schönborn (1999) and Doglioni and Carminati (2008), and also along the major Valsugana thrust by Bosellini (1985). Despite the absence of deep seismic reflections or adjacent well data, the deep structures of the Friuli Alps have been unravelled by Nussbaum (2002) who constructed large scale profiles within the area based on kinematically balanced surface data. His reconstructions amounted to 50 km of shortening since the beginning of the Late Miocene, in correspondence with the estimates made by Schmid et al. (1996) and Schönborn (1999). Nussbaum (2002) does however note that this amount is conservative and a minimum, as the introduction of a more intricate structure with more thrusts and longer décollements would result into increased shortening. This larger amount of shortening is also expected by Ustazewski et al. (2008), who suggests a total of 190 km of shortening, from the Miocene onwards. Paleostress reconstructions of the Friuli region by e.g. Castellarin and Cantelli (2000) and Bartel et al. (2014a) have tried to put the different phases of deformation into a timeframe. Most studies show a general trend with N-S to NE-SW shortening during the Eocene, NE-SW to NNE-SSW shortening during the Oligocene, N-S to NNW-SSE shortening in the Miocene and NW-SE shortening during the Pliocene, but differences between studies do occur. The two oldest phases are considered as Dinaridic and the younger two as Alpine.

A detailed understanding of the interfering tectonics in this area can provide crucial information on the geological evolution of the Friuli Alps. The area is also of special interest because of its occurring lithology: most

of it is either a deep marine or shallow marine (platform) deposit. As deep marine facies are 'softer', they are more susceptible to deformation than shallow marine facies. Along these lines, it has been argued that these deep marine deposits, together with the evaporite deposits occurring in the area, have acted as décollement surfaces for the more massive shallow marine carbonate platforms, resulting into 'thin-skinned tectonics', enabling the platforms to travel long distances along these décollements, leading to larger amounts of shortening than predicted by Nussbaum (2002). Furthermore, the subduction of Adria underneath the European plate (Lippitsch et al. 2003; Kissling et al. 2006; Ustaszewski et al. 2008) is expected to have resulted in more north vergent structures in the Southern Alps than has been observed by previous studies (Luth et al., 2013).

In order to test the 'thin-skinned tectonics' theory and the interfering tectonics, field data has been collected along a 54 km long NNE-SSW profile in the eastern part of the Friuli Alps, from the foreland of the orogeny near the town of Tarcento to the hinterland east of the village of Pontebba; this profile line is also indicated on the geological map in figure 2. A similar N-S profile has also been reconstructed in the western part of the Friuli Alps by Engelen (2016; see fig. 10 for location). In short, the particular aims of this project are (1) to construct a map showing major facies changes (deep vs. shallow water), to (2) infer kinematics and study overprinting criteria to arrive at a clear separation of Dinaridic and Alpine structures and to (3) construct a balanced cross section by hand and with the aid of a software programme (*MOVE*; Midland Valley, 2014), based on the field data and existing maps. This will lead to an estimation of the amount of shortening in this area from the Paleocene until recent. Furthermore, the balanced cross section will provide constraints on the structural and paleo-geographical evolution of the area in the context of the Alpine-Dinaridic orogenic system.

2. Geological setting

The Friuli Alps, located in NE Italy (figs. 1 and 2), form the eastern part of the Southern Alps and are surrounded by the Dolomites in the west, the Carnic Alps in the north, the Julian Alps in the east and the Friuli plain to the south. The Southern Alps curve southeastwards, where they turn into the Dinarides. While both the Alps and the Dinarides formed due to the convergent motions between the European and African plates (fig. 3) that caused the 'overall' Alpine orogenesis, both mountain belts have a different strike (fig. 1).

The Southern Alps are an active fold-and-thrust belt that is entirely made up of material from the Adriatic microplate, which in general consists of sedimentary rocks of Mesozoic age that developed within a shallow sea, forming mostly vast carbonate platforms (Schönborn, 1999; Nussbaum, 2002). The mountain belt has formed due to the northward motion of the Adriatic indenter that collided with the European plate (Nussbaum, 2002; Schmid, 2008). The region was mainly affected by southwest vergent thrusting related to Dinaridic tectonics during the Paleogene and by south vergent thrusting in response to the formation of the Alps since the Neogene until present (Doglioni and Bosselini, 1987). The visible uplift of Quaternary terraces and recent seismic activity in the Friuli area are evidence for this still ongoing phase of deformation (Benedetti et al, 2000). The present-day slightly arched shape of the mountain belt is caused by three different factors, according to Schönborn (1999): Mesozoic rifting, basin and carbonate platform formation, Jurrassic to ongoing convergence in several different directions and the shape of the indenting Adriatic microplate. In the following sections a brief summary is provided of the tectonic evolution of the Alps and the Dinarides respectively.
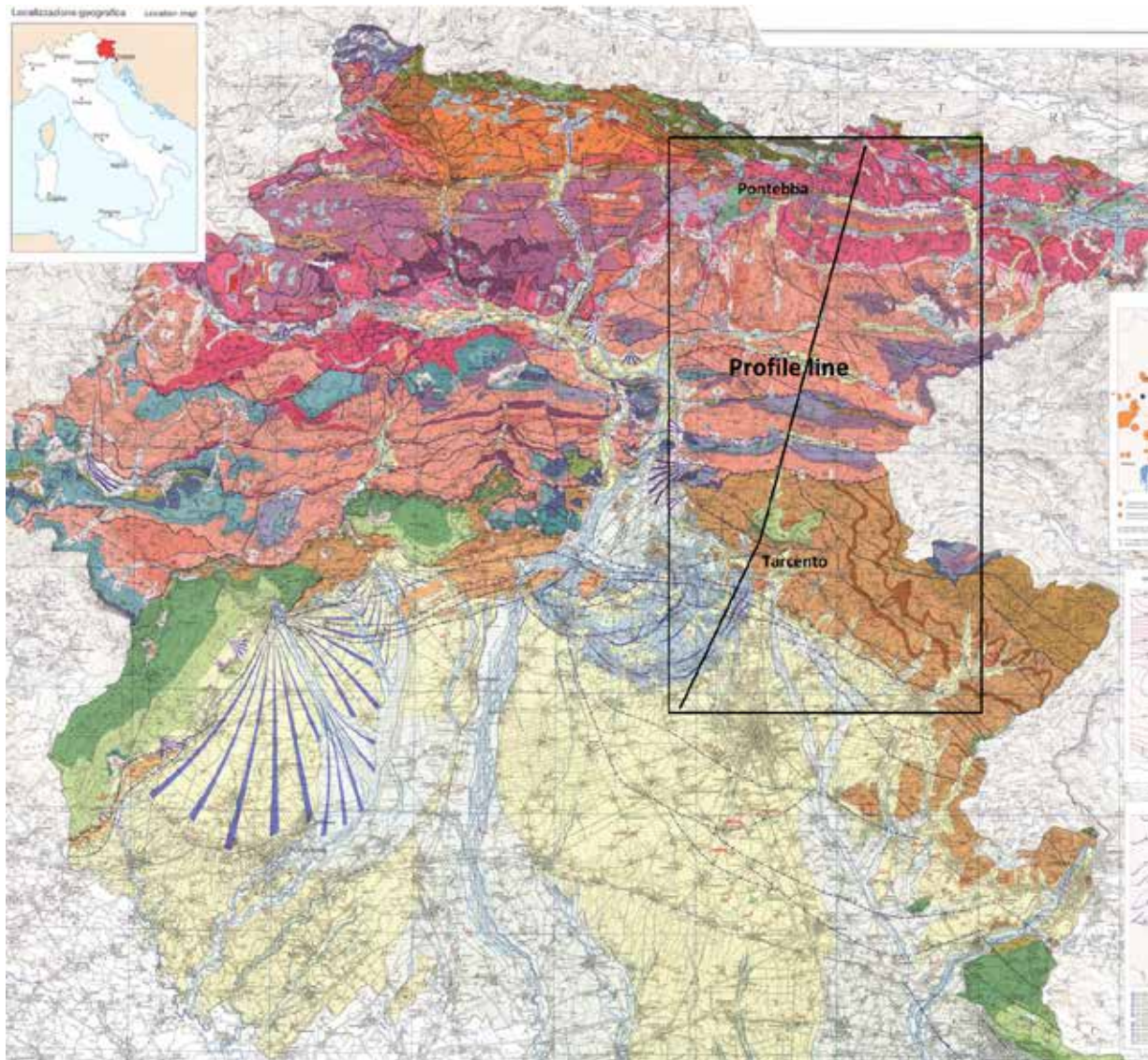
Figure 2. Geological Map of the Friuli Alps; the study area and profile line are indicated. After Carulli et al., 2006, for a detailed version, see appendix A.

2.1. Alpine Tectonics

Cretaceous Orogeny

During the late Triassic, while Pangea was breaking up, the European and African plates became separated from one another by the Neotethys. A small part of this Neotethys, called the Triassic Meliata Ocean started to close during the Late Jurassic (Schmid et al., 2008; fig. 3) due to the northward motion of Africa. The final closure of this Ocean and its subsequent subduction below the Neotethys led to the Cretaceous orogenic phase of the Alps. During this phase, nappe stacking of material derived from the Adriatic plate took place to form the Austroapline nappes (Schmid et al., 2008). These Austroalpine nappes became metamorphosed due to subduction and peak PT conditions reached UHP (ultra-high pressure) levels in the south eastern part of the present day Alps (Pohorje Mountains, Slovenia; Janák et al, 2004). This Cretaceous or Eo-Alpine deformation affected only the central and western parts of the Southern Alps (Doglioni and Bosellini, 1987) and most of the deformation took place along inherited rift structures from the Permo-Triassic to Middle-Jurassic rifting phase (Bosellini and Doglioni, 1986). At the end of the Cretaceous the area was subjected to extension again, as deep intercontinental basins started to form and the high grade metamorphic rocks became exposed (Willingshofer et al., 1999).
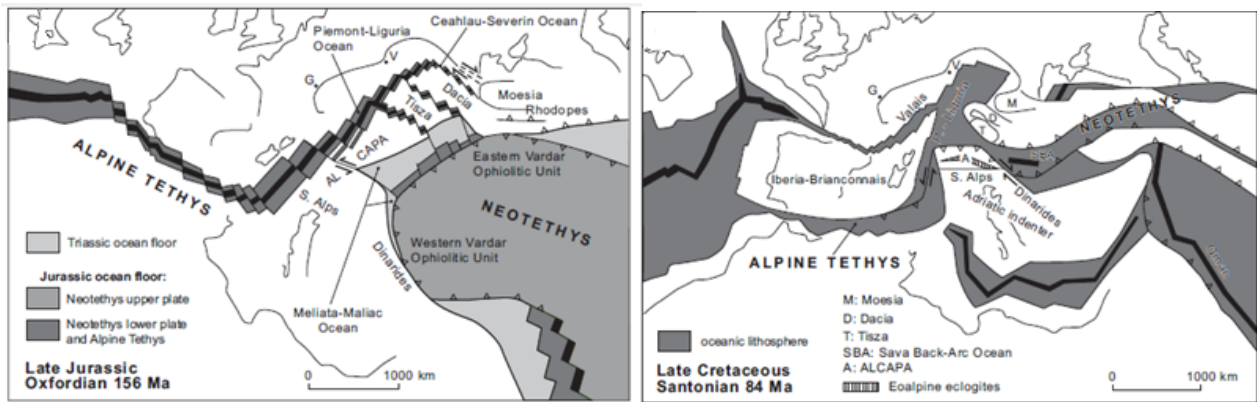
Figure 3. Closing of the Meliata Ocean, related to the formation of the Alpine Tethys and the northward movement of the Adriatic indenter/African plate. (Schmid et al., 2008).

Paleogene

The closing of the Meliata Ocean was also partially caused by the opening of the Alpine Tethys in the west at the end of the Jurassic (Schmid et al., 2008). The opening of this branch was in turn related to the opening of the Atlantic Ocean and it separated the European and Adriatic (or Apulian) plates, while it was opening up more and more towards the east, where it eventually connected with the Neotethys (fig. 3). This Alpine Tethys started to close just before the start of the Paleogene, around 80 Ma, as both the Adriatic and the African plate started to drift northwards. Subduction of the European plate beneath the Adriatic microplate started at the beginning of the Paleogene (Schmid et al., 1996). During this convergence, firstly the Penninic nappes, consisting of material derived from the European distal margins and Alpine Tethys were thrusted upon the autochthonous Helvetic nappes of the European plate. The actual continental collision took place during the Eocene (Neubauer et al., 2000), when the allochtonous Austroalpine nappes were placed upon the Penninic nappes. Together, these three different nappes or superunits form the Tertiary nappe stack within the Alps. This structural sequence can for example be observed really well within the Tauern Window (Schmid, 2004; Bartel, 2014a; fig. 4). All the rocks that nowadays make up the Southern Alps also used to be part of the Adriatic microplate. They formed at its northwestern part, where the southern passive continental margin of the Alpine Tethys was located (Castellarin and Cantelli, 2010; Doglioni, 1986). According to Schmid et al. (1996; 2008) Adria and Europe have experienced a total amount of Paleogene N-S shortening of about 450-600 km, making it the most dominant deformation phase.

Neogene to recent

N-S shortening continued after the Paleogene, along structures such as the Periadriatic Fault, which forms a large fault system along the boundary between the Austroalpine domain and the Southern Alps. While the largest part of the Alps is a mostly north vergent system, the Southern Alps contain mostly southward directed thrusts and folds (fig. 4). The Periadriatic Fault was most active during the Oligocene, when volcanics intruded the fault zone (Fodor et al., 2008) and is roughly 700 km long; running from north-western Italy to Slovenia (Ratschbacher et al., 1991). Most of the motions along this fault are dextral strike-slip, with sometimes a vertical component (Mancktelow et al., 2001; Bartel et al., 2014a).

The Neogene is the period that marks the beginning of post-collisional shortening in the Southern Alps, starting between 20 and 17 Ma and ending during the Messinian (Ustaszewski, 2008). The 20° to 30° counter-clockwise rotation of the Adriatic indenter that moved northward caused an increase in the amount of shortening towards the east, so the Eastern and Southern Alps have experienced much more shortening than the Western and Central Alps (Ustaszewski et al., 2008; fig. 5). According to Ustazsewski et al. (2008) a total of 190 km of Neogene N–S shortening took place in the Southern and Eastern Alps, of which most was accommodated in the south-directed thrusts in the Southern Alps. This amount of shortening decreases to almost 0 km near Torino in Western Italy (Schmid and Kissling, 2000), near the rotation pole of the Adriatic indenter (Ustazsewski et al.,

2008). Schmid et al. (1996) state that shortening in the Western part of the Southern Alps already started after the Adamello intrusion-phase during the Oligocene and arrived at 56 km of shortening along the Milan and Lecco thrusts located north of Milano. This shortening led to the creation of the foreland thrust wedge of the Southern Alps and ceased around 7Ma, as is indicated by a late Messinian unconformity. Nussbaum (2002) estimated a minimum of 50 km of shortening in the Friuli Alps since the beginning of the Late Miocene and Schönborn (1999) concluded the same for the Dolomites.
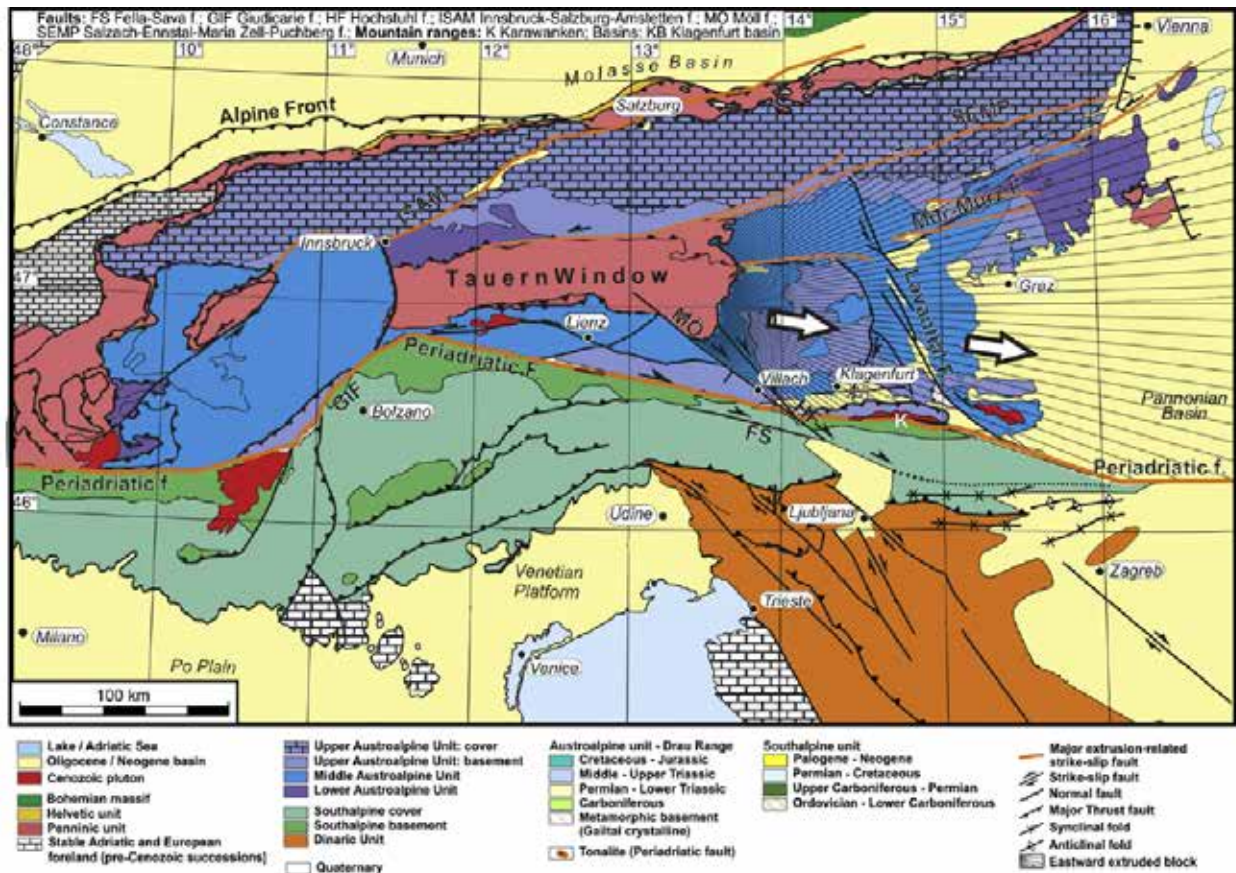

Figure 4. Tectonics of the Eastern Alps after Bartel et al., 2014a. The Periadriatic Fault is a major zone of orogen-parallel dextral strike-slip faults that separates the south verging Southern Alps from the rest of the Alps (north verging). The east-directed lateral extrusion (indicated by the white arrows) of the central Eastern Alps into the Pannonian Basin is a result of these movements.

Another process that accommodated for the ongoing N-S shortening is the eastward lateral extrusion of the Eastern Alps during the Miocene (Ratschbacher et al., 1991; fig. 4), which was also partially caused by the gravitational collapse of the orogen due to the thickened lithosphere beneath the mountain chain (Frisch et al., 2000). This escape of tectonic blocks was in turn accommodated by rollback of the Carpathian slab to the East and the opening of the Pannonian Basin, creating space for the 'escaping' material (Ratschbacher et al., 1991; Horváth et al., 2006). The formation of the Penninic windows such as the Tauern window is a result of this large-scale orogeny parallel extension in the Eastern Alps (Frisch et al., 2000). The shape and the amount of counterclockwise rotation of the Adriatic indenter are also of big influence on the lateral extrusion to the East (Ratschbacher et al., 1991).

The point where the Alps merge with the Dinarides is also a point where the polarity of subduction changes (Kissling et al. 2006; Ustaszewski et al. 2008; fig. 1). In the Alps, the European plate is the one being subducted underneath Adria, while in the Dinarides, the Adriatic plate forms the lower plate (Schmid et al. 2008). This switch has been identified on tomographic images of the Eastern Alps by Lippitsch et al. (2003). The length of the northward dipping slab on these images is approximately 210 km (Lippitsch et al., 2003), which can be explained by the 190 km of Neogene N-S shortening implied by Ustaszewski et al. (2008). Handy et al. (2014) suggests that the polarity change was triggered by tearing of both the European and Adriatic slabs and

intracrustal and crust–mantle decoupling during the Alpine collision. In turn, this decoupling makes the extension in the Pannonian basin and the roll-back subduction of the Carpathians possible.
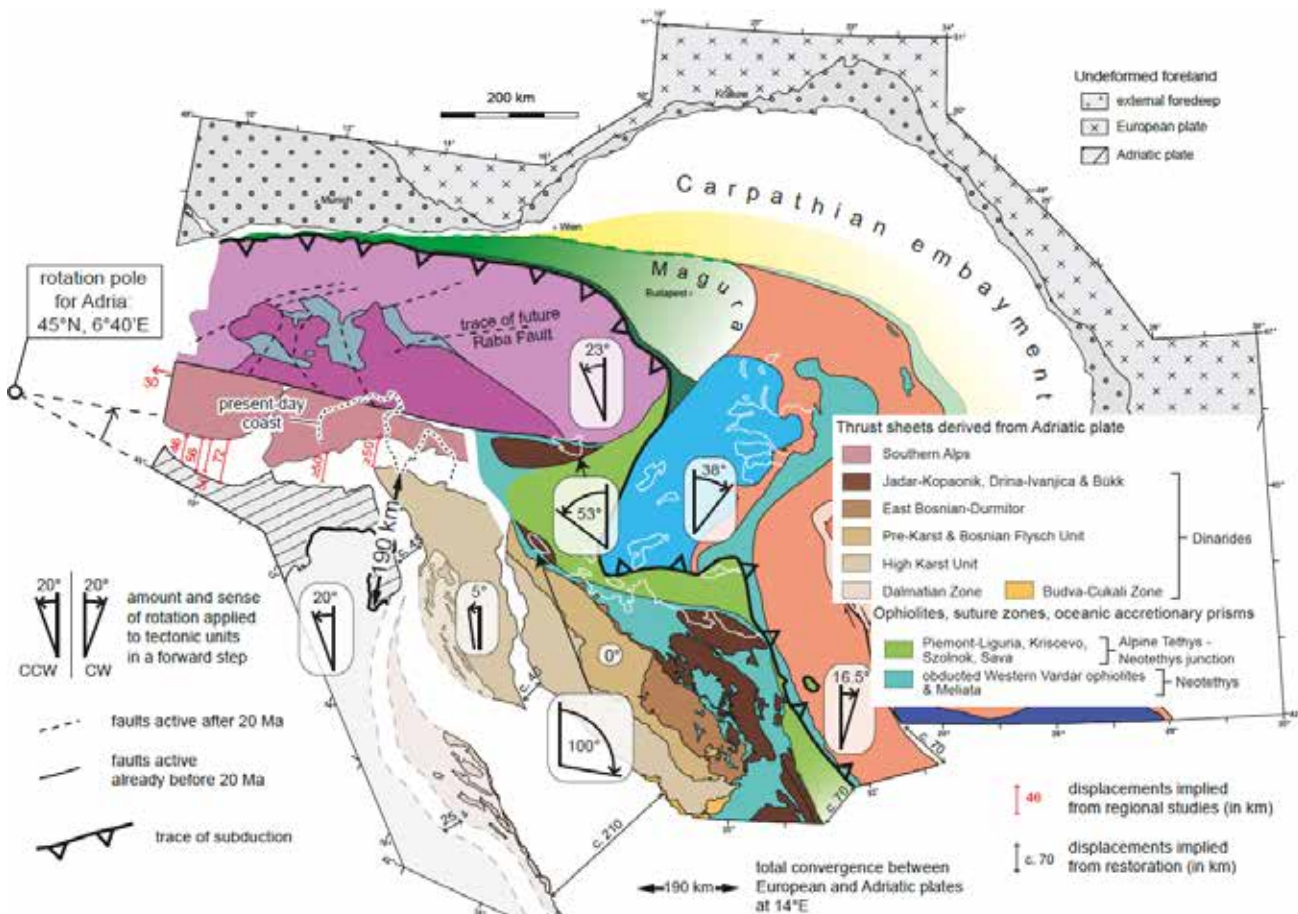
Figure 5. Early Miocene restoration of the AlCaDi-system (Ustaszewski et al., 2008, simplified after Schmid et al. 2008). The present-day coastal outline can still be seen as a comparison; numbers in black represent the Neogene displacement in km as found by Ustaszewski et al. (2008); numbers in red are the displacements in km derived from other regional studies such as those by Schönborn (1992; 1999) and Nussbaum (2000). The location of the rotation pole for the Adriatic indenter near Torino is also indicated.

2.2. Dinaridic Tectonics

The Dinarides formed due to convergence between the European and African plates, similar to the Alps, and are largely made up of Mesozoic and Cenozoic sedimentary rocks and ophiolites (Schmid et al., 2008). The evolution of the Dinarides took place within the Alpine orogeny at large, so both geological histories have a lot in common. During the late Triassic to Late Jurassic, the Dinaridic branch of the Neotethys started to open. North to northeast subduction followed in Late Jurassic-Early Cretaceous times, while the Neotethys was closing (fig. 3). This led to the obduction of ophiolites that were derived from, for example, the Triassic Meliata Ocean (Babic et al., 2002). During the Late Eocene-Early Oligocene, nappe-stacking onto the former distal margin of the Adriatic plate occurred (e.g. Pamić et al., 1998), resulting into the formation of the Dinaridic mountain chain. Because of the counter-clockwise rotation of the Adriatic indenter from the Neogene onwards, the Dinarides have experienced more shortening than the (Southern) Alps during this period (fig. 5). Ustaszewski et al. (2008) derived a total of maximum 235 km (25+210 km) of Neogene shortening within the southern tip of the Dinarides. This shortening mainly took place in the external Dinarides, along for example the dextral-transpressive Split-Karlovac Fault. But the northward motion of Adria was also accommodated by dextral strike-slip movements along reactivated thrusts within the internal Dinarides (Schmid et al., 2008; Ustaszewski et al. (2008)). Neubauer and Ilić (2005) note that, although visible offsets in this internal area are in order of a few kilometers, the total displacement along the multiple faults in the area is cumulative and thereby difficult to obtain.

According to Schmid et al. (2008), the Dinarides can be divided into seven different zones, from SW to NE (fig. 5). The External Dinaridic Platform, which comprises Triassic deep-water facies and Cenozoic flysch of the Budva-Cukali Zone and carbonate platforms of the Dalmatian Zone and the High Karst Unit that are all derived from the proximal parts of the Adriatic margin. The Internal Dinaridic Platform, that includes the Pre-Karst Unit and the Bosnian Flysch. The East Bosnian-Durmitor, Drina-Ivanjica and Jadar-Kopaonik thrust sheets, which contain more distal parts of the Adriatic passive margin. The Western Vardar Ophiolitic Unit, that thrusted over these three thrust sheets and is made up of the previously mentioned ophiolites. And the Sava Zone, which forms the Cenozoic suture zone between the Dinarides and the Tisza and the Dacia Mega-Units to the (north)east.

The main tectonic structures in the Dinarides are of Paleogene age and southwest vergent, which can be observed best in the central parts of the orogen (Pamíc et al., 1998). However, these influences can also be seen in the Southern Alps that are part of the foreland of the Dinarides (figs. 2 and 4). From the Neogene onwards these structures became overprinted by south vergent Alpine tectonics. There is no exact border between both contractional regimes, but the border NE of Udine defined by Schmid et al. (2004) is most widely used (see also fig. 4). The Dinaridic phase also seems to have affected the sedimentary cover of the Dolomites, leading to thin-skinned tectonics in this area with ramp-flat structures, according to Doglioni and Bosellini (1987). They also mention that in the Friuli area the basement might have been involved as well, causing thick-skinned tectonics.

2.3. The Friuli Alps

The oldest formations found in the Friuli Alps consist of folded Hercynian basement and molasses of Late Carboniferous to Early Permian age (Nussbaum, 2002; fig. 8). These formations are covered by the Bellerophon formation which are shallow marine evaporites and carbonates deposited in a sabkha environment that prograded westward (Nussbaum, 2002; Carulli et al., 2006). During the Middle Triassic, the whole area experienced a period of rifting as the Meliata Ocean started to open (Nussbaum, 2002; Schmid et al., 2008). This rifting phase created several basins of different depths (Viel, cited in Nussbaum, 2002), which resulted in the formation of areas with fast growing carbonate platforms of the Serla and Schlern formations, that were separated from one another by deep lagoons (e.g. Bosellini, 1984). In the late Triassic, the massive peritidal carbonate platforms of the Dolomia Principale formed, reaching thicknesses of 1000 to 1700 m (Nussbaum, 2002). Meanwhile some small basins started to form as well, inside in for example the at that time still developing Friuli platform (Cati et al., 1987b; Schönborn, 1999; Nussbaum, 2002; fig.6).
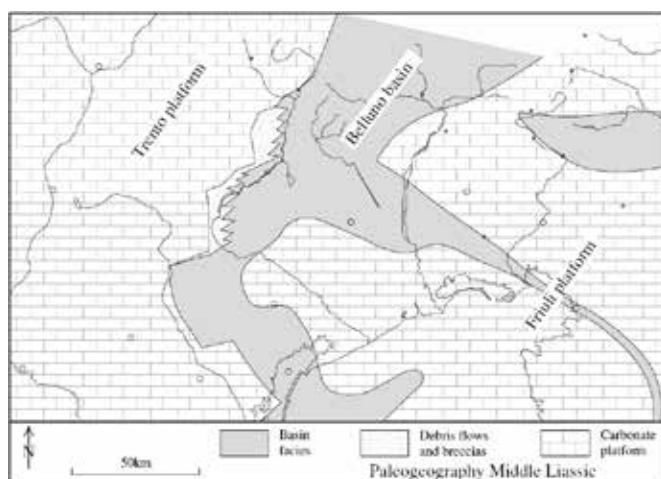
Figure 6. The basin-platform configuration of the Friuli area in Early Jurassic times. The formation of the Belluno basin resulted into two different platforms; one that would drown and another that would remain relatively shallow during the entire Mesozoic. Modified by Nussbaum (2002) after Schönborn (1999).

The presence of these topographic highs and lows would become of great influence on both the Dinaridic and Alpine deformation phases and would often determine the orientations of the developing major thrusts (Schönborn, 1999). From the Early Jurassic onwards, these massive carbonate platforms became affected by extension and subsidence related to the opening of the Alpine Tethys (Nussbaum, 2002; Schmid, 2008; fig. 3).

Eventually it resulted in the formation of the deep N-S trending Belluno basin that divided the platform in two (Schönborn, 1999; fig. 6); the Western part of the platform (Trento platform) eventually drowned, but the Eastern part (Friuli platform) remained relatively shallow during the entire Mesozoic (Nussbaum, 2002).

Throughout the Paleogene and Neogene, the Friuli platform became covered with flysch and molasse deposits, linked to the subsequent rise of the Dinarides and the Southern Alps. The first syn-orogenic flysch was dated as Late Cretaceous/Paleocene (Schönborn, 1999; Carulli, 2006) and was deposited in the deep-marine foreland basins that bordered the beginning mountain chains. In time, those basins would become shallower leading to the deposition of the post-orogenic shallow-marine or terrestrial Late Oligocene to Miocene molasse sediments (Nussbaum, 2002). According to Schönborn (1999) the initial flysch deposition was disturbed by several sinistral strike-slip zones along the northwestern border of the Friuli platform, leading to an irregular deposition pattern with older flysch in the North and younger flysch in the South. The foredeep succession can be divided into an eastward thickening Dinaridic sequence and a northward thickening Alpine sequence (Schönborn, 1999).

In general, the exposed rocks of the Friuli Alps can be divided into basinal, platform, shallow and slope/ramp deposits (fig. 7). The alternation of rigid carbonate platforms and softer basinal/slope deposits consisting of shales and evaporates, led to flat-ramp-flat thrust structures; with ramps cross-cutting the platforms and flats developing in the evaporites and shales (Nussbaum, 2002). These flats acted as décollement horizons during Dinaridic and Alpine tectonics, along which the rigid platforms were displaced over long distances. Schönborn (1999) and Nussbaum (2002) distinguish two major décollement horizons: the Bellerophon formation and the Raibl formation, which divide the stratigraphy into three different units (fig. 8; for a detailed description of the stratigraphy see also appendix B). Some minor décollements are also located at the base of the Lower Cretaceous, the base of the Paleocene flysch and the Oligocene flysch.
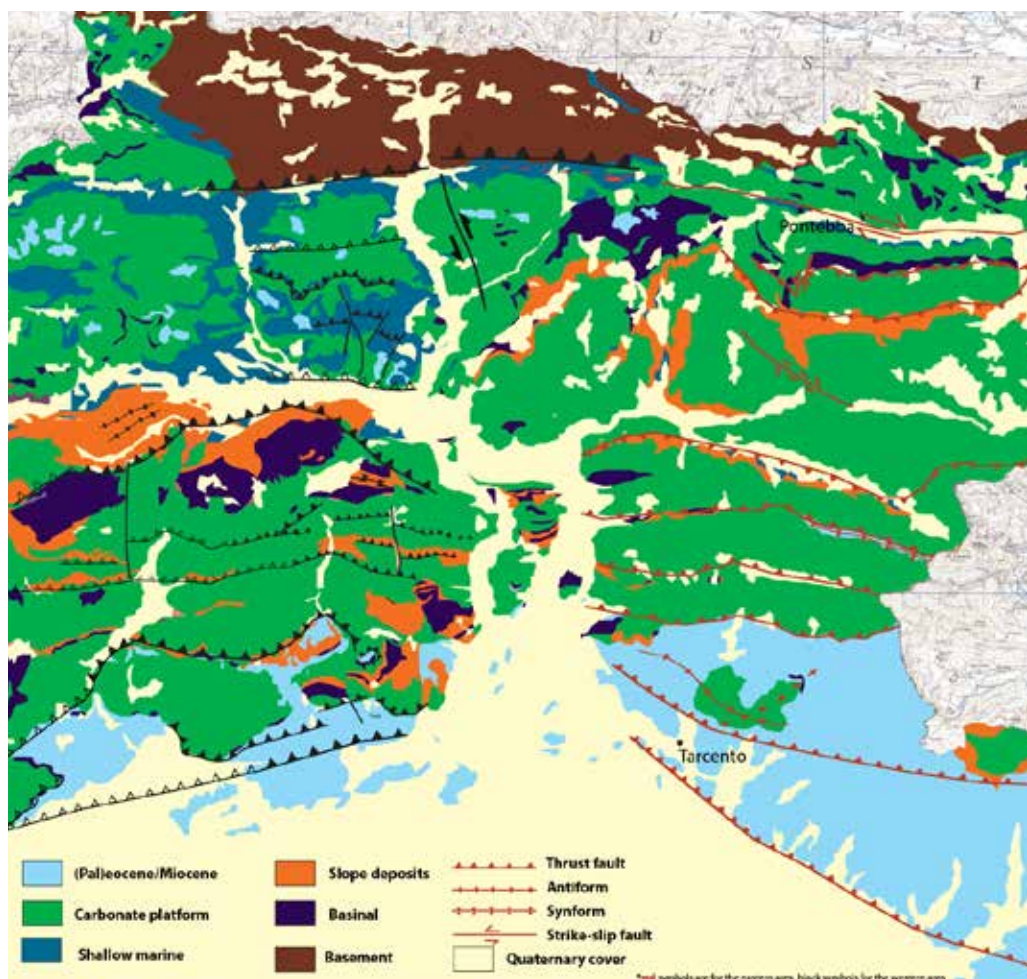
Figure 7. Facies map, showing the distribution of the different facies occurring in the study area of the Friuli mountains. Modified after Carulli (2006).

Due to erosion, an uneven distribution because of rifting, or both, the Cretaceous limestones thin towards the east, while the Paleogene flysch thickens due to the approaching Dinaridic chain (Nussbaum, 2002). This causes a major unconformity between the Eocene flysch and the Cretaceous formations (Carulli et al., 2006; Nussbaum, 2002; fig. 8). At some places only a small part of the stratigraphy is missing, but at other places the entire Cretaceous is absent.
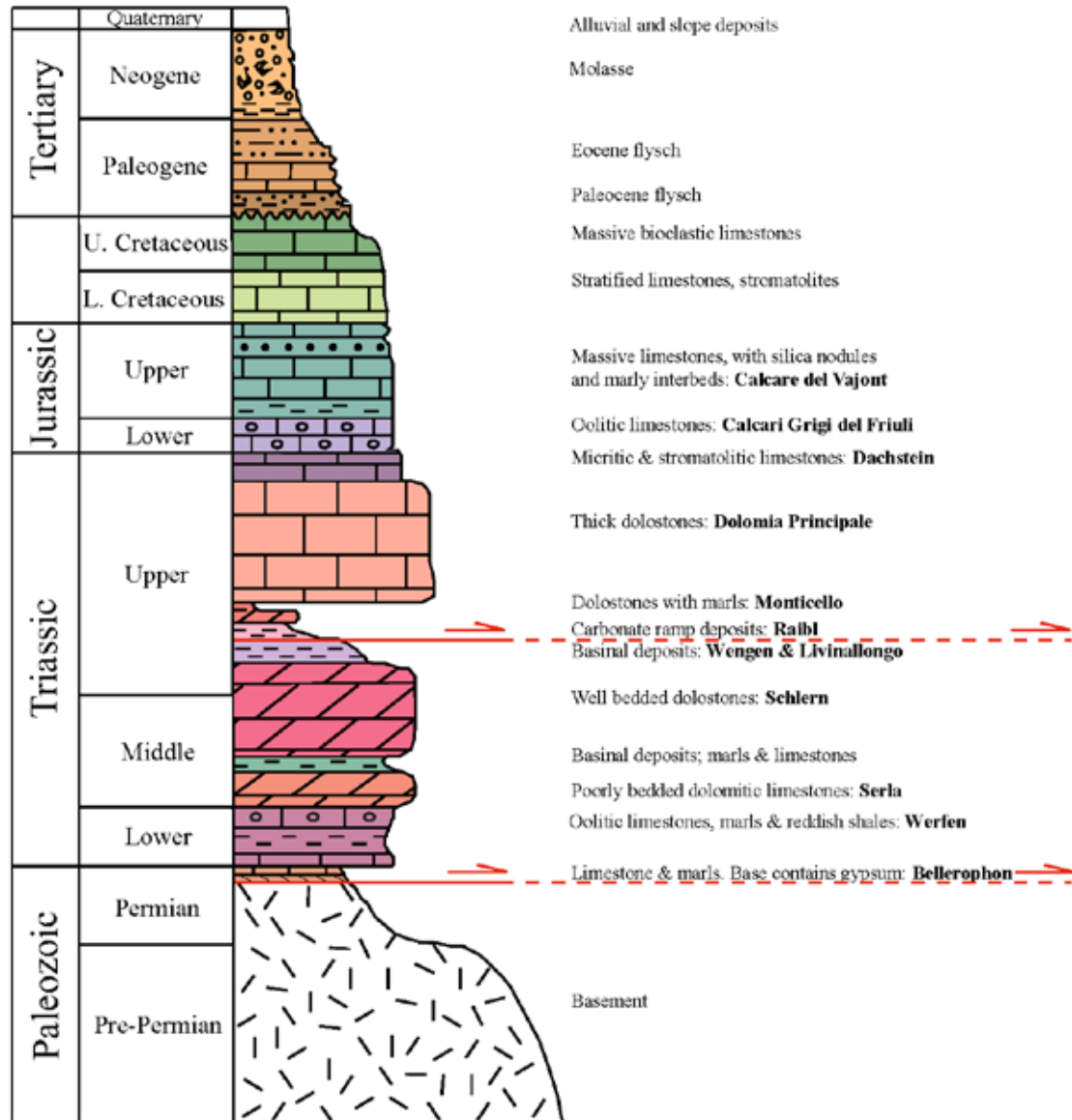
Figure 8. Tectonostratigraphic column of the Friuli Alps, modified after Nussbaum (2002). Formation descriptions are from Carulli et al. (2006), major décollement horizons are indicated in red. Colour coding is similar to that of the geological map in appendix A. For a detailed description of the formations see appendix B.

Paleostress reconstructions of the Friuli region by Bartel et al. (2014a) have led to the distinction of five different deformation phases: (1) N–S shortening during the Eocene and Oligocene; (2) NW–SE shortening in the Oligocene; (3) NE–SW shortening during the Oligocene and Miocene; (4) N–S shortening in the Miocene; and (5) NW–SE shortening during the Pliocene. Castellarin and Cantelli (2000; 2010) however, obtained a slightly different reconstruction: (1) NE-SW Dinaridic shortening during the Eocene; (2) NNE-SSW Dinaridic shortening from 28 to 16 Ma; (3) NNW-SSE shortening from 12 to 7 Ma; and (4) NW-SE shortening from 7 Ma onwards (fig. 9). More studies on paleostress reconstructions in the Southern Alps have been conducted by for example Bressan et al. (1998).
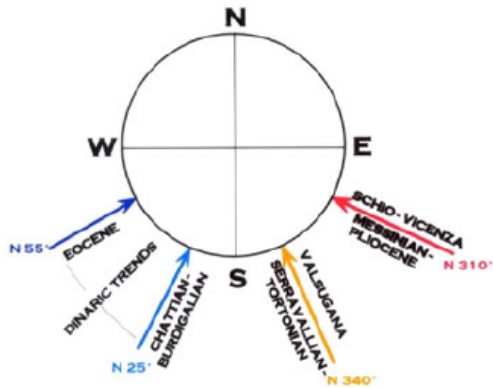
Figure 9. Shortening axes of the different deformation phases active in the Southern Alps according to Castellarin et al. (1998).

Nussbaum (2002) describes a balanced N-S cross section at almost the exact same location as the cross section constructed for this study, which gives more insight into the geometrical structures of the Friuli Alps at depth. Four different thrust systems are distinguished by Nussbaum (2002): the Carnia thrust, the Friuli thrust, the Maniago thrust and the Dinaridic thrust system, that were active at different times (figs. 10 and 11). The Carnia thrust system in the north was responsible for stacking of basement units and became reactivated as a dextral strike-slip fault system during subsequent Alpine deformations (fig. 11). The Friuli thrust started out as a flat in the Bellerophon formation, ramped up and split into a south-vergent thrust and a backthrust (Nussbaum, 2002). This steep north-vergent backthrust is called the Fella-Sava line, where recent seismicity occurred in 1965 and 1976 according to Müller, Slejko et al., and Carulli et al. (cited by Nussbaum, 2002). During these earthquakes, the backthrust was reactivated as a dextral strike-slip fault (Nussbaum, 2002). Nussbaum (2002) marks the frontal thrust of the Friuli system as a major one, as it puts Upper Triassic strata onto Eocene flysch, accounting for a great deal of displacement (the most southern yellow thrust in fig. 11). From subsurface data and data from the Bernadia well by AGIP (1977), Nussbaum (2002) concludes that the southern part of the profile consists of two different anticlines: one created by NW-SE Paleogene Dinaridic thrusts and one by the subsequent E-W thrusts of the Neogene Maniago system. According to Nussbaum (2002), the formation of the first anticline caused the tripling of the Cretaceouos and Eocene units, which implies a minor décollement at the base of the Lower Cretaceous. Other Dinaridic structures observed by Nussbaum (2002) is the décollement in the Bellerophon formation that ramps up through the Mesozoic units in a couple of splays with minor shortening, in the northernmost part of the external Dinarides.
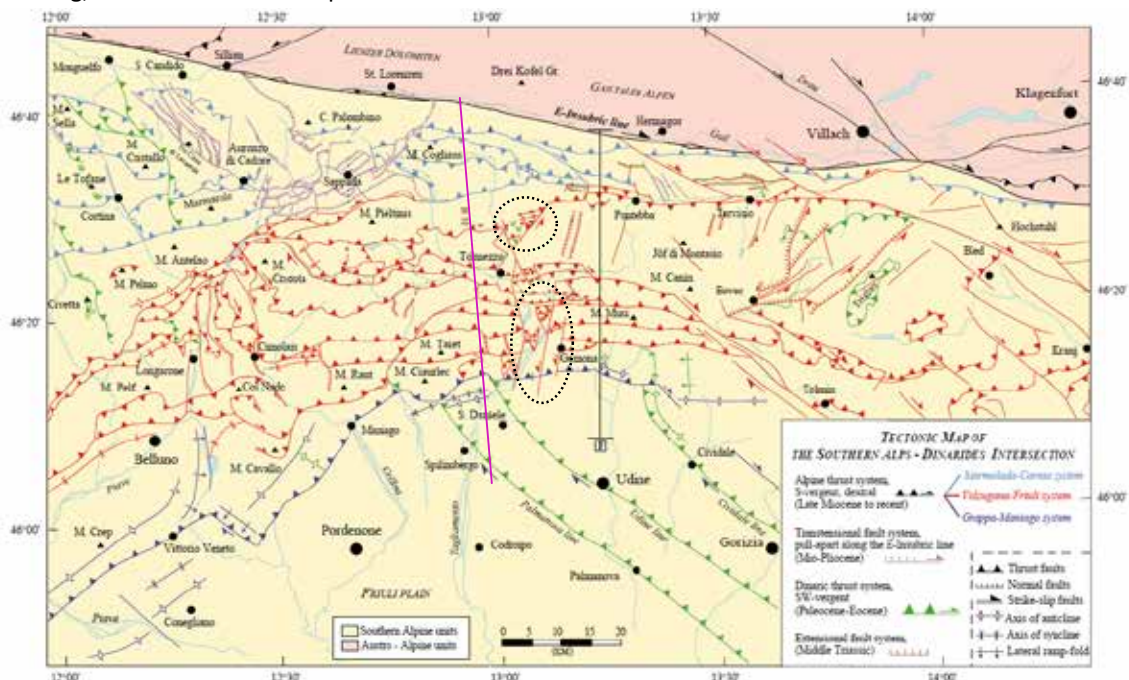
Figure 10. Location of the cross section (F, in black) by Nussbaum (2002). The four different thrust systems identified by Nussbaum (2002) are indicated by the light blue (Carnia), red (Friuli), dark blue (Maniago) and green (Dinaridic) colours. The pink line is the location of the profile by Engelen (2016). The area between the Western and Eastern profiles is characterised by the presence of two transverse zones, located within the black ellipses (Nussbaum, 2002; see section 6.3).
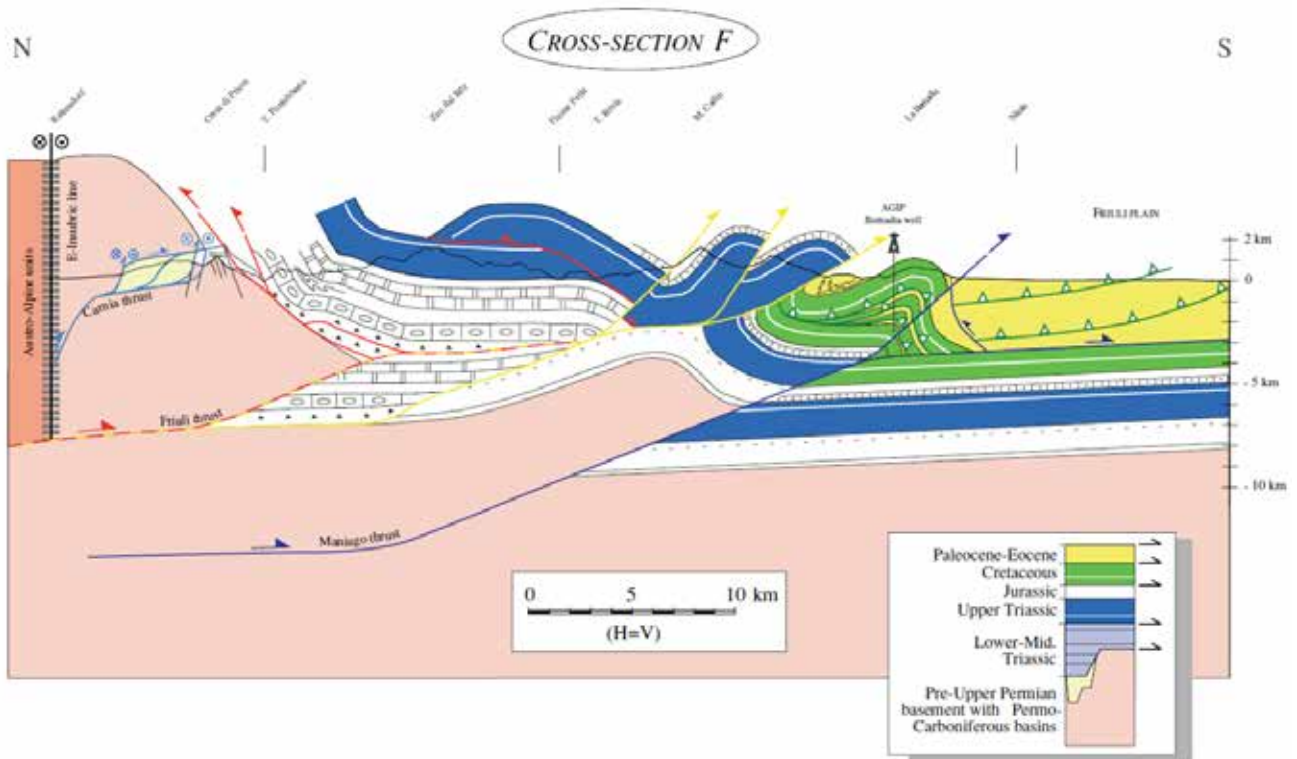
Figure 11. N-S cross section by Nussbaum (2002). The location of the profile line is indicated with the letter F in figure 10; the northern half of this profile lies about 8km west of the profile constructed for this study. The four different thrust systems are also indicated by the light blue (Carnia), red (Friuli), dark blue (Maniago) and green (Dinaridic) colours.

3. Methodology

In order to provide new structural (geometric and kinematic) constraints for the reconstruction of the tectonic evolution of the Friuli Alps and to further discriminate between the Dinaridic and Alpine phases of deformation, fieldwork has been conducted in the eastern part of the Friuli-Venezia Giulia region. The results presented in this report are based upon the data gathered during this fieldwork. For convenience, the main area of study was located along a 54 km long NNE-SSW oriented profile line, roughly between the towns of Pontebba (hinterland) and Tarcento (foreland) (fig. 2). A geological map (appendix A, original scale 1:150000) was used to identify places of interest, such as the locations of big thrust or strike-slip zones and particular formations. This map was also used to create a facies map (fig. 7), on which the transitions between deep and shallow water facies zones are shown.

During the same fieldwork, additional data was also collected in the western part of the region (Engelen, 2016), along another N-S profile line roughly 30 km west of this eastern profile line. The geometries from these two profiles has been compared to each other during a later stage of the research (see paragraph 6.2).

All geological data, such as lithology and younging direction and structures such as bedding, foliations, fold axes, faults, lineations, slickensides, stylolites, tension gashes, etc. were studied and when possible measured. A higher confidence level was given to large-scale structures such as thrust directions, fold axes and fold vergence, because small-scale indicators might be influenced by local heterogeneities and are preferably only used statistically over large areas (Nussbaum, 2002). Measuring the structures was done by the dip direction-dip method and kinematic information was retrieved in the field by measuring slickensides with steps, Riedel shear systems, offsets of markers or drag of bedding planes close to fault planes.

Stereographic projection programs *Stereo32* (Röller and Trepmann, 2007, version 9.4) and *Win-Tensor* (Delvaux, 2014, version 5.0.5.) were used to determine the three principle stress directions (σ1, σ2 and σ3) and the associated stress regimes (R') and to present an overview of the field data. Due to a lack of outcrops with sufficient directional kinematic indicators, such as striae with steps, Riedel shears or visible offsets, all field data was merged for use in both programs. In *Win-Tensor*, the entire dataset was separated again into fault subsets

that have the same orientations for their principle stress directions. These different subsets are likely to represent different phases of deformation.

The collected data and new insights on the deformation phases have been used to reconstruct a N-S striking cross section (for the location of the cross section see fig. 2; cross section presented in fig. 24). This interpretation will provide the input for a quantitative 2D reconstruction of the area by means of balancing the cross section using *MOVE* software (Midland Valley, 2014). *MOVE* was used to detect space problems and geometrical errors; this was done by separating the interpreted section into different fault blocks, leaving one of these blocks at its original position as a reference. These blocks were then individually unfolded using the *flexural slip unfolding algorithm*. Afterwards, the unfolded blocks were put back together and space problems such as gaps and overlaps along the section could be identified and manually corrected. The modified cross section was then refolded again into its original position, making it geometrically valid (see also *MOVE* 2014, tutorial 16). During this process, the same layer should be unfolded between two adjacent fault blocks, so one layer should always function as a template for unfolding. The other layers are then passively unfolded, relative to the template, while maintaining the thicknesses between the layers. Also, every fault block should be "pinned" before unfolding at a position where no slip between layers occurs; for example parallel to the axial planes of folds or at a horizontal part of the section.

Further restoration of the cross section was then obtained by restoring the fault offsets, fault by fault, using the *move on fault algorithm (fault parallel flow)*. Starting with the youngest fault and finishing with the oldest one, based on fault and stratigraphic relationships (see also *MOVE* 2014 tutorial 14), bringing the cross section back to its original (pre-deformation) structure. The main assumption during restoration is that the cross section behaves as a layer cake model, which implies the conservation of area. So no layer thickness changes and bedding parallel flexural slip only.

Finally, from this restored section, the total amount of contraction can be derived by using the *section analysis tool*, which can calculate the line lengths of the model at the start and finish of the restoration. However, only deformation in the direction parallel to the location of the profile can be obtained from this reconstruction, so in order to assess the amount of Dinaridic deformation as well, the selected profile had to slightly bend some more towards the SW at its southern end.

The balanced and reconstructed cross section will provide clear constraints on the pre-shortening structure of the study region. Also, different steps of deformation can be recognized more easily and the interpreted layout of the deep structure will be geometrically valid. When a distinction can be made between younger Alpine and older Dinaridic structures, restoration of the Alpine structures will show what the original geometry and transport directions are of the pre-existing Dinaridic structures.

4. Field results

In total, 57 stops have been visited in the Eastern Friuli Alps, at various locations (see appendix C for an overview of the locations and their structural and lithological descriptions). Of these stops, 11 were located in the "Southern Paleocene-Eocene/Miocene Flysch Zone" (see fig. 7 for a facies map), plus 3 other stops in a narrower flysch outcrop to the NE of this zone (fig. 12a). The other stops were located in either rigid carbonate platform facies (34 stops, fig. 12b) or softer basinal/slope facies (9 stops, fig. 12c).

4.1. General structures

Because all formations older than the Bellerophon formation remained attached to the crystalline basement during Alpine thrusting (Nussbaum, 2002), these formations are regarded as part of the basement. Almost all structures observed in the field are typical for brittle deformation, except those in the Belleophon formation, which seem to have been formed by a combination of brittle and ductile deformation. Since this formation consists partly of evaporites, high temperatures were not necessarily needed to obtain ductile deformation. The 'soft' shale and evaporite layers are characterized by many and well defined deformation features such as folds and faults, while little deformation structures could be recognized in the rigid platform carbonates. The

décollements identified by e.g. Schönborn (1999) and Nussbaum (2002); the Bellerophon and Raibl formations, are usually tight or even isoclinaly folded, with significant amounts of shearing and steeply dipping bedding planes (fig. 12c). The Paleocene (formation 19a) and Eocene flysch (formation 19b), which locally contains thick carbonate platforms as well, are also relatively soft. They are less intensively folded than the décollement strata, but are also often found in an (almost) vertical orientation (fig. 12a).

Various different 'fault zones' can be identified in the field as well; these fault zones are brittle throughout, containing cataclasites and fault breccia. The zones are often 20 to 60 m wide, which indicates that a significant amount of deformation has affected these areas, along relatively large structures. The other formations laying on top of the fault zone material is overall still intact and the contact between the intact layers and the fault zone is relatively shallow inclined (less than 45°). This suggests thrusting rather than normal faulting, sometimes combined with some oblique motions (fig. 13a). Usually these zones are indicated on the geological map by Carulli et al. (2006) as south vergent thrusts as well. The zones were located at stops 1.6 near Pontebba, 3.1 and 7.3 near Resuitta, 6.2 near Chiusaforte, 9.1 near Venzone and 10.7 near Valbruna.

Another noteworthy characteristic of these zones is the occurrence of so-called 'mirror planes' on the surface of some fault rocks, where the frictional forces have been so powerful that they polished the rock surface to be as smooth as that of a mirror, perhaps indicating past events such as earthquakes (fig. 13b).
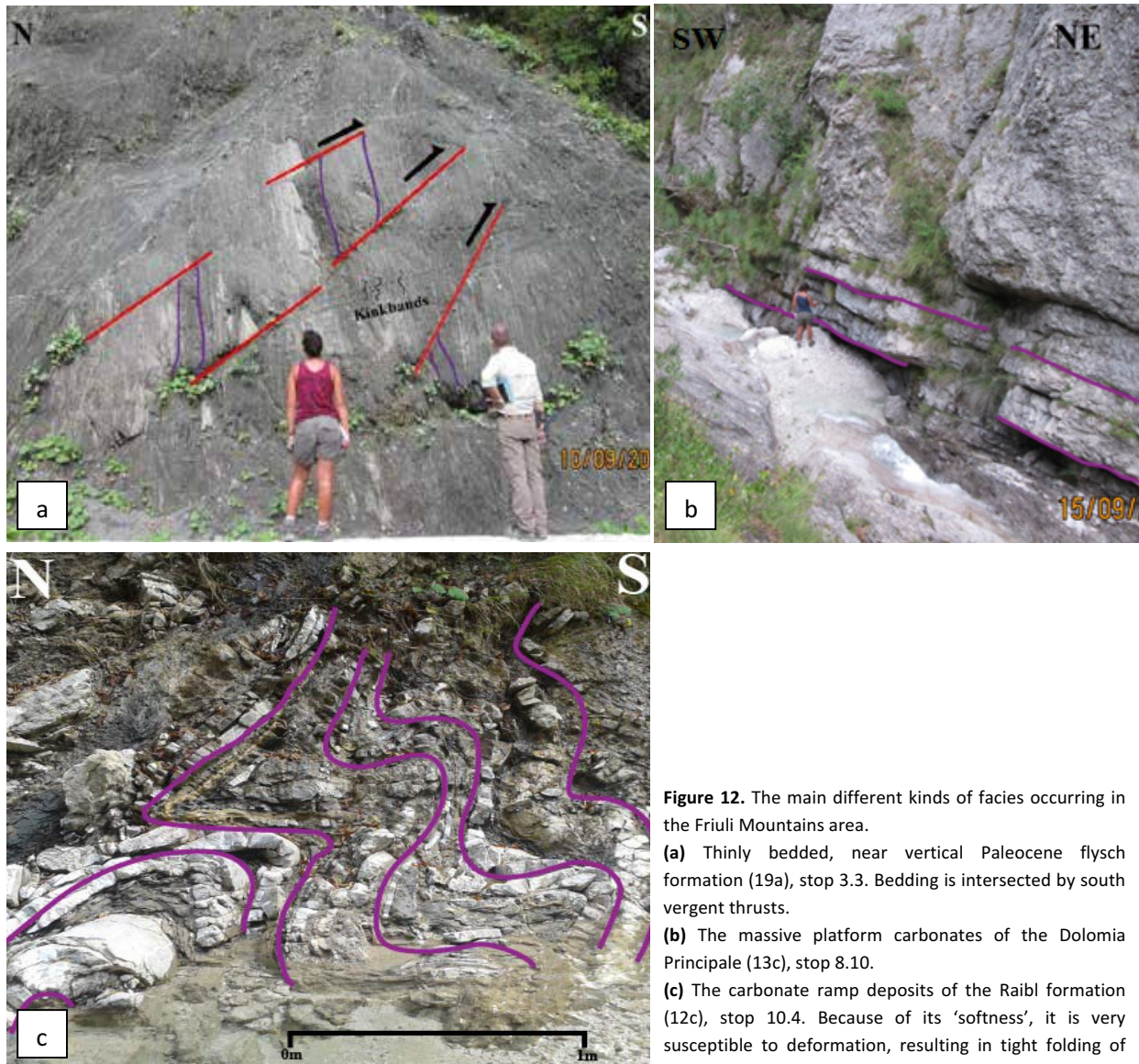
Figure 12. The main different kinds of facies occurring in the Friuli Mountains area.

(a) Thinly bedded, near vertical Paleocene flysch formation (19a), stop 3.3. Bedding is intersected by south vergent thrusts.

(b) The massive platform carbonates of the Dolomia Principale (13c), stop 8.10.

(c) The carbonate ramp deposits of the Raibl formation (12c), stop 10.4. Because of its 'softness', it is very susceptible to deformation, resulting in tight folding of the bedding planes.
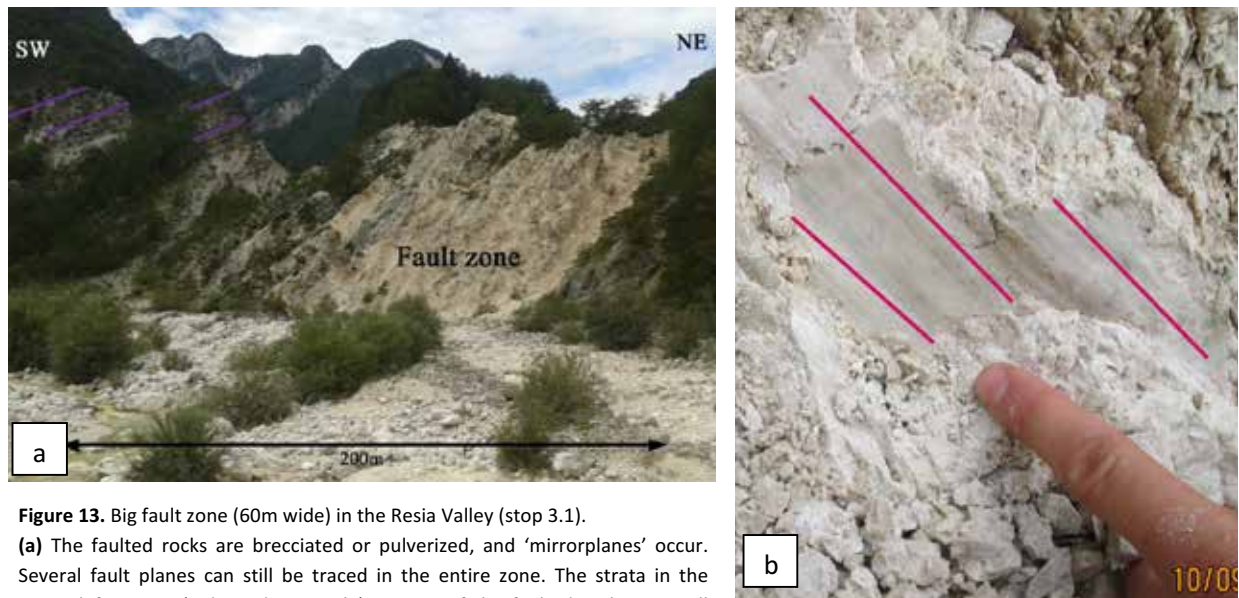
Figure 13. Big fault zone (60m wide) in the Resia Valley (stop 3.1).

(a) The faulted rocks are brecciated or pulverized, and 'mirrorplanes' occur. Several fault planes can still be traced in the entire zone. The strata in the upper left corner (indicated in purple), on top of the faulted rocks, are still intact. The inclination of the contact plane between the two is shallow.

(b) Detail of a 'mirrorplane' on a fault rock of the fault 'zone' in fig. 13a, striae are visible, but it is unclear whether the movements were either down-dip or up-dip.

The younging directions, needed to identify overturned formations for the construction of the N-S profile, were obtained from structures such as burrows, load casts and wave ripples (figs. 14a and b). The measured bedding plane (S_0) orientations, which were mainly S to SE dipping (black lines in fig. 15a), were also incorporated into the N-S profile if they were located close enough to the profile line. But as is apparent from fig. 15, the bedding planes do show a wide variation in their orientations, suggesting that they have been subjected to large scale folding, applied from multiple directions.

Not on every fault, clear kinematic information could be retrieved; based on fault orientation, four different fault sets could be recognized: N-S dipping (fig. 15c: towards 340°– 20° and 160°-200°), NE-SW dipping (fig. 15d: towards 25°-65° and 205°-245°), NW-SE dipping (fig. 15e: towards 120°-160 and 300-340) and some E-W dipping faults (fig. 15f). The rose diagram (fig. 15b), on which all these faults are plotted, shows that south dipping fault planes are statistically most abundant.

However, as various faults also expressed strike slip or oblique motions, and not only dip-slip, this plot is not entirely representative of the stress regimes that affected this area. Faults that did have kinematic indicators, such as calcite steps, Riedels, shears and folds, were incorporated in *Win-Tensor*. From the combination of these field observations and the data analysis in *Win-Tensor* and *Stereo32*, four different deformation phases could be inferred, which are described in the next paragraph.
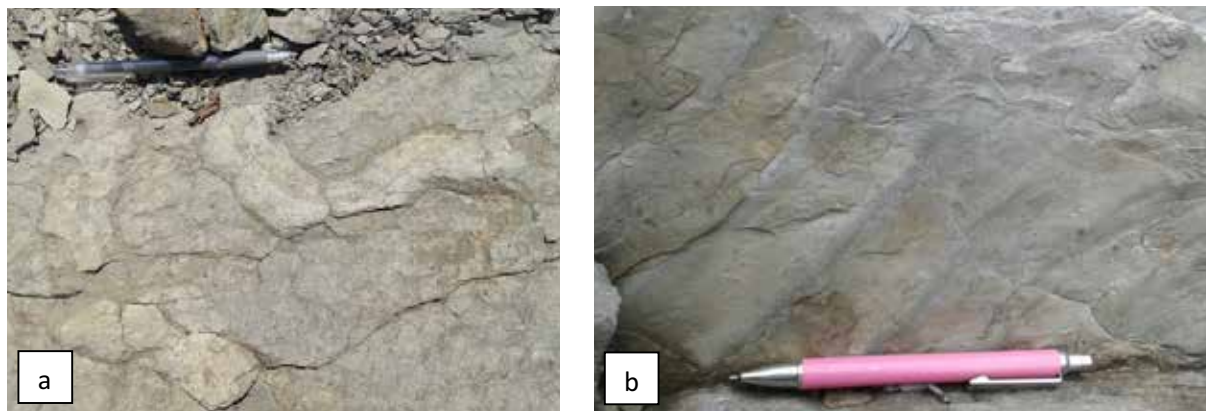
Figure 14. Younging direction indicators.

(**a**) Burrows indicating that the flysch is overturned, stop 8.3 east of Tarcento. (**b**) Wave ripples on the top-side of the bed, near Pontebba at stop 5.3.
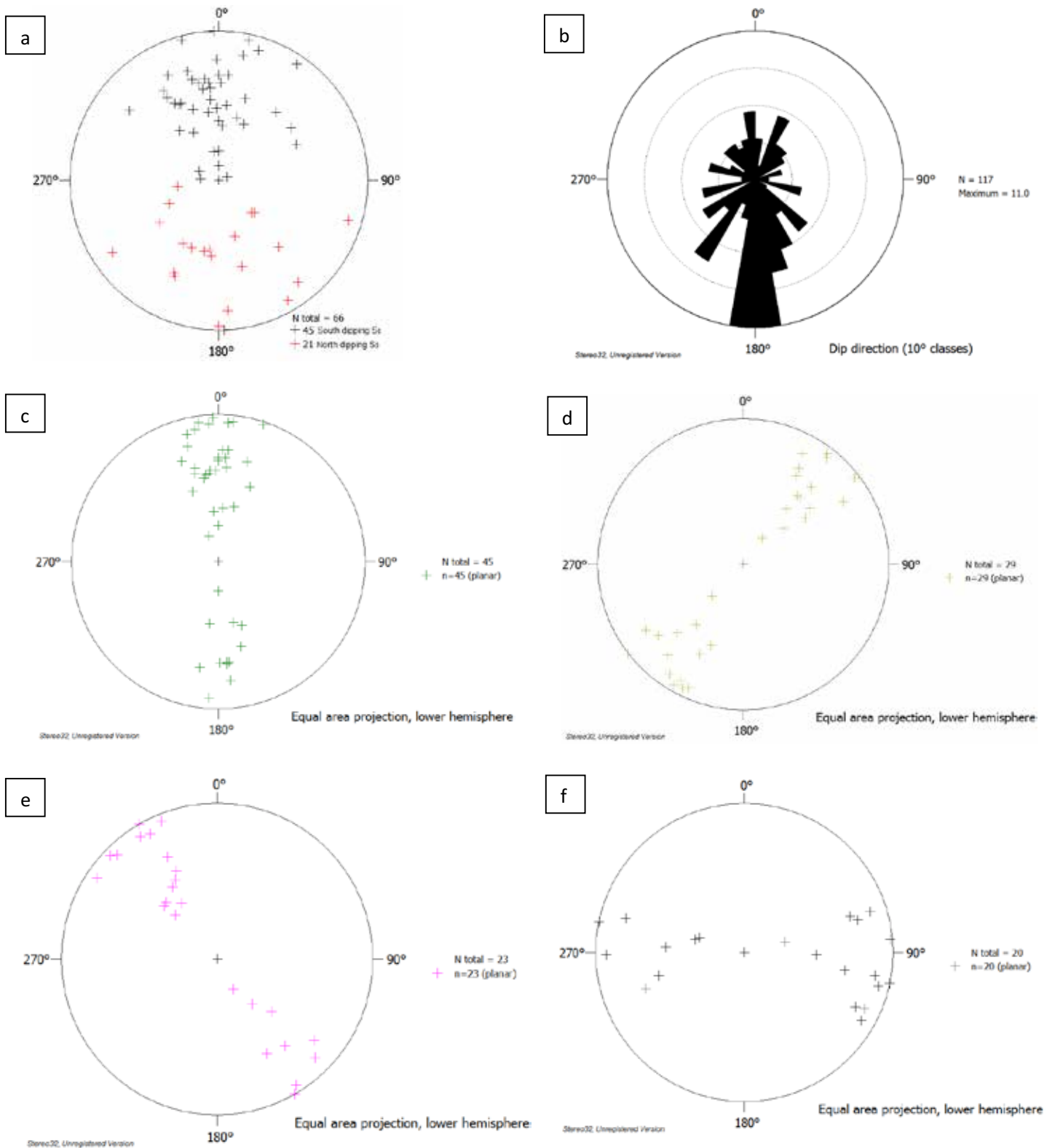
Figure 15. Stereoplots.

(a) All measured bedding plane (S_0) orientations, presented as poles. Most of the bedding planes dip towards the S to SE; which is indicated by the black poles (45 planes of a total of 66 planes).

(b) Rose diagram of the 117 measured fault planes; the south dipping planes are statistically most abundant.

(c) The N or S dipping fault plane set is the most abundant of the four different fault sets presented as poles, with a total of 45 fault planes.

(d) NE-SW dipping fault planes, 29 in total.

(e) NW-SE dipping fault planes, 23 in total.

(f) E-W dipping fault planes, 20 in total.

4.2. Deformation phases

The combined field results and stress analysis led to the identification of four different deformation phases (A to D in chronological order) that are characterized by their own stress regimes and typical deformation structures. Phases A, C and D clearly formed distinct sets in the *Win-Tensor* analysis and could be recognized as separate phases in the field as well. Phase D2 was only distinguished in the field; the faults that make up its tensor in figure 17a also fitted within the tensors of the other phases. However, because these faults were all located in the same area, they were plotted as one separate phase and together they form a stress tensor that describes a different deformation phase than the other three.

The order of these subsequent deformation phases could be deduced from overprinting relationships observed in the field; for example at stop 9.2 where more prominent layer parallel faults belonging to a certain phase were cross-cutting a previously formed cleavage that belonged to another phase and at stops 9.1 and 10.4 where striae and asymmetrical folds of one phase were intersected by strike-slip faults of a different phase. Only the timing of phase D1 was more difficult to determine, because the structures belonging to this phase were not clearly influenced by other structures. This could be because phase D1 is actually the youngest phase, or because all normal faults belonging to this oldest phase have been (partially) inverted during subsequent phases. Taking the regional geology of the area into account, the last option seems more likely, as the Triassic, Jurassic or Late-Cretaceous rifting phases must have left some traces.

The big fault zones probably have experienced multiple deformation phases as well, since thrusts, normal faults and strike-slip faults occur together at these locations. But unfortunately no cross-cutting structures were found at these stops. For example, when the faults of stop 3.1 were all plotted together, they mainly seemed to fit within phase D3, but the high amount of strike-slip faults also suggested some phase D4 influences (fig. 21b).

4.2.1. D1: N-S extension

The oldest deformation phase (D1) has a horizontal, roughly N-S extensional axis ($\sigma3$) and a near vertical shortening axis ($\sigma1$), indicating N-S extension (fig 16a). The R' value of 0.5, calculated in *Win-Tensor*, is also typical for a pure extensional regime (Delvaux and Sperner, 2003).

The faults that characterize this phase are mostly normal faults, which are all plotted in figure 16a that contains 15 measurements form different outcrops. The rose diagrams (figs. 16 and c) indicate that most faults have a E-W oriented strike with a mostly steep dip angle. Compared to the amount of thrusts faults in the area, normal faults are actually quite rare, which is most likely caused by (partial) overprinting of these oldest faults.

Most normal faults were observed in the carbonate platform rocks of for example the Monticello and Dolomia Principale formations at stops 6.1 and 10.7, but some were found within the thicker high carbonate-content layers of the flysch as well (stop 7.6). When offsets were visible, they were usually relatively small, on a 1 to 6 m scale (fig. 16d), suggesting that normal faulting did not affect the area to a very large extend. But due to the likely subsequent reactivation of these faults, the offsets measured in the field are not representative for the amount of extension associated with this first phase.
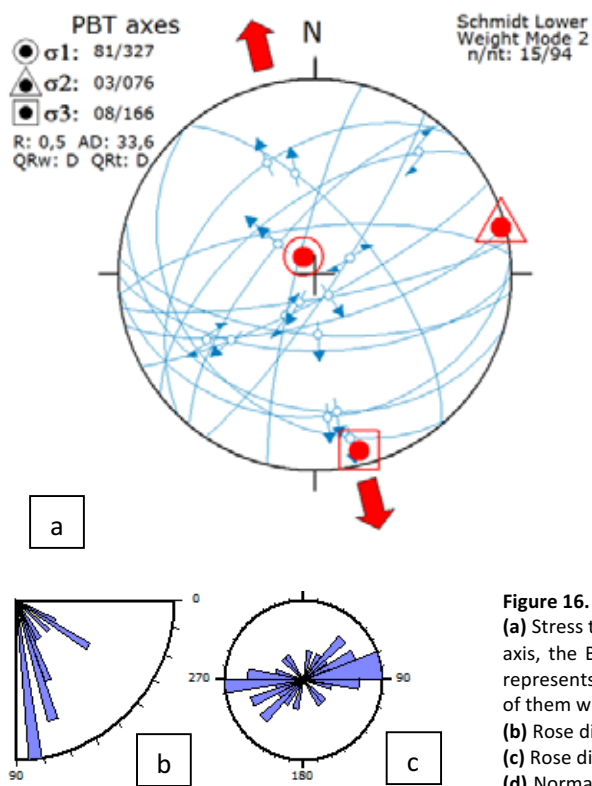
Figure 16. Phase D1: N-S extension.
(a) Stress tensor defining phase D1. The P or σ1 axis (circle) depicts the contraction axis, the B or σ2 axis (triangle) is the neutral axis and the T or σ3 axis (square) represents the extension axis. The faults are from several different outcrops, most of them were found in the carbonate platform facies.
(b) Rose diagram for the dip angle of the faults defining phase D1.
(c) Rose diagram for the strike of these faults.
(d) Normal fault, with possible Riedel shear and striae plunging towards 174/60°S, and an offset of 1-1.5 m, located at stop 6.1, near Resiutta.

4.2.2. *D2: NNE-SSW shortening*

The second deformation phase that can be identified in the Eastern Friuli Alps is a phase defined by a NNE-SSW shortening axis (fig. 17a; based on 7 measurements). Characteristic structures belonging to this phase are (S)SW dipping thrust faults and NW or SE plunging fold axes (fig. 17c). Most of these structures were observed in the Eocene flysch of the "Southern Flysch Zone", located close to the Dinaridic Chain, at stops 4.1 to 4.4 and 8.1 to 8.9 (the blue area in fig. 7; for more information see appendix D).

Some of the observed thrusts were up to several meters long, but the precise amount of offset was often not clearly visible. Fold structures include for example a 10 m wide fold with a 285/11° plunging axis (intersection of the black great circles in fig. 17c) and a kinkband with a 290/05° fold axis (red cross in fig. 17c).

A Cretaceous outcrop of roughly 2 by 4 km wide, consisting of formations 16c and 17a, which is surrounded in the field by the flysch of this "Southern flysch Zone" is also affected by NNE-SSW shortening. These Cretaceous rocks form a 1,5 km wide anticline with a fold axis plunging towards 136/07° (pink fold limbs; fig. 17c, see also fig. 24f).

At two locations outside of the flysch "Zone", representative structures for phase D2 were found as well. This included (W)NW directed thrust faults within the Raibl formation at stop 6.5/10.1, near the town of Dogna and the occurrence of a 2m wide fold in the carbonate platforms of the Monticello or Dolomia Principale formations, with a fold axis plunging towards 154/55° at stop 9.2 (blue fold limbs in fig. 17c). At this last stop, the intersection of the bedding and observed cleavage also plunged to 169/53°, indicating the same NE-SW shortening (fig. 17c). Along the bedding planes, bedding parallel slip features were observed that intersect these cleavage structures.

Figure 17. Phase D2: NNE-SSW shortening.

(a) Stress tensor defining phase D2; for the explanation of the used symbols see fig. 15. Most faults are located in the "Southeren Flysch Zone"; mainly at stop 4.1, except for one fault that is located in the Raibl formation at stop 6.5/10.1.

**(b)** Cleavage (S_1, indicated in blue) in the Monticello or Dolomia Principale formation at stop 9.2, whose intersection with the bedding (S_0, in purple) indicates NE-SW shortening. Later, bedding parallel thrusting (S_2) towards the north took place as well, which intersects the cleavage. This indicates that at least two different deformation phases have affected these rocks.

(c) Stereoplot for all the D2 folds, the coloured lines represent the limbs of three different folds, the red cross is the fold axis of a kinkband (see main text for more information).

4.2.3. D3: N-S shortening

The third phase is the most pronounced phase of deformation within the field work area and could be recorded at several different places. The stress tensor in figure 18a, which contains 29 measurements from different outcrops, shows that the orientation of the shortening axis (σ1) is roughly SSE trending and horizontal, while the extensional axis (σ3) is nearly vertical. This indicates a contractional regime, which is also confirmed by the R' value of 2.65. Phase D3 is characterized by WNW/ENE plunging fold axes, small scale N and S vergent asymmetrical folding in the softer facies and large scale north- or southward thrusting in the more rigid facies. The rose diagram for the fault plane strikes also shows a mostly E-W oriented strike with a great variation in fault dip angles (figs. 18 b and c). Furthermore, the majority of the poles that represent the 14 S_1 foliations measured throughout the entire area have a preferred orientation dipping towards the north (fig. 18d), suggesting south vergent folding and thrusting.

The stereographic projection of all the fold axes observed in the field, indicate that most axes plunge relatively shallow (<45°) towards the WNW or to the ENE (fig. 19). This implies that the majority of the folds formed due to N-S contraction. The folds observed in the softer basinal formations (formations 8b and 10a; see appendix A and B) and in the Raibl formation (12c) are usually asymmetrical and can either be tight or open folds (figs. 12c and 21a). Chevron folds also occur (fig. 20b), of which some show a collapsed hinge. Another feature that these folds have in common is a considerable amount of layer parallel shortening. This is indicated by the high amount of shearing within the softer layers of these formations, while the more rigid layers seem to be less affected. This type of deformation is typical for flexural slip folding (fig. 21b and c). The scale of the folds is overall relatively small and varies from folds with wavelengths up to 4 m with an amplitude of 1 m within the more rigid layers and folds with an average wavelength of 15 cm and amplitude of 10 cm in the softer layers

(fig. 21a). The vergence of these folds, based on the orientation of their longer and shorter limbs, is not constant and is for example towards the north at stop 5.3 (fig. 22a) and to the south at stop 2.3 while located at the same latitude and within the same basinal formations. In the Raibl formation (12c) at stops 6.5 and 10.1-10.4 (fig. 22b) near Dogna, the same type of asymmetrical folds are also south vergent.

At stop 10.4, a cross-cutting relationship was observed as well, as the south vergent asymmetrical folds in the Raibl formation were intersected by dextral shear planes with shearing towards the SE (fig. 20). These shear planes must belong to a younger deformation phase (phase D4).
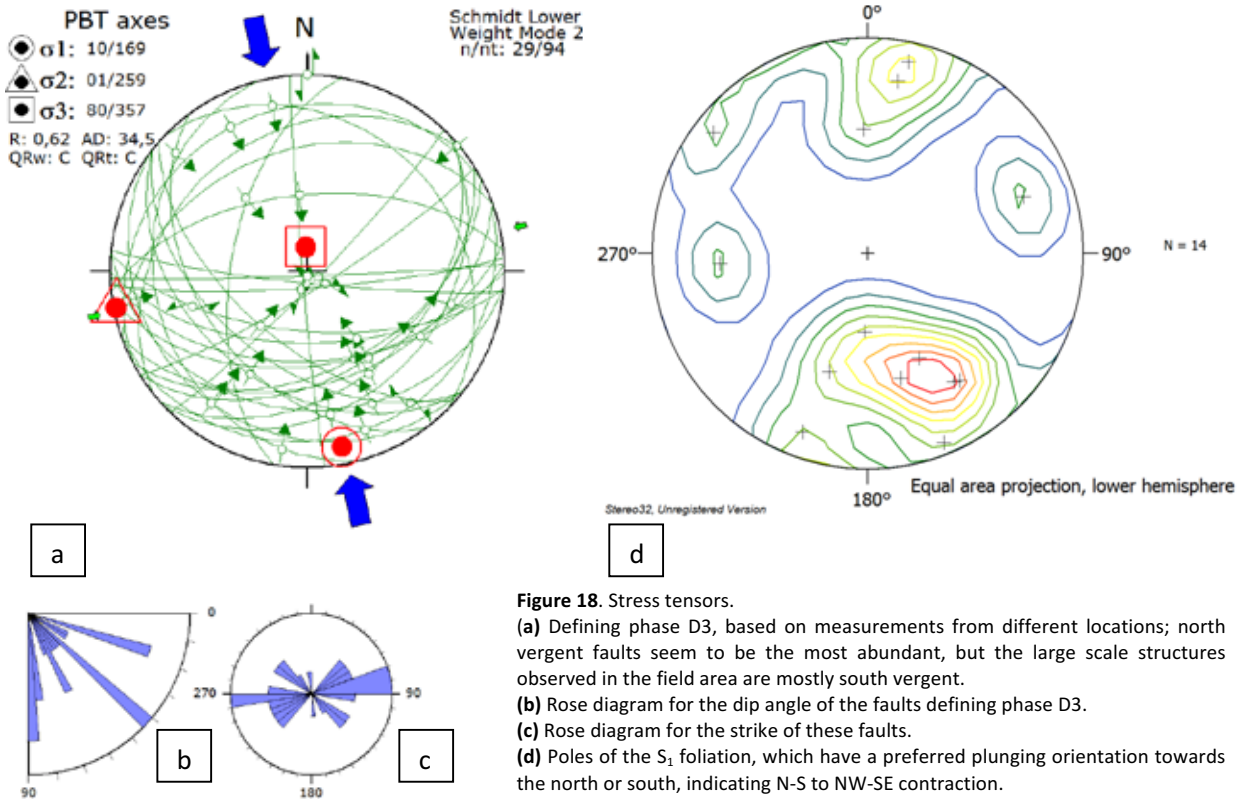
Figure 18. Stress tensors.
(**a**) Defining phase D3, based on measurements from different locations; north vergent faults seem to be the most abundant, but the large scale structures observed in the field area are mostly south vergent.
(**b**) Rose diagram for the dip angle of the faults defining phase D3.
(**c**) Rose diagram for the strike of these faults.
(**d**) Poles of the S_1 foliation, which have a preferred plunging orientation towards the north or south, indicating N-S to NW-SE contraction.

The phase D3 deformation structures were not only observed in the soft strata of the ramp, slope and basinal deposits, but also in the more rigid carbonate layers and in the flysch, in the form of large scale north- and southward thrust faults, with offsets of up to tens of meters. A division between north directed thrust in the northern part of the area and south directed thrusts in the southern part of the research area was recognized as well.

An example of a north vergent thrust that showed at least a couple of meters of offset, was found at stop 10.2, within the Schlern formation (fig 23a). The most southern north vergent thrusts are located within the large "Thrust Zone" at stop 3.1, in the Dolomia Principale formation, based on the stress tensor belonging to this outcrop (fig 23b). Most large scale thrusts, are however south vergent, which does not become immediately apparent from the phase D3 stress tensor in figure 18a, but is in accordance with the geological map of Carulli (2006; fig. 2). Examples of these structures can for example be found at stops 3.2/3.3 and 9.1.

At stops 3.2 and 3.3, which is located in the narrow flysch zone, the main direction of transport is to the S(SE), as is indicated by small scale thrusts and kinkbands (fig. 12a). On the larger scale, thrusting here has created large offsets, as younger flysch of Paleocene age lies in the valley, while the nearby hilltops in the north consist of older carbonate platforms of Triassic to Jurassic age (fig. 23c). Another noteworthy feature is that the flysch at stop 3.3 has an almost vertical orientation, while the flysch in stop 3.2 has not, suggesting that the flysch might have been overturned in a footwall syncline. Calcite steps found at stop 3.2 indicate dextral shearing towards the SE as well (fig. 23d), but sinistral shearing was also observed at adjacent surfaces. This indicates that several smaller faults with different shearing directions were associated with the big south vergent fault occurring in this area.
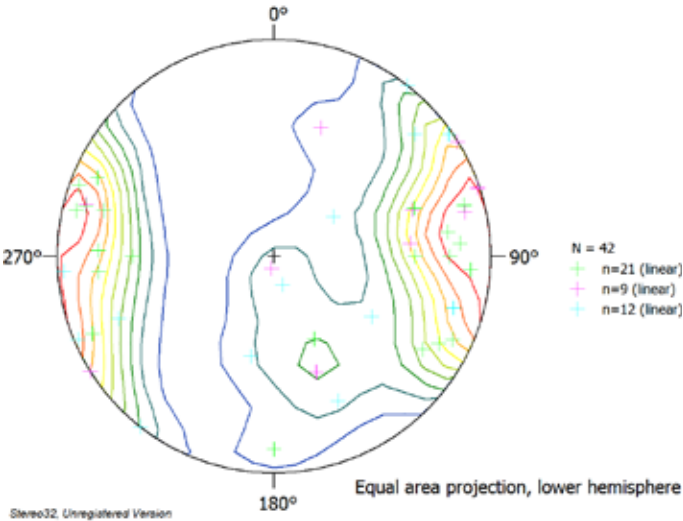
Figure 19. Stereographic projections of all fold axes occurring in the field work area; green crosses are fold axes measured in the field, pink crosses are derived from fold limbs measured in the field and blue crosses are derived from the intersection between the bedding (S_0) and the S_1 foliation.
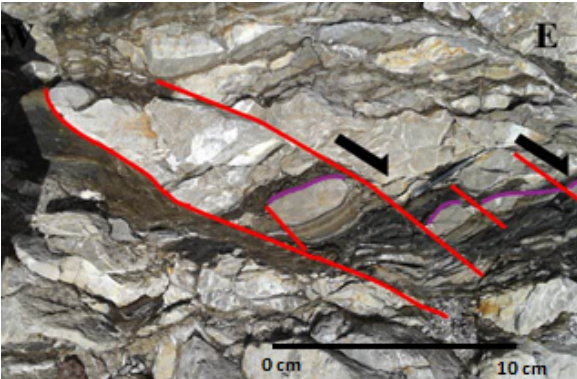
Figure 20. Dextral SE directed shearing planes that intersect the asymmetrical folded Raibl formation at stop 10.4, near Dogna. The strike-slip folds, with an average offset of 10 cm belong to a subsequent deformation phase.
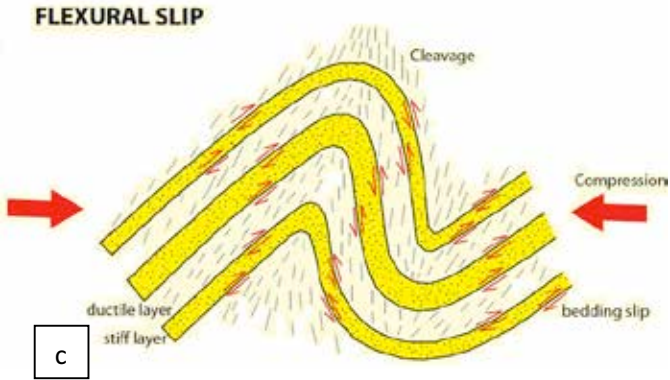
Figure 21. Phase D3 folding.
(a) Open folds of several wavelength and amplitude within the basinal facies (formations 8b and 10a), at stop 5.3 where tight folds also occur. The inset shows Here, the folds are north vergent.
(b) Tight chevron folding in the Raibl formation (stop 10.4), also with an E-W fold axis, but south vergent. The darker layers are softer and show more deformation, indicating flexural slip folding within these mechanically soft units that are sandwiched between the stiffer units
(c) Image modified from Hatcher (1995), that shows how more deformation can occur in the softer layers of an alternating soft/hard rock formation, combined with bedding parallel slip, due to flexural slip folding.

Figure 22. Field book overview sketches indicating the different vergences and stratigraphic successions occurring in the area. Sketches are not drawn to scale.
(a) North vergent asymmetrical folds in the basinal formations at stop 5.3, which could be caused by the overthrusting of the Schlern formation. The bedding planes are almost vertically orientated at some places along the same outcrop.
(b) South vergent asymmetrical folds in the steeply orientated Raibl fomation at stop 10.2 and 10.3. The vergence could be caused by overthrusting of the Schlern formation to the south. Both the carbonate platforms located to the north (Schlern) and south (Monticello/Dolomia Principale) of the narrow outcropping zone of the Raibl formation are less steeply oriented, indicating that the massive platforms might indeed have slid along the softer underlying facies.

At stop 9.1, in the Dolomia Principale formation, striae (green lines) are visible on the bedding planes and a Riedel shear, that both indicated south directed layer parallel shortening (fig 23e). These structures were in turn, cut by a strike-slip fault (265/88°) with horizontal striae, belonging to a younger deformation phase (D4).
Bedding parallel slip features were also observed at stop 9.2 and were inferred from the occurrence of fault gauge and significantly brecciated rocks along the bedding planes. The direction of thrusting was towards the north (355°), indicating N-S shortening. These bedding parallel slip features intersect older cleavage structures (belonging to deformation phase D2, see 4.2.2.) and are far more prominent, indicating that layer parallel slip must have happened after the cleavage was formed.
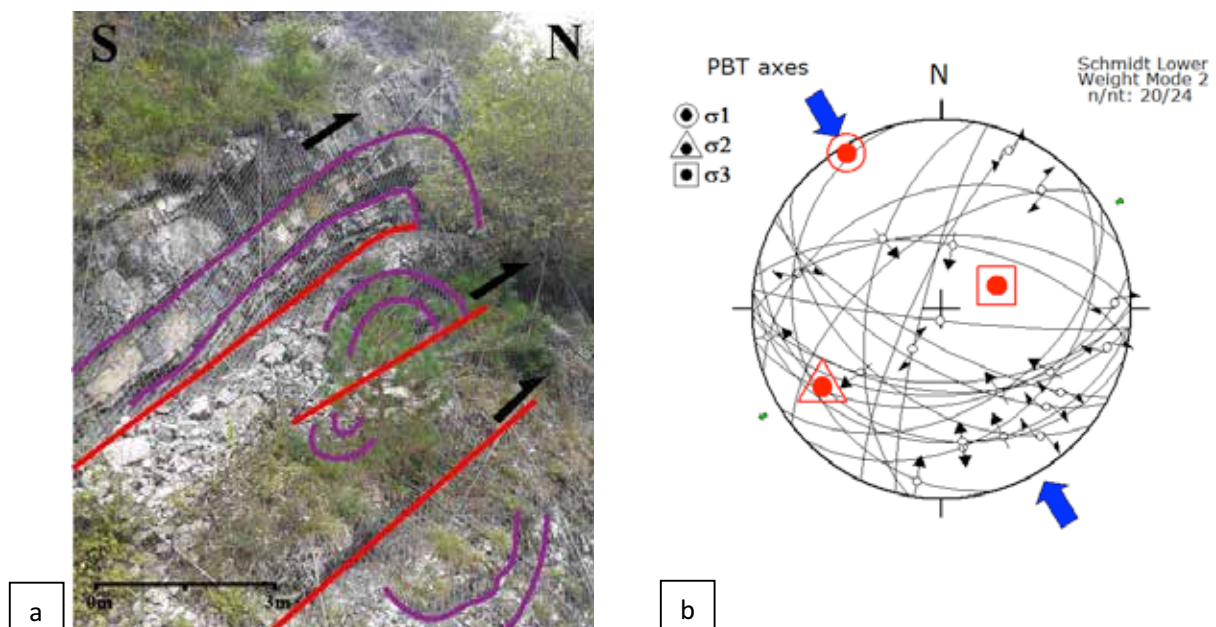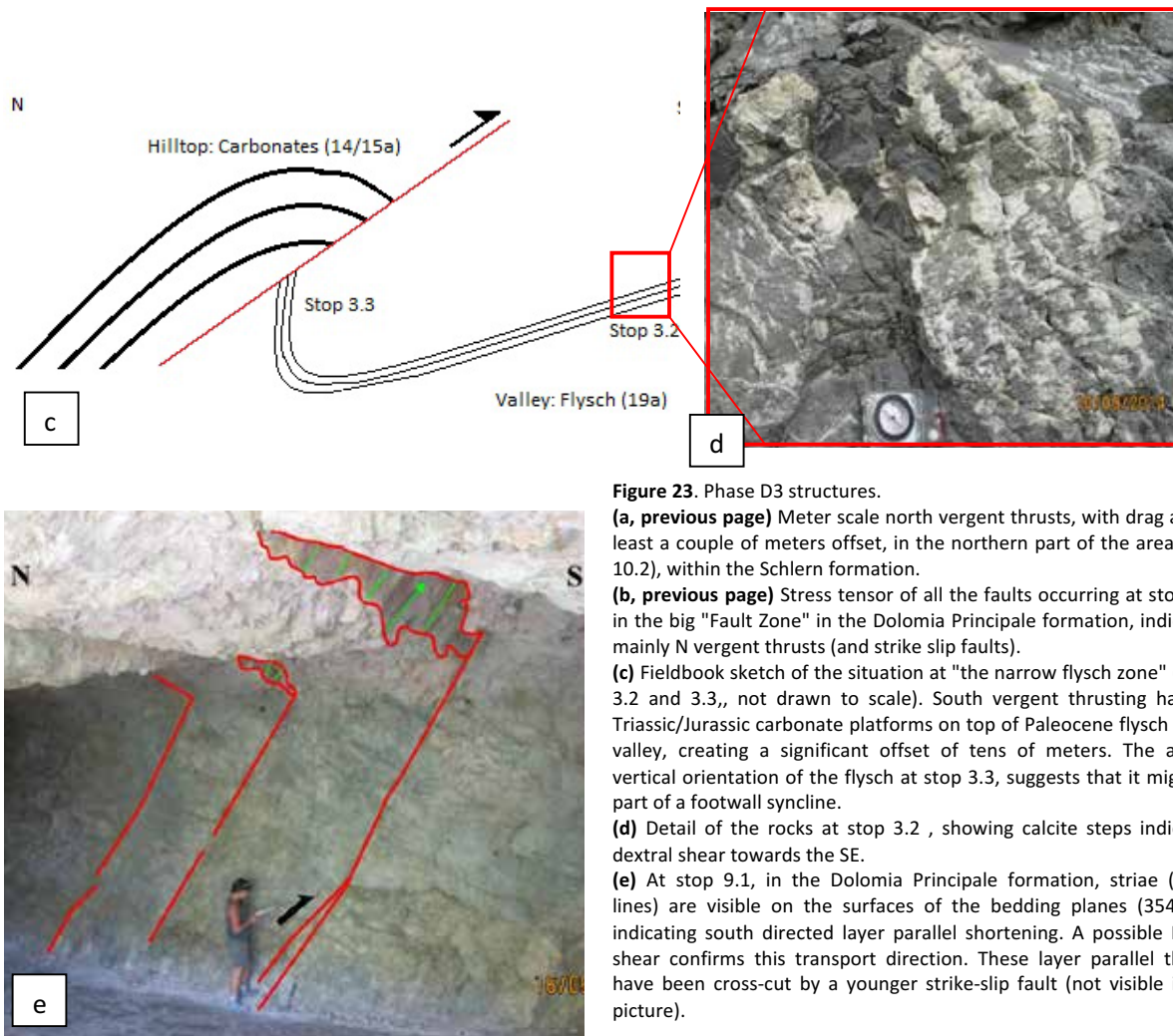
Figure 23. Phase D3 structures.

(a, previous page) Meter scale north vergent thrusts, with drag and at least a couple of meters offset, in the northern part of the area (stop 10.2), within the Schlern formation.

(b, previous page) Stress tensor of all the faults occurring at stop 3.1, in the big "Fault Zone" in the Dolomia Principale formation, indicating mainly N vergent thrusts (and strike slip faults).

(c) Fieldbook sketch of the situation at "the narrow flysch zone" (stops 3.2 and 3.3,, not drawn to scale). South vergent thrusting has put Triassic/Jurassic carbonate platforms on top of Paleocene flysch in the valley, creating a significant offset of tens of meters. The almost vertical orientation of the flysch at stop 3.3, suggests that it might be part of a footwall syncline.

(d) Detail of the rocks at stop 3.2 , showing calcite steps indicating dextral shear towards the SE.

(e) At stop 9.1, in the Dolomia Principale formation, striae (green lines) are visible on the surfaces of the bedding planes (354/58°), indicating south directed layer parallel shortening. A possible Riedel shear confirms this transport direction. These layer parallel thrusts have been cross-cut by a younger strike-slip fault (not visible in the picture).

4.2.4. D4: E-W strike-slip

The youngest deformation phase has a horizontal NW-SE trending shortening axis (σ1), a horizontal NE-SW trending extensional axis and a R' value of 1.34, indicating a strike slip regime. The dataset used to create the stress tensor in figure 24a contained 26 measurement, obtained from outcrops from the whole area.

Phase D4 is mainly characterized by dextral roughly E-W trending strike-slip faults, as is also indicated by the plotted faults in figure 24a and the rose diagram that shows the general strikes of the faults (fig. 24c.) The dip angle of the faults varies, but steeply dipping faults are the most common (fig. 24b). Many of the strike-slip planes are bedding parallel.

In the field, these faults could be observed within the E-W trending vertical bedding of the Bellerophon formation at stop 1.6, that crops out along the river east of Pontebba. The river is located along the Fella-Sava Line, a backthrust that has been re-activated as a dextral strike-slip fault (Nussbaum, 2002), which explains the strong strike-slip character of this area. Here, cm-scale offsets of calcite veins and layer parallel faults with Riedel shears, show dextral strike slip movements (figs. 23f, 24d and 24e). Other structures that formed during this phase are tension gashes (280/78°; fig. 23f) and stylolites (004/82°), which both have their σ_1 axis in the N-S plane. The rocks in this strike-slip zone are brecciated at some locations and smooth mirror planes also occur, indicating severe brittle deformation. This zone is indicated as a major thrust fault on the geological map by Carulli (2006; fig.2) and it is likely that the strike-slip faults are a reactivation of older structures that have become overprinted.

The 'Thrust Zone' at stop 3.1, can also be identified as a strike-slip zone, as most of the faults from this area plot within the Phase D4 stress tensor as well (figs. 23b and 24a); these faults might be (partial) reactivations of

c

older faults. The previously mentioned dextral shear planes that intersect the south vergent asymmetrical folds in the Raibl formation at stop 10.4 (fig. 20) also belong to this phase and must be younger than phase D3. The amount of displacement along these strike-slip faults is usually not more than 10 to 20 cm and have strong dip-slip component as well, defining them as oblique faults.

Sinistral strike-slip faults were also observed, for example in the basinal 8b and 10a formations, in combination with what seems to be a normal fault or another strike-slip fault. (fig. 24g)

The S_0 of the flysch in the southern 'Flysch Zone', which encompasses the Cretaceous formations on the NW and SE side, has an orientation of 312/26° at stop 8.9 in the north and 150/50° at stop 8.3 in the south. This could be interpreted as an approximately 15 km wide anticline, with a SW plunging foldaxis that could be caused by shortening along the σ1 axis of deformation phase D4 (figs. 24a and e). So, in this area, two different anticlines might exist on top of one another; the one that was observed in the Cretaceous outcrop that formed during deformation phase D2 and this younger one.
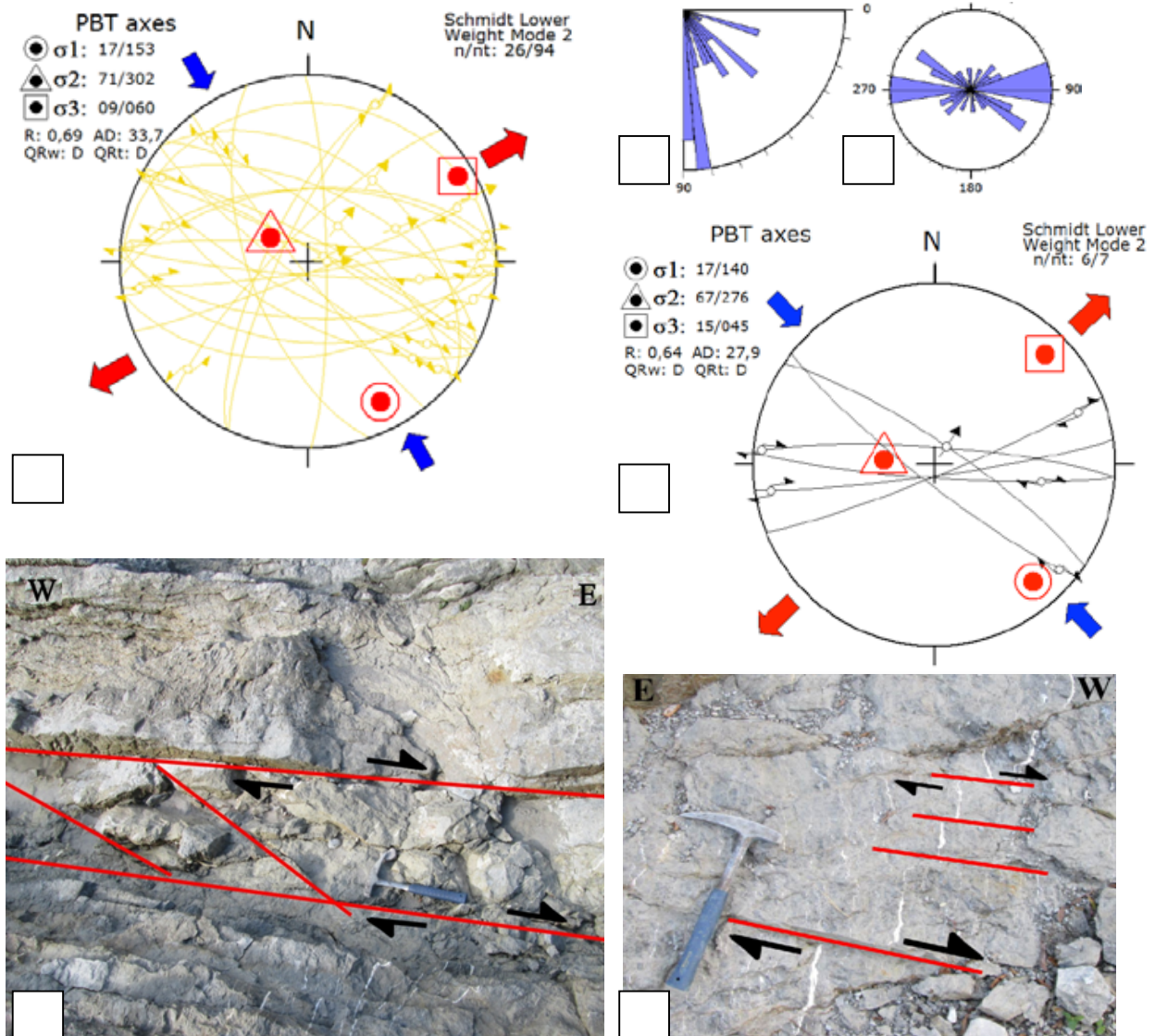
Figure 24. Phase D4.
(a) Stress tensor defining phase D4, creating mostly strike-slip faults. Most of these faults are from stops 3.1 in the Dolomia Principale formation (fig. 23b) and 1.6 (fig. 24e).
(b) Rose diagram for the dip angle of the faults defining phase D4.
(c) Rose diagram for the strike of these faults.
(d) When the 6 faults of stop 1.6 are plotted together, they create almost the same stress tensor as the one created for phase D4 (fig. 24a).
(e) Stop 1.6, east of Pontebba, showing bedding parallel dextral shear, as is indicated by the Riedel shears.
(f) Tension gashes (280/78°) found in the Bellerophon formation at stop 1.6, which have their σ1 axis in the N-S plane and are caused by dextral shearing. They have been cross-cut by dextral shear planes, causing 2-10 cm offsets.

Figure 24 (continued). Phase D4.

(g) Stop 5.3, in the basinal formations of 8b or 10a. A sinistral strike-slip fault (38/44°) is cut by a normal fault (or other strike-slip fault; 358/88°) which is cut again by another sinistral strike-slip fault (108/26°). The sequence is indicated in the figure.

(h) Stops 8.3 and 8.9 encircled in red, where two flysch bedding planes have been measured that could be part of a large scale antiform. The green circles indicate the antiform in the Cretaceous outcrop, that formed during phase D2.

4.3. Cross section

The observed structures and deformation phases described above have resulted in the interpretation of a 54 km long N-S profile (fig. 25). The most important observations from the field were used to construct this profile, such as the orientation of the bedding (S_0), formation type, the younging direction and the location and kinematics of the major fault zones. The black pins at the topography of the profile represents the measurements of the bedding (S_0) at that stop. Only stops located within a radius of 4 km near the profile line were incorporated into the profile. The dip measured at many of the stops had to be corrected first, because their accompanying strikes differed from the strike of the cross section.
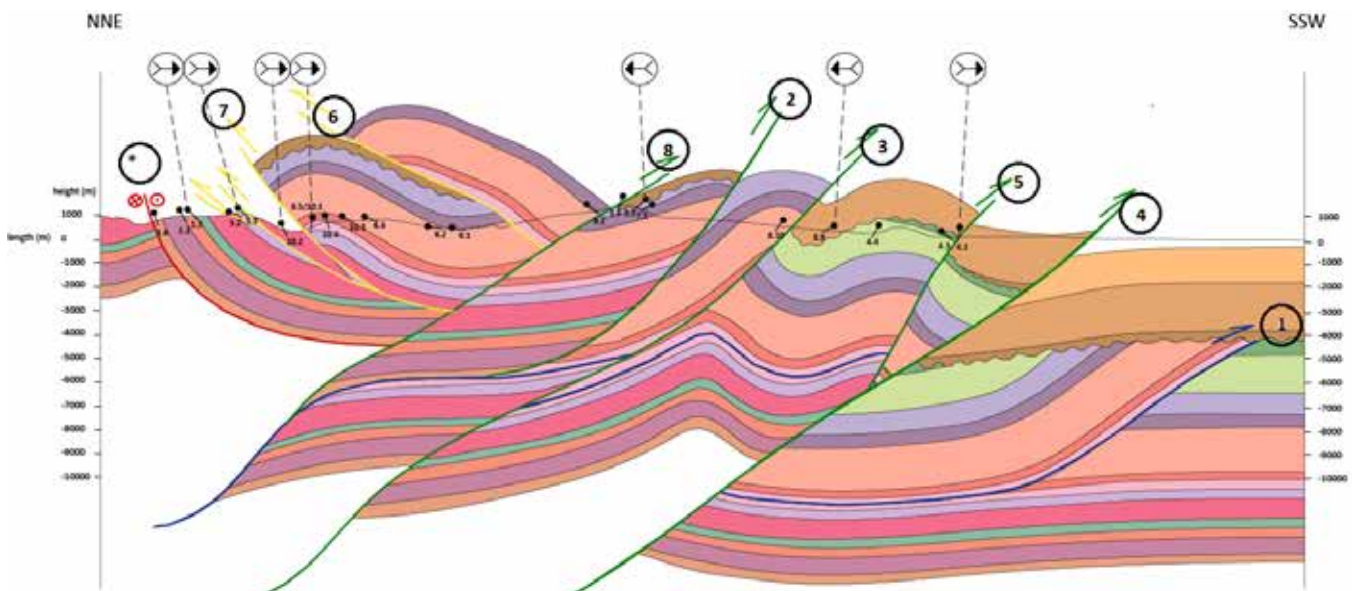
Figure 25 (a). N-S profile of the Eastern Friuli Alps, drawn to scale, legend at the next page (fig. 25b). For location see fig. 2, for the tectonostratigraphic column see fig. 8. The younging directions are indicated with arrows. The different colours of the faults represent different fault "groups" or faults that were active during the same period or have the same characteristics. The encircled numbers show sequence of their formation, which is explained in more detail in chapter 5.
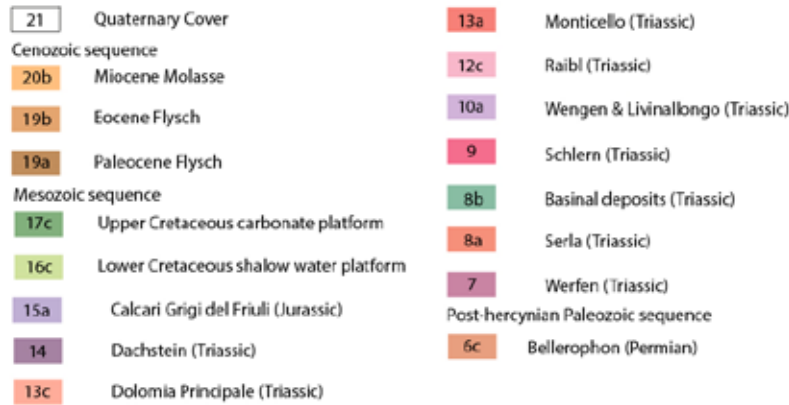
Figure 25 (b). Stratigraphic legend for figure 25a.
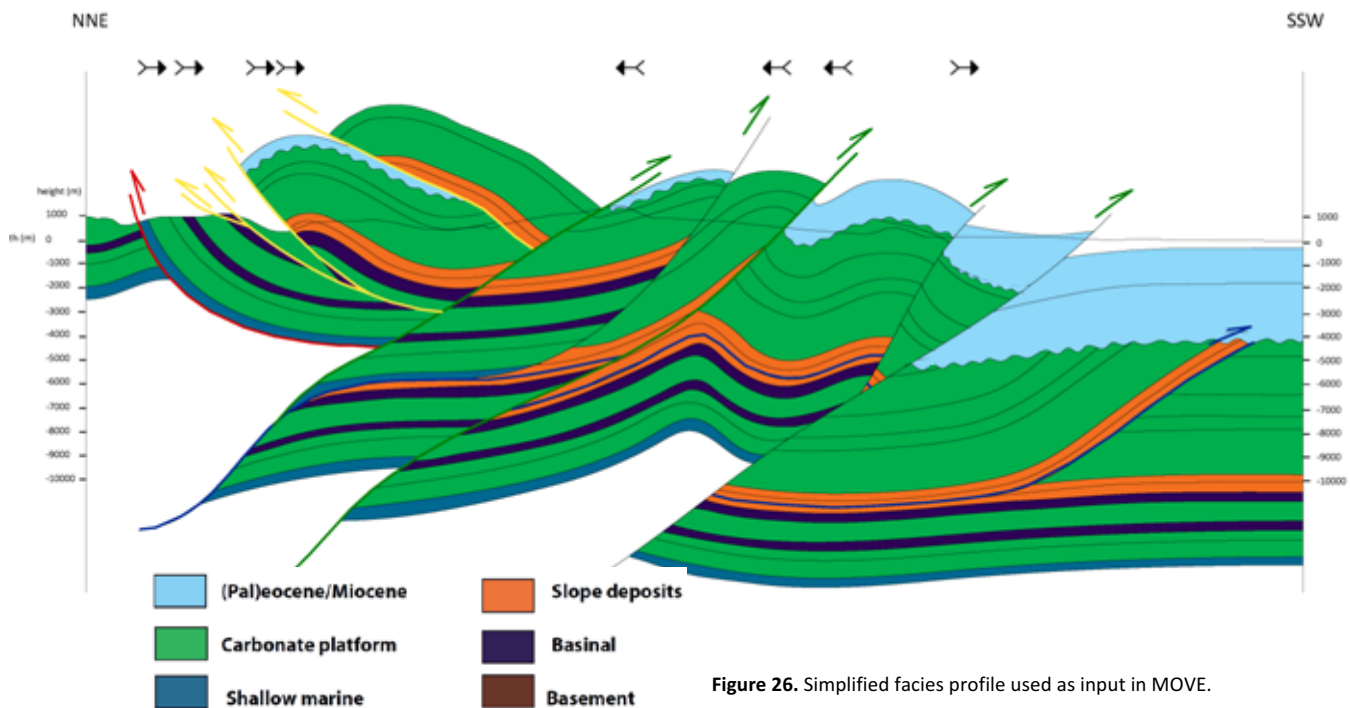
Figure 26. Simplified facies profile used as input in MOVE.

As input for MOVE, a simplified version of this profile has been used, where all formations are shown in terms of their depositional environment (fig. 26; see also fig. 7 for the facies map). The profiles have not been subjected to any vertical exaggeration, as this would have an lead to erroneous geometrical interpretations.

The cross sections show that the base of the Bellerophon (red line) and Raibl (blue line) formations have acted as gliding surfaces for the overlying formations (fig. 25, 26). Both of these formations are soft basinal or shallow marine deposits that caused thin-skinned thrusting that resulted in shortening over long distances. The Raibl formation was mainly the gliding surface between the basement and everything else on top of it. It only crops out along the large reactivated strike-slip fault in the north; the Fella-Sava Line. The only way that such a stratigraphically low formation can crop out at the surface, is when it has been brought up previously during a thrusting event. Which is why the current strike-slip motions measured at stop 1.6 must have completely overprinted older thrusting indicators. There are no field-based constraints for the amount of shortening that occurred along the Bellerophon formation; in theory it could have gone on and on, which is why the red coloured fault line is not continued in both cross sections. This is also the case for the amount of shortening along the Raibl formation, even thought this blue coloured fault line is continued throughout the cross-sections. The shortening distances along these faults that are chosen for the modelling in *MOVE* are arbitrary ones that can be regarded as minimum amounts of shortening. Constraints for these amounts of shortening

might be found in other parts of the Alps, but the relationship between the Friuli Alps and the part of the Alps to the north of this profile are not shown, since the field area was restricted to the Friuli Alps only.

Major thrusts occur at stops 3.2 and 8.10, where the older platform carbonates have been put on much younger flysch. These major thrusts are interpreted as thick-skinned thrusts that also cut through the basement. In the field these thrust could be recognized by the observations of hanging wall anticlines an footwall synclines, in which the formations were often steeply orientated. The thrust in between stops 3.2 and 8.10 is also drawn as a major thrust in the profiles, but no constraints for this fault were found in the field. The same applies to the most frontal thrust that puts the flysch on top of Quaternary sediments in the foreland.

The profile also shows that the Cretaceous carbonates thin out towards the NNE, which is caused by either erosion or an uneven distribution due to rifting, or both. Erosion certainly must have played a role, as the base of the overlying flysch is a major unconformity.

5. Cross section balancing

5.1. MOVE

The simplified cross-section in figure 26 served as the input for *MOVE.* The modelling program was used to create a geometrically valid version of this cross-section, in other words; a balanced cross-section. The input profile proved to be quite accurate, as only small adjustments had to be made during the restoration process to arrive at the final profile in figure 27, which represents the present day configuration.
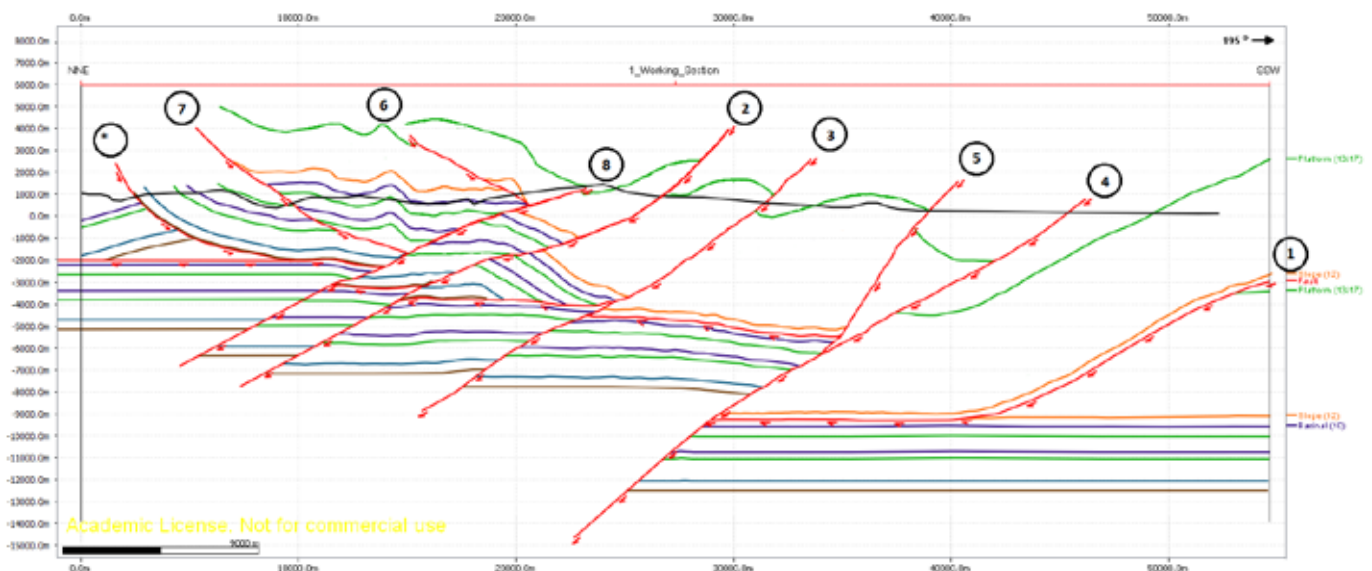
Figure 27. Balanced cross-section in MOVE that represents the present day configuration.

The deformation history could be inferred by restoring the movements along every single fault, one by one, as explained in chapter 3. Because *MOVE* only assumes plane strain, movements in other direction than the plane of the cross-section could not be restored. So, for example strike-slip faults or oblique components of faults could not be modelled. It is also not possible to reactivate a thrust in an opposite direction.

The coloured lines represent the upper boundary of the different facies, derived from the profile in figure 26; so brown is the top of the basement, blue is the top of the shallow marine facies and so on. The top of the most upper carbonate facies layer (in green) does not represent the same type of carbonate formation throughout the profile, as can be concluded by looking at figure 25. This top needed to be simplified, because unconformities could not be modelled in *MOVE.* The faults are all drawn in red and have been numbered from 1 to 8 for identification, according to the order in which they formed (fig. 27).

Below, every single fault restoration stage is shown, starting with stage 0 and ending with the present day configuration (stage 8). These stages are not to be confused with phases D1 to D4 that were derived from the field results in chapter 4.2.
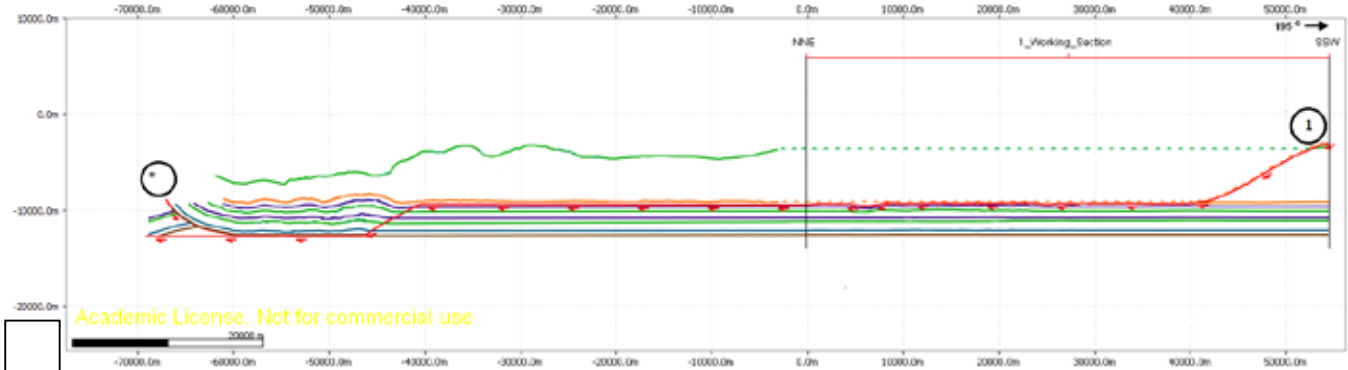
Stage 0: Shortening along the Bellerophon and Raibl formations (thin-skinned thrusting).

During this stage a decollement fault developed within the base of the Bellerophon formation (the brown line), causing all overlying sediments to slide towards the SSW, on top of the basement formations. These basement formations are not drawn in the profiles but are represented by the white 'area' underneath it.

At some point, the decollement fault ramped up and continued along the next "weaker or softer" material of the Raibl formation, creating the first flat-ramp-flat structure. This fault continued untill it ramped up again, this time to continue on top of the Upper Cretaceous formation. This fault has been indicated with a (1). This stage causes the highest amount of shortening in the Friuli Alps and accounts for 57 km of the total shortening.

It is uncertain whether shorting along the remainder of the Bellerophon formation continued as well, but this option is not taken into account for this reconstruction, as no contstraints for this theory were found in the field. Another possiblity is that shortening had already taken place along the entire base of the Bellerophon prior to this stage, but this has also not been taken into account.

The northern side of this profile shows a backthrust along the base of the Bellerophon formation as well, which is indicated with an (*). The relative timing of the formation of this thrust is unknown, as it could not be modelled in MOVE due to a lack of data. The backthrust could have formed during this stage as well, including it in the overall shortening along the Bellerophon formation. It is however more likely that this backthrust formed together with the other backthrusts during one of the thick-skinned stages (stage 6), because they all share the same E-W strike that does not fit with the assumed direction of thin-skinned thrusting.
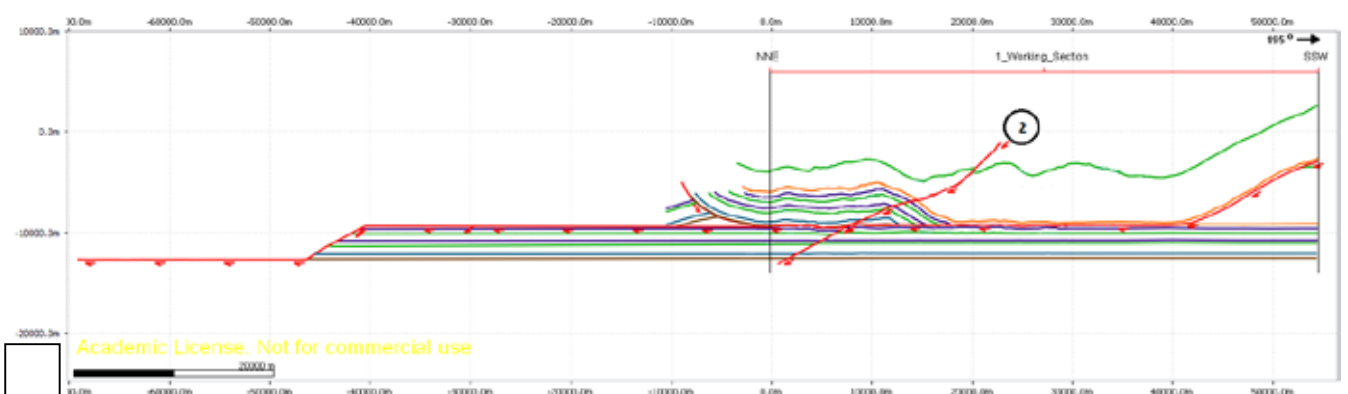
Stage 1: Onset of thick-skinned south vergent thrusting

After a considerable amount of shortening along the two décollement horizons, a south vergent thrust developed that started in the basement (fault no. 2). This thick-skinned thust caused 1.2 km of offset in the Triassic and Jurassic formations.
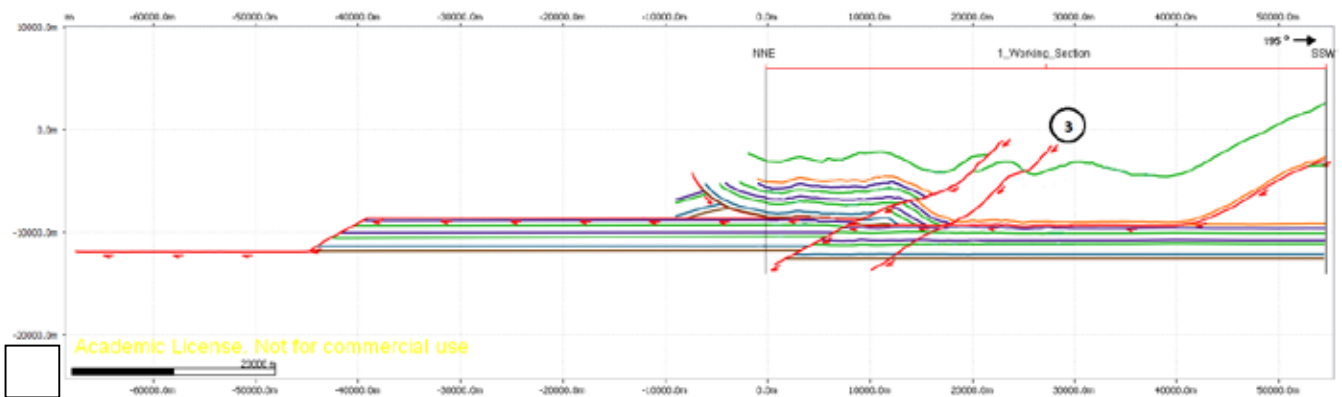
Stage 2: Continuation of thick-skinned south vergent thrusting.

A second thick-skinned south vergent thrust develops in sequence, more towards the south (fault no. 3). This stage causes the formation of hanging wall anticlines and footwall synclines that could be recognised in the field. The offset of 1 km puts the formation of the Dolomia Principale (Triassic) on top of the Eocene Flysch. So the thrust has to be of Eocene age or younger. The flysch is not shown in the *MOVE* reconstruction profiles, because a period of erosion somewhere near the end of the Cretaceous or beginning of the Paleocene, affected these sediments, and erosion could not be modelled in MOVE. The relationship between the flysch and the underlying platform carbonates is shown in figures 25 and 26.
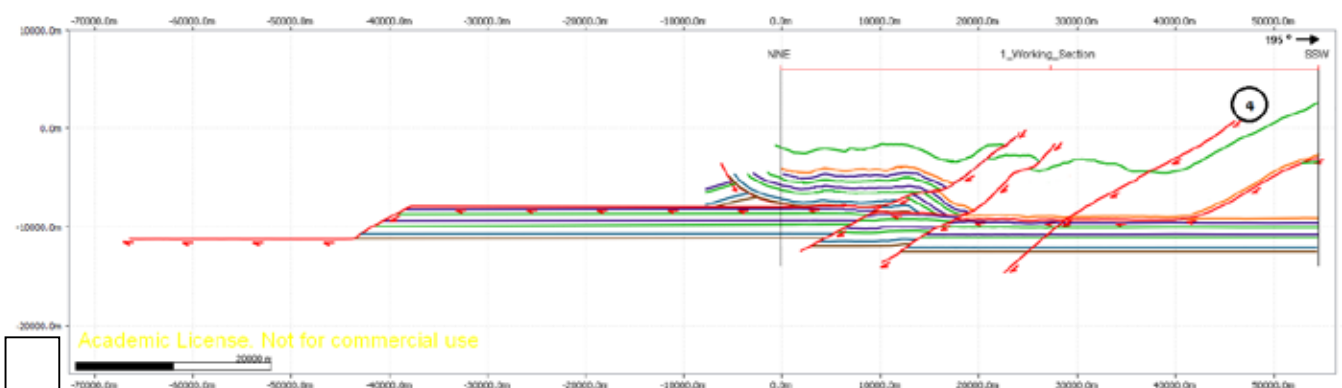
Stage 3: Continuation of thick-skinned south vergent thrusting.

A third thick-skinned south vergent thrust develops in sequence, which will be the frontal thrust in the south to reach the surface (fault no. 4). This thrust is one of the major thrust faults, that causes 4.4 km of offset between the Cretaceous sediments in the hanging wall and the footwall. At greater depth the major offset can also be observed in for example the Bellerophon formation.
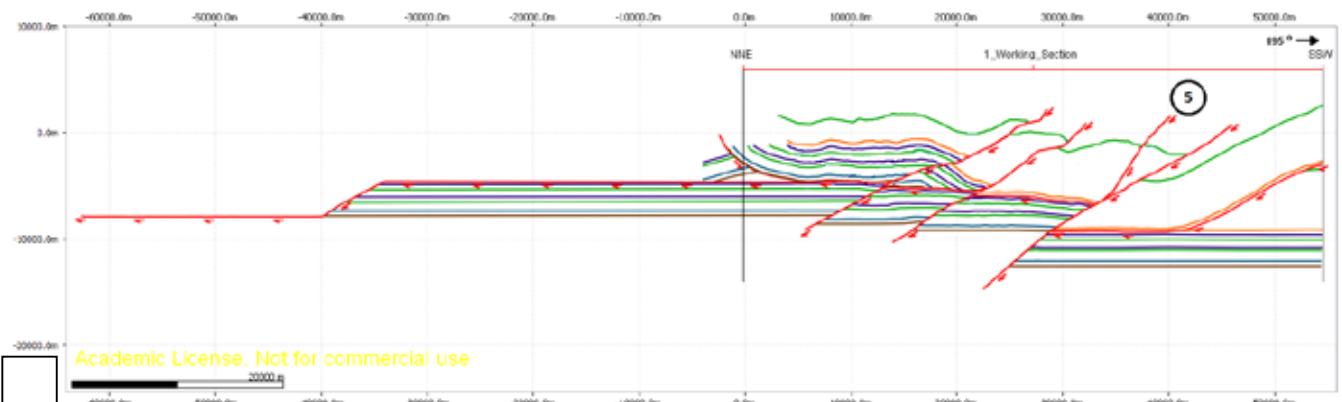
Stage 4: Continuation of thick-skinned south vergent thrusting.

A second branch forms, out of sequence, along the previously formed thrust (fault no. 5). This fault, with 1.6 km offset, causes the antiform that was observed in the field in the Cretaceous formations.
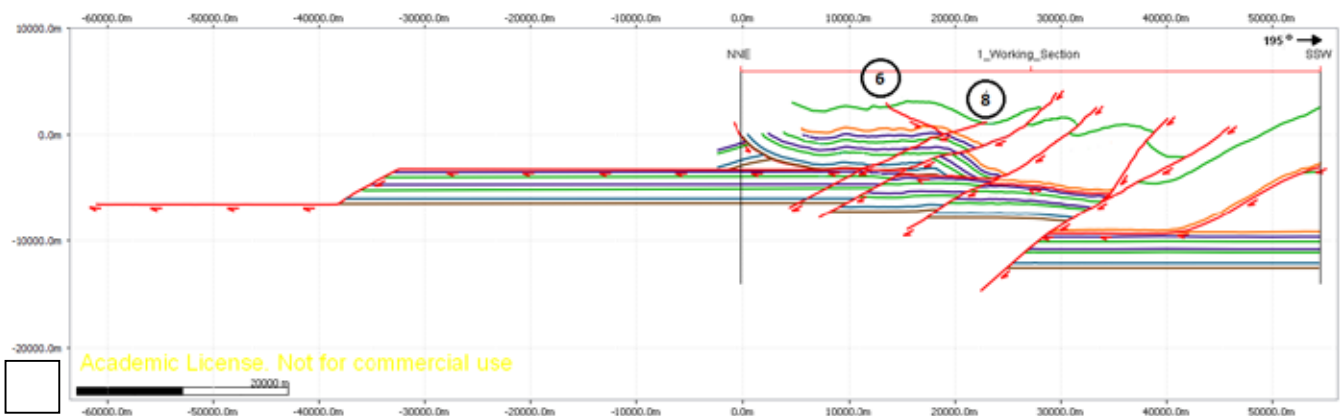
Stage 5: South and north vergent thrusting.

This time an out of sequence thrust is formed more towards the north, but no sifnificant movements occured yet during this stage (fault no. 8). Along a northvergent backthrust that branched off this fault, shortening does take place, causing the formation of a hanging wall anticline and only minor offset (0.6 km)in the Dolomia Principale formation (fault no. 6). The fault only seems to affect the wedge shaped part in the hanging wall, creating a pop-up structure and does not cut trough the south vergent thrust of which it branched off.
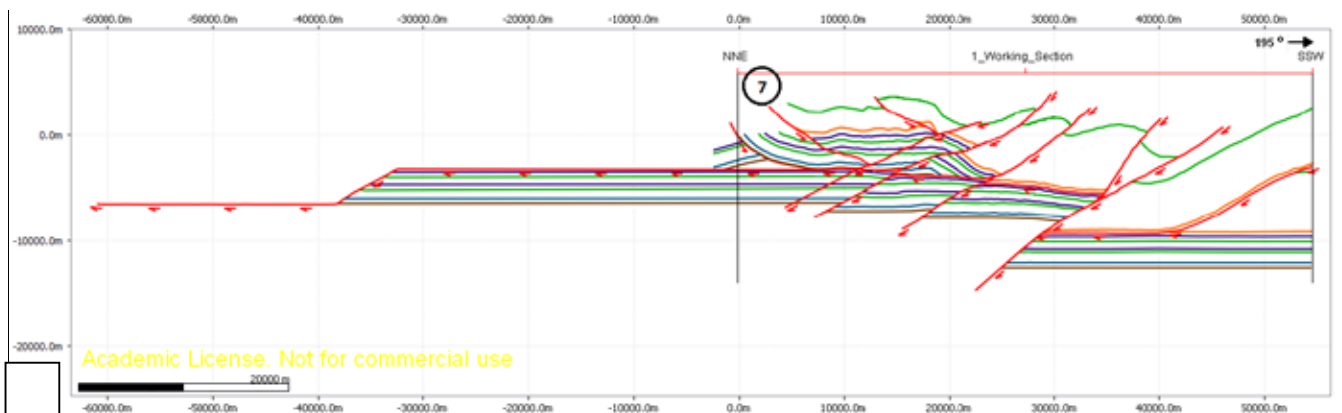
Stage 6: North vergent thrusting.

A second north verging thrust branches off the same south vergent thrust, causing little offset as well (fault no. 7, only 0.6 km). It is more likely that the north vergent backthrust that causes the offset in the Bellerophon is formed during this stage instead of stage 0, as the Bellerophon is an already weakend layer.
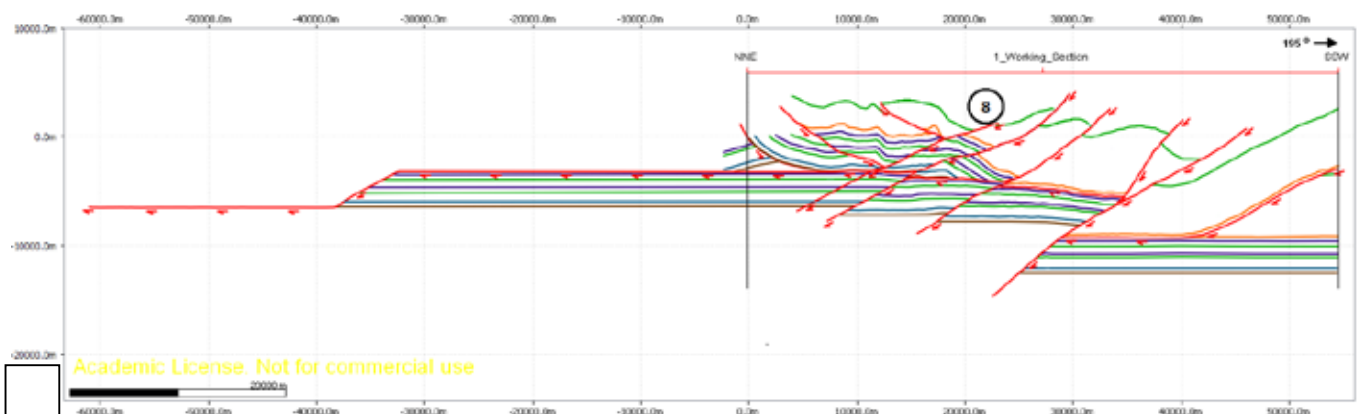
Stage 7: South vergent thrusting.

The already existing south vergent thrust no. 8 that did not cause any significant movements during the previous stages is reactivated again. This causes 2 km of offset in the formations at depth, but at the surface this influence becomes smaller because it partially cancels out the displacements caused by the older north vergent backthrusts.
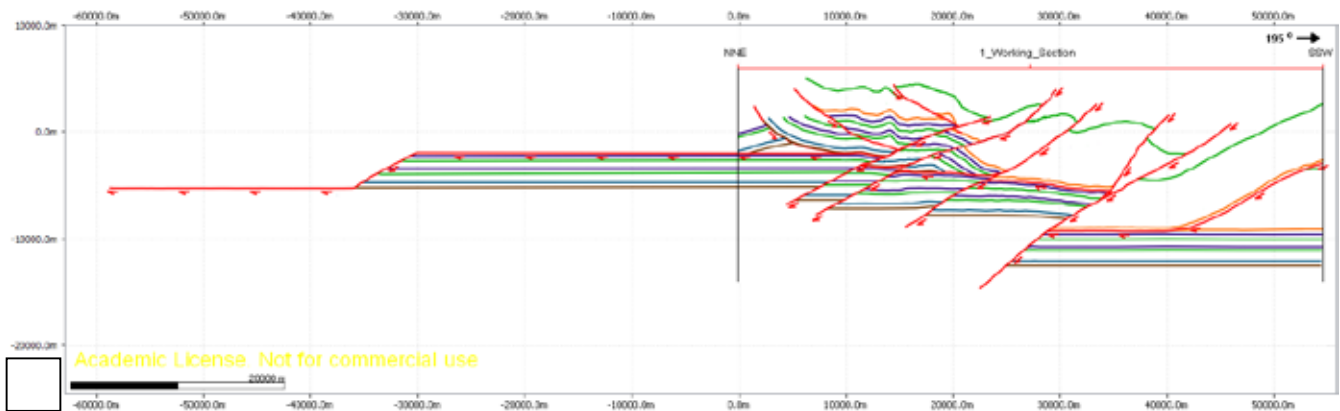
Stage 8: Present day configuration.

The final stage shows the present day configuration as a result of the restaurations in *MOVE*. The profile in this figure (and its enlarged version in figure 27) is slightly different from the hand-drawn profile that was solely based on field observations (fig. 25). The main differences are:

- The doubled continuation of the older and deeper formations (Bellerophon to Raibl) towards the north that was needed to show the flat-ramp-flat structure in these formations.
- This ramp-flat structure also resulted in the occurrence of these same older and deeper formations in the upper fault block between faults nos. 2 and 3.
- The absence of extra north vergent backthrusts that branch off of backthrust no. 7 for simplicity.
- The absence of erosional features, because this could not be modelled. Because of this, no formations overlying the erosional horizon could be shown either (the Eocene flysch and Neogene molasses etc.).
- The deeper formations have remained in an almost horizontal position, which was not the case in the original input profile.

The thinning of the Cretaceous formations towards the north is not really clear because these layers have been taken together with the Jurassic and Triassic layers for simplicity.

5.2. The amount of shortening in the Friuli Alps

As mentioned previously, the thin-skinned flat-ramp-flat detachment faulting in the Bellerophon and Raibl formations caused the most shortening in the Friuli Alps, accounting for 57 km of shortening. During the subsequent stages of thick-skinned thrusting an additional 11 km of shortening was added to this amount, resulting in a total 68 km of shortening. This amount must be considered as a minimum amount, as there were no constraints of the amount of shortening along the Bellerophon and Raibl formations. As these formations were involved in the biggest part of the shortening, due to their ability of facilitating thin-skinned tectonics, the amount of actual shortening within the Friuli Alps might be a lot higher.

6. Discussion

6.1. Interpretation of field data and cross section balancing

The main objective of this study was to reconstruct the structural and paleo-geographical evolution of the Friuli Alps. Crucial information on this could be obtained from a detailed understanding of the interfering tectonics in this area. Special interest went out to the occurring lithology in the project region that consisted of an alternation of 'soft' basinal and 'rigid' platform carbonate formations. These softer formations were expected to behave as décollement surfaces that would facilitate thin-skinned tectonics.

The balanced profile in *MOVE* (chapter 5) shows that a first phase of thin-skinned tectonics and subsequently a phase of thick-skinned tectonics in the Friuli Alps is indeed geometrically correct and fits with the structural and kinematical surface data. The profile also shows that the occurring lithology has been of great influence on these types of regional tectonics.

The field results and the results from the *MOVE* reconstruction are combined and discussed below, in order to arrive at a complete interpretation of the geological evolution of the area.

6.1.1. *Extension (>90 Ma)*

The mostly steep dipping normal faults that characterize this first N-S extensional phase (D1) are not well spread in the study area, making it hard to assign them to a certain time frame due to a lack of interference structures (see also section 4.2.1). Most normal faults were observed in the carbonate platforms of the Monticello and Dolomia Principale formations. Considering the regional geology of the area, it is likely to assume that the normal faults are associated with the Jurassic or Triassic rifting. The more incompetent flysch layers also recorded two separate phases of normal faulting, but these structures are probably local accommodation structures (caused for example by hinge collapse), which do not reflect large-scale extension. The small amounts of normal faults in the area and their relatively small offsets can be attributed to the reactivation of these faults during subsequent phases. The extensional phase (D1) was not incorporated into *MOVE* due to the lack of sufficient data.

6.1.2. *Erosion (±80 Ma)*

Several phases of erosion must have affected the area during the evolution of the Friuli Alps. The most striking of these phases is the one that accounts for the unconformities shown in the profiles (figs. 25 and 26) and the stratigraphic column (fig. 8), which must have taken place prior to the thin- and thick-skinned tectonic phases. This erosional phase was not taken into account in the reconstruction of the balanced profile, because it could not be modelled in *MOVE*.

At some locations more towards the north (stops 3.2 and 3.3) the erosion had to be substantial, because Upper Cretaceous/Paleocene flysch (formation 19a) was deposited right on top of Lower Jurassic carbonate platforms (formation 15a). This large hiatus was aided by the nature of the Cretaceous limestones (formations 16c and 17c) that were probably never deposited here, because they consisted mainly of reef limestones built locally by stromatolites and rudists (Nussbaum, 2002). At places where no reefs developed, stratigraphically low formations were subjected to erosion. The division of the area into several basins and heights during the Triassic and Jurassic rifting phases also supported this uneven distribution, as the reef carbonates mainly developed in relatively shallow areas.

The Upper Cretaceous/Paleocene flysch does not seem to be affected by this phase of erosion, thus the onset of this major erosional phase must have occurred approximately around 80 Ma. Nussbaum (2002) also recognised this hiatus (between 90 and 80 Ma). However, the Cretaceous/Paleocene flysch is considered as a transgressively deposited formation by Nussbaum (2002), which did not get deposited throughout the entire area. This explains why it absent in the "Southern Flysch Zone", where only younger flysch has been deposited. In the profiles and stratigraphic column described in this report, these two periods of erosion and non-deposition are not clearly separated.

6.1.3. *Thin-skinned tectonics (60 - 30 Ma)*

Dinaridic Orogeny (Paleogene)

The balanced profiles confirm that the Friuli Alps were first subjected to thin-skinned tectonics during stage 0, which did not involve any deformation of the basement rocks and was accommodated along the weaker décollement horizons of the Bellerophon (marls and in the West Friuli area also gypsum) and Raibl formations (marls). The thin-skinned tectonics are characterised by flat-ramp-flat geometries, associated fault-bend folds in the handing wall (an antiform-synform pair) and low angle faults which can be recognised in figure 27 and the profiles belonging to stages (0) and (1). The detachment faults ramp up towards the SSW, which is the direction of tectonic transport. The creation of a ramp usually happens at a location where the current detachment surface starts to gain in strength due to the deformation (strain hardening; Fossen, 2010). They cut

through the overlying beds and continue along another stratigraphically higher 'weak' layer; creating multiple layers along which shortening can take place. Thin-skinned tectonics typically cause great amounts of horizontal displacement, with relatively little vertical displacement.

In the reconstructed profiles, most of the detachment faults do not really crop out at the surface in this area, making it hard to say anything about the true direction and amount of displacement along these faults. The backthrust in the north along the Bellerophon formation does surface (in red in fig. 25), but is not completely representative as it is not certain that this part of the formation also used to be part of the décollement surface before it was activated as a backthrust. And even if it was part of the décollement, most features are likely to have become overprinted by subsequent backthrusting and strike-slip faulting. No information can be obtained from the most frontal part of the detachment fault in the south as well, as it does not surface within the range of this cross-section.

Even though no constraints were found in the field on these thin-skinned thrusts indicated in the profiles, they were introduced in this reconstruction in order to arrive at a greater amount of shortening compared to a geological history where only thick-skinned thrusting would occur. The idea that these formations facilitated thin-skinned thrusting comes from studies by Nussbaum (2002) and Doglioni (1985 and 1987) and from observations at locations where the softer formations did crop out in the field, even though these horizons are not indicated as décollements in the profiles. This included not only outcrops in the Bellerophon formation at stop 1.6, but also in the Raibl formation at stops 6.5, 10.1 and 10.4, and the basinal formations 8b and 10a at stops 2.3 and 5.3. It seemed like these formations had experienced far more deformation than the platform carbonates, which was indicated by several features such as the accommodation of high amounts of internal shearing in less competent layers (fragmented material, small scale parasitic folds and calcite steps), a near vertical orientation of the bedding and the occurrence of mirror planes and severe asymmetric folding. These features suggest a kind of detachment folding that was caused by thin-skinned tectonics (fig. 28).

In the profile in figure 25, these locations are indicated in yellow as north vergent backthrusts, that developed during a later stage in the evolution of the Friuli Alps (see chapter 5). It is possible that these backthrusts were not only indicative for detachment faulting along the same formations at depth, but also that they were actually reactivations of another detachment fault set along these layers. This option was not included in the balanced reconstruction because reactivations in different directions could not be modelled in *MOVE,* but if this extra décollement set was also active during the thin-skinned phase (D2), it could have accounted for an even larger total amount of shortening than is indicated by the reconstruction in this report.

Furthermore, as is also mentioned previously, the amounts of shortening along the Bellerophon and Raibl formations are not constrained by any field indicators. It is for example unknown whether the Bellerophon formation continued to be a detachment surface towards the south as well, after it formed a ramp towards the Raibl formation, or whether a preceding phase of detachment faulting along the entire Bellerophon had occurred before phase 0. So the 57 km of thin-skinned shortening can be considered as a minimum amount.

Nussbaum (2002) and Doglioni (1985; 1987) both related the thin-skinned tectonics with décollements in the Bellerophon and Raibl formations, which were observed in the Friuli area and Dolomites respectively, to the Paleogene Dinaridic orogeny. This, because of their (N)NW-(S)SE strikes that correspond to the features described in this report for deformation phase D2 (see section 4.2.2.) and because they were cross-cut by younger E-W striking structures that belonged to the subsequent Alpine phase (N-S directed shortening belonging do deformation phase D3, see section 4.2.3.).

The onset of the Dinaridic orogeny is marked by the deposition of the Dinaridic syn-orogenic flysch that is said to be of Thanetian age (Upper Paleocene; Cousin (1981), formation 19b; Carulli (2006)). From the field data, it can be concluded that the Eocene flysch (formation 19b) in the "Southern Flysch Zone", was affected by Dinaridic NNE-SSW shortening. This means that the thin-skinned thrusts related to this phase (D2) were active between 60 and 30 Ma.

The Dinaridic folds and faults observed in the field, as described in section 4.2.2., did not seem to be an obvious result of thin-skinned tectonics. However, the offsets they created were also not very large, so they did not indicate thick-skinned tectonics either. Some Dinaridic structures were discovered in the northern half of the

Eastern Dinarides (stops 6.5/10.1 and 9.2), indicating that the influences of this mountain chain reaches further than might be expected from the geological maps by for example Carulli (2002). However, most of the structures belonging to this phase (D2) were observed in the "Southern Flysch Zone", were mainly Dinaridic flysch (and Cretaceous limestones) was exposed. This flysch thins towards the SSW, perpendicular to the strike of the Dinarides, as the foreland basin associated with this mountain chain becomes shallower (Schonborn, 1999), even though this seems to be the opposite in figure 25. The deposition of the Dinaridic flysch and the associated thin-skinned tectonics lasted until the mid-Eocene (Nussbaum, 2002).

Figure 28. Detachment folding in the weak Raibl formation at stop 10.4, with smaller scale parasitic folds. The base of this formation acted as a detachment surface. The fault at this location is indicated as a backthrust in figures 25 to 27, but this backthrust might have been a reactivation of a former thin-skinned detachment fault (D2). Evidence of this reactivation is that the folds within this area have a roughly east-west oriented axis that fits better within the N-S shortening thick-skinned phase (D3). It is also possible that these folds are not related to detachment faulting at all, but only shows that the Raibl formation at depth could have been a detachment surface.

6.1.4. Thick-skinned tectonics (23 Ma)

Alpine Orogeny (Neogene)

It can be inferred from the balanced profile that the thin-skinned tectonics phase was followed up by a phase of thick skinned tectonics (stage 1 to 7). During this type of deformation, steeply dipping thrusts were created that cut trough all formations and previously formed décollements, involving the basement as well. Shortening occurred along a N-S axis, that is described as deformation phase D3 in section 4.2.3. The thick-skinned thrusts cause significant vertical offsets, as can be noticed in the profiles, but not so much horizontal displacement, resulting in a smaller amount of overall shortening for this phase. It is very likely that the thrust faults belonging to this phase (D3) are all splays of one or two basal thrusts, located at depth, that originated in the brittle-ductile transition zone.

At the surface, the thick-skinned thrusting could be recognised by three different features:
- The occurrence of wide brittle thrust zones.
- Tilting of the bedding to an almost vertical position due to the formation of hanging wall anticlines and footwall synclines caused by drag along the fault plane.
- The observation of stratigraphically older formation on top of younger formations, caused by large scale vertical offsets.

Wide brittle thrust zones were found in the northern half of the eastern Friuli region, at stops 1.6, 3.1 and 10.2/10.7. The 20 to 60 m wide zones consisted of brecciated rocks, indicating a significant amount of

deformation along large scale structures. The shallowly inclined contact surface between these zones and the unaffected formations found on top of it, indicates thrusting. Carulli (2006) identified most of these zones as north vergent thrusts and evidence for this direction of thrusting was also found in the field, except at stop 1.6. It is however likely that this backthrust also belonged to this phase, as they all share the same strike. Evidence for reactivations of these zones as strike-slip zones during a subsequent phase (D4) was also encountered at these locations.

Vertical tilting of the bedding was mostly observed in the softer formations, such as the Bellerophon, Raibl and basinal (8b, 10a) formations in the north and the flysch formations in the south. As large scale tilting could be caused by the formation of hanging wall anticlines and footwall synclines related to thrusting, these observations were indicative for the occurrence of large scale thrusts in the vicinity.

As was mentioned in the previous section, the vertical dip orientation of the Bellerophon, Raibl and basinal formations could already have been initiated during the previous phase of thin-skinned tectonics (D2). It is however likely that these weak formations (also) accommodated further deformation during the thick-skinned phase (D3), which is confirmed by the mainly south and north verging asymmetrical folds occurring in their less competent layers, which fits within the N-S shortening regime of this phase. The change in vergence is most likely caused because these folds are small wavelength parasitic folds that are part of a much larger (km scale) folding phase (fig.29). The formation of these parasitic folds is usually caused by the different bed thicknesses of the affected formations.
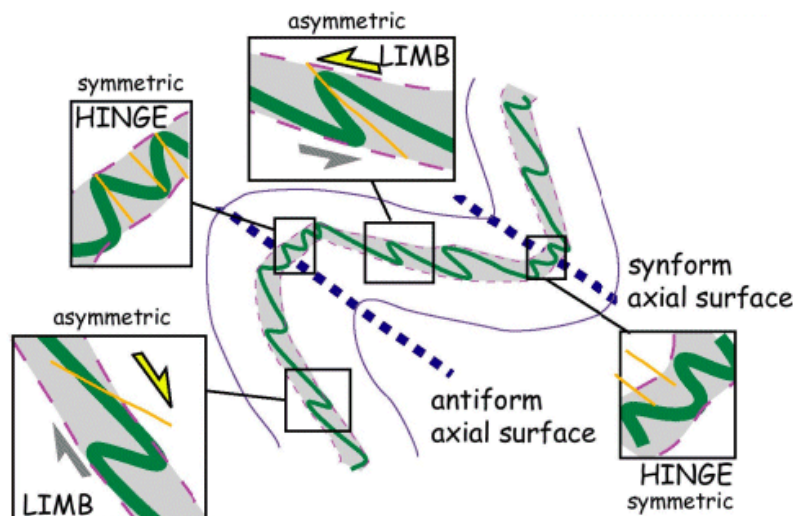
Figure 29. Image of the University of Leeds, that shows how asymmetric small scale parasitic folds with opposite vergences can be part of the same large scale folding phase. In this case that would be a phase of km-scale folding due to N-S shortening (D3) .

The main direction of transport in the north during this thick-skinned phase (D3) remains towards the north, resulting in backthrusts that most likely overprinted all potential former kinematic indicators. The backthrusts themselves are actually no thick-skinned thrusts, as they have no influence on the underlying basement. They might have formed as a consequence of the formation of fault no. 8, which is a thick skinned thrust.

However, within the vertical oriented flysch in the southern part of the area, mainly south vergent features were observed, such as for example the smaller scale thrusts and kink-bands at stop 3.3. This stop is also located in the valley where older Triassic/Jurassic limestones were found at a topographically higher point than the younger flysch, indicating large scale thrusting (fig. 23c). Although the Paleocene and Eocene flysch are also partially composed of less competent layers, just like the Bellerophon, Raibl and basinal formations, they did not display as many intense deformation features (asymmetric folding, internal shearing). This indicates that the flysch was subjected to less deformation related only to thick-skinned thrusting, while the other formations experienced indeed both tectonic regimes.

Two south vergent thrusts (faults 2 and 4 in fig. 27) lacked clear field data constraints, but were inferred from the geological map, as thrusts are the only structures that can put older formations on top of younger formations. The most frontal thrust is for example responsible for a large amount of vertical displacement as it puts Eocene flysch on top of Quaternary sediments.

The south vergent thrusts are the most pronounced deformation features of the area, which lead to the characterization of the Southern Alps as a south vergent fold and thrust belt. All these major thrusts are interpreted as thick-skinned and fit within the N-S shortening regime related to the Alpine orogeny (deformation phase D3), that started in the Neogene. This is reflected in the profiles, in which the thrusts cut trough molasses of Upper Oligocene and Miocene age. The most frontal thrusts even affects Quaternary sediments, so stages 3 to 7 must show really recent stages, assuming the order of thrusting presented in fig. 27. Recent activity along this fault is also confirmed by the presence of focal mechanisms of some major earthquakes on this fault in 1976 (Bressan, 2009; Nussbaum, 2002).

The order of thrusting was chosen because it would first lead to the formation of the typical south vergent thrusts and then to the formation of north vergent backthrusts, when deformation could no longer be accommodated along the south vergent thrusts. This requires however an extra out of sequence thrust (no. 8). Considering this unnatural out of sequence thrust and the involvement of Quaternary sediments and recent seismicity in the frontal thrust, it might have been more logical to put thrust no.4 at the end of the sequence.

In the *MOVE* reconstruction, the thick-skinned thrusting did not take any drag into account along the thrust faults, which is why the sections at depth have remained horizontal compared to the original input profile (fig. 25). It is more likely that drag did occur in reality, especially at depth where deformation is expected to behave more ductile. This absence of drag is also the reason why the top of the carbonate platforms in the initial state profile (stage 0) is slightly irregular. Prior to any deformation, the top of the carbonates should actually decrease gradually towards the north where no Cretaceous limestones were deposited, but it was left irregular intentionally to be able to arrive at the hanging wall anticlines and footwall synclines in the present state, that are normally caused by drag along the faults.

In the research area, which only comprises the eastern half of the Friuli Alps, no outcrops of Miocene molasses were found. Although field evidence is absent, these formations were included in the subsurface of the foreland based on the profiles on the geological map by Carulli (2006). According to literature, molasse sediments were mostly deposited in the Veneto basin, of which outcrops can be found to the SW of the area of interest. This basin used to be part of both the Dinaridic and Alpine foreland basins and contains conglomerates of which the deposition marks the onset of Alpine uplift (Nussbaum, 2002). Viaggi and Venturini (1995) dated these conglomerates as Messinian.

6.1.5. *Dextral transpression (<8 Ma)*

The ongoing convergence between the African and European plates and the counter clockwise rotation of the Adriatic plate are not only accommodated along thrust faults in the Friuli area, as mentioned in the previous section. It is for example also integrated in large strike-slip faults such as the Periadriatic Fault. Smaller scale strike-slip faults were also observed in the research area, which are most likely linked to these bigger structures. These strike-slip motions mark the youngest deformation phase (D4), as they crosscut most other geological structures in the field. The recent seismicity on the youngest thrust faults indicate a slight overlap between these last two phases.

Only one strike-slip fault is shown in figure 25 at stop 1.6 in the Bellerophon formation. This fault is an important one, as it is a large scale structure that is easily recognised in the field. In reality other strike-slip faults were also observed near stops 3.1, 6.2 and 10.7, which were left out of the profile for simplicity and because strike-slip motions perpendicular to the strike of the profile could not be modelled in *MOVE*.

Most of these strike-slip faults are indicated as thrusts on geological maps (Carulli, 2006; appendix A). This is because these faults used to be thrusts during the N-S shortening/Alpine phase (D3), but have been reactivated as strike-slip faults during this younger phase (D4). Evidence for the overall strike-slip motions within these big fault zones can be found in the many smaller scale shear planes with different directions of movement and the completely brecciated material. At these locations, mirrorplanes were often found as well, which indicate a significant amount of deformation (fig. 30).

Figure 30. Strike-slip zone at stop 10.7, in the carbonate ramp deposits of the Monticello formation. The fault zone is large, 20 to 30m wide, just as at stop 3.1, and comprises cataclastic limestones with many small scale faults in multiple directions. The shear planes have been indicated in pink and the striae in purple. Directional shear sense indicators such as calcite steps were absent. The two largest planes were smoothly polished (mirrorplanes).

The dextral E-W trending strike-slip that can be observed at stop 1.6 is a good field example of the stresses that are at work during this youngest phase (figs. 23f and 24d, see also the stress tensor in fig. 24a).

The area surrounding this location is part of the Fella-Sava Line, which is a large scale north vergent backthrust that has been reactivated as a transpressive dextral strike-slip fault (Nussbaum, 2002; Merlini et al. cited in Bressan, 2009). Towards the west, the Line continues as a south vergent thrust (see appendix A and Engelen, 2016), which eventually braches onto a large south directed thrust within a megaflower structure that is called the Valsugana Line (Bosselini and Doglioni, 1986). Both the Fella-Sava Line and the Valsugana Line are linked to the dextral transpressive Periadriatic Fault. Bressan (2009) also confirms this NW-SE/NNW-SSE oriented contractional strain to the west of the area of interest, while deformation to the east of the Fella-Sava Line was mostly accommodated along dextral strike-slip faults as well. N-S shortening remains the most prevalent in the area south of the Fella-Sava Line where no indication for strike-slip movements were found.
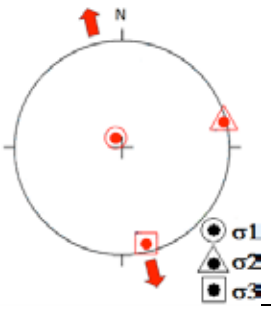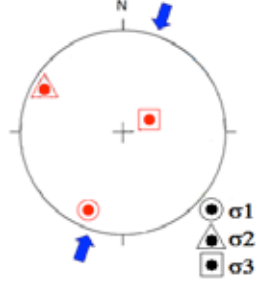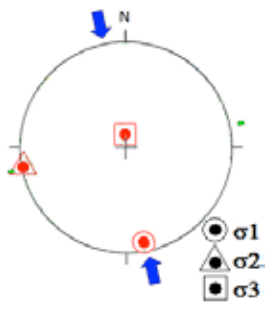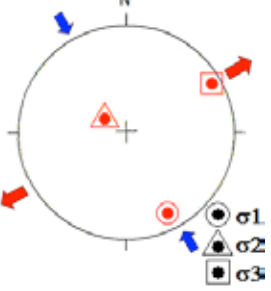
Only relative time constraints on the youngest phase were obtained from the field results. Venturini and Carulli (2002) related strike-slip structures observed in the central Friuli area (near Venzone) to Pliocene NW-SE shortening of pre-existing E-W striking structures (5 Ma). Venturini (cited in Bressan, 2009) noted that this was also the force behind the transpressive reactivation of the E-W oriented Fella-Sava backthrust.

Fodor et al. (1998) arrived at 30-40 km of dextral displacement along the Fella-Sava fault in NW Slovenia, based on the displacement of Oligocene and Triassic rocks. Bartel et al. (2014b) suggests that the offset along this fault could not have been more than 20 km. Bressan (2009) notes that recent seismicity did occur along this fault, however with a small magnitude. Tiberi et al. (2012) linked at least one large historical earthquake to this fault, that occurred in 1348.

As the Fella-Sava Line is related to the Valsugana Line and the Periadriatic Fault, absolute timing could also be inferred from these structures. The earliest activities along the Periadriatic Fault are reflected by Oligocene intrusions (Fodor, 2008). Structures that indicated actual dextral transpression along this fault, were dated as early Miocene (24-17 Ma) by Fodor (1998). Venzo (cited in Bosselini and Doglioni, 1986) noticed that the youngest sediments involved in the Valsugana thrust are of Tortonian age (10 Ma).

Based on the previous information, the period from the Late Miocene to the early Pliocene qualifies as the most suitable moment for the onset of the dextral transpressional phase in this area, which is still active today.

Deformation phase	Tensor	Main features	Timing
D1	N-S extension	E-W striking normal faults with relatively small offsets (1-6 m) and steep dips. Most faults are likely (partially) overprinted by younger faults.	> 90 Ma Late Cretaceous or older
*		Erosion and irregular deposition of Cretacous limestones and Upper Cretacous/Paleocene flysch.	±80 Ma - 60 Ma
D2	NNE-SSW shortening	(S)SW verging thrust faults and NW or SE plunging fold axes. Faults can be several meters long, without clear offset. Fold size varies between 2 m and 1.5 km. Most of these structures were observed in the "Southern Flysch Zone", located close to the Dinaridic Chain. **Thin-skinned tectonics**, interpreted as Dinaridic structures.	60 - 30 Ma
D3	N-S shortening	WNW/ENE plunging fold axes, small scale asymmetrical folding towards the north and south, with considerable amounts of bedding parallel slip in the softer facies and large scale north- or southward thrusting in the more rigid facies. Fault dip angels vary. S_1 foliations with an E-W to SW-NE oriented strike. Occurrence of tension gashes and stylolites. **Thick-skinned tectonics**, interpreted as Alpine structures.	23 Ma - recent
D4	E-W to ENE-WSW transpression	Dextral E-W to ENE-WSW trending strike-slip faults, with a shortening component along the NNW-SSE axis. The dip angle of the faults vary, but steeply dipping faults are the most common. The strike-slip faults might be reactivations of older thrusts. The majority of strike-slip faults was found at stops 1.6 and 3.1. Possible anticline within the flysch, in the "Southern Flysch Zone".	8 Ma - recent

Table 1. Summary of the four different deformation phases of the Eastern Friuli Alps, based on field observations and MOVE interpretation.

The summarised deformation history in table 1 and figure 31 (right image) largely agrees with the paleostress reconstructions of the Friuli region by Castellarin and Cantelli (2000, see fig. 9) and Bartel et al. (2014a, see fig. 31, left image). All three studies show a shift of approximately 90° for the orientation of the principal stress axis: NE-SW to NW-SE. The difference between the results from this study and the one by Castellarin and Cantelli (2010), is that the latter shows a wider range of Dinaridic trend (N55°-N25°, fig. 9). They also suggest

that the Alpine phase is shorter lived, being active between 14 and 7 Ma only. Bartel et al. (2014a) proposes that NE-SW Dinaridic shortening started much later, during Late Oligocene times (24 Ma), resulting in a later onset of Alpine N-S shortening as well (around 16 Ma). Bartel et al. (2014a) also introduces a N-S and a NW-SE shortening phase before the Dinaridic phase.
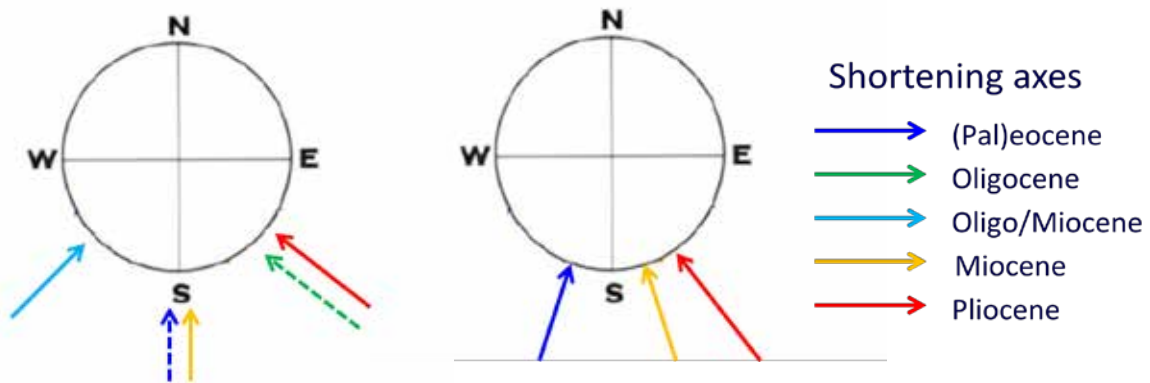
Figure 31. Paleostress comparison to other studies.
On the left: Paleostress reconstruction by Bartel et al (2014a) largely agrees with the one constructed by Castellarin and Cantelli (2000, see fig. 9) and with the one presented in this study (**on the right**). The colored arrows represent the direction of shortening at different time periods.

6.2. Separation of Dinaridic and Alpine structures

In the field, Dinaridic and Alpine structures could be distinguished from one another by their differences in orientation, even though Alpine N-S vergent structures were far more abundant than the Dinaridic SW vergent ones.

The separation of both structures in the cross-section was far more difficult. This was caused, first of all, by the strike of the cross-section. Normally, balanced cross-sections are constructed parallel to the main transport direction, because it assumes plane strain and conservation of area (no movement outside of the section plane). This means that one straight section cannot properly represent two phases with a different transport direction. This shortcoming was supposed to be remedied by the slight angle of the profile to the SSW, which was increased even more towards the SW in the most southern part of the section. Unfortunately, this led to a profile that was maybe even harder to interpret correctly, as neither the pure N-S vergent structures as the SW vergent structures could be properly displayed. Nevertheless, the profiles serve well to explain the overall geological structure of the area, but there is always some sort of distortion of the true direction and amount of movement.

The second difficulty was the possibility of complete overprinting of Dinaridic structures by Alpine ones. No clear evidence for the relation between Dinaridic structures and thin-skinned tectonics was observed in the field, because the structures related to possible thin-skinned tectonics were found in the softer facies that facilitated backthrusting as well, causing overprinting of all possible indications for Dinaridic SW vergent movements. Existing literature however, confirmed that Dinaridic deformation was mainly expressed along these softer detachment surfaces, which is why all the thin-skinned thrusts drawn in the profiles are interpreted as Dinaridic ones. (Schönborn, 1999; Nussbaum, 2002) But it is for example possible that the deeply located thin-skinned thrust in figure 27 (no. 1) is actually also part of an early Alpine phase that reactivated the Dinaridic structures, as they could be interpreted as strictly south vergent features as well, due to a lack of kinematic data on the thin-skinned thrusting phase. This interpretation is more in line with that of Nussbaum (2002, see section 2.3) and Engelen (2016, see section 6.3).

It is also likely that the out of sequence splay along the most frontal surfacing Alpine thrust (no. 5 in fig. 27) is in fact a reactivated Dinaridic thrust. The occurrence of a Dinaridic thrust at this location would be more in line with the Cretaceous antiform on top of it, which is almost certainly caused by Dinaridic deformation.

6.3. Comparison to the Western Friuli Alps

The research presented in this report was part of a larger project concerning the geological evolution of the entire Friuli Alps. This research has its focus on the eastern part of the project area, while the research performed by Engelen (2016) focused on the western part. Both areas largely contain the same stratigraphic formations and the same methods were used during both researches. In this section, the geological interpretation from Engelen (2016) will be compared with the one described above and their differences will be discussed.

Deformation phase	Stress Tensor (Win Tensor)	Characteristics	Affected formations
D1: NE-SW extension		Tilted normal faults (NW-SE oriented): cm/m scale.	Werfen Val Degano (11)
D2: NE-SW (ENE-WSW) shortening		SW (WSW) vergent thrusts. ENE-WSW oriented open/tight folds: dm/m scale. Top SW-WNW ductile shearing. NE-SW oriented tension gashes.	Mid-Triassic volcanics Werfen Bellerophon
D3: N-S (NNW-SSE) shortening		SSE vergent thrusts: m/hm scale. S vergent asymmetric folds: dm/m scale. E-W oriented syn- and anticlines: hm scale. S1 foliation. Occurrence of tension gashes.	Eocene flysch Chiampomano (15b) Dolomia Principale Raibl Buchenstein Werfen Bellerophon
D4: NW-SE shortening		NE-SW plunging open folds: dm/m scale Top NW shearing	Chiampomano (15b) Dolomia Principale Bellerophon
D5: NW-SE shortening and WSW-ENE extension		WNW-ENE oriented dextral and sinistral strike-slip faults: dm/hm scale; former thrusts reactivated as strike-slip faults. NNW-SSE striking normal faults: dm/m scale.	All formations

Table 2. Summary of the five different deformation phases of the Western Friuli Alps (modified after Engelen, 2016).

The main difference between the deformation phases summarised in tables 1 and 2 is the additional NW-SE compression phase (D4) by Engelen (table 2), which leads to a total of five deformation phases instead of four. This phase was observed at only a few field locations and is expressed by thick-skinned SE-vergent thrusts and NE-SW plunging open folds. In the East, these kind of structures would have been combined with those from phases D5 to one last deformation phase.

Another difference is the orientation of the σ1 axis during phase D2; which lies more towards the N-S axis in the Eastern area. The Eastern area also shows more D2 influences, as it is closer located to the Dinaridic chain. No tight folds were observed in the east for this phase, but km-scale folding is absent in the west, indicating the abnormality of the Cretaceous anticline (fig. 24h). Engelen (2016) also mentions that top WNW to NW ductile shearing was observed in the lower Bellerophon formation, which has a higher gypsum content than the Bellerophon formation occurring in the East. These shearing structures confirm that this surface formed indeed a décollement along which westward thrusting was facilitated (Dinaridic thrusting). Engelen (2016) explains that the somewhat northward directions of these shears could be caused by rotations due to subsequent

deformation phases. He also notes that shortening in the Eocene flysch was mostly accommodated along NE-SW directed layer parallel slip, something that is less clear in the Eastern area.

The most striking difference during phase D3 is that north vergent thrusts and folds do not seem to occur in the Western Friuli region (see also appendix A and fig. 32), while they are typical for the northern half of the Eastern part. As mentioned previously, Engelen (2016) interprets the "soft" Bellerophon, Raibl and also the Biancone (16b) and Eocene flysch formations as main décollements for the S-vergent movement of the D3 phase as well. The sequence of thrusting is interpreted quite different compared to the East, but thin-skinned thrusting is also succeeded by thick-skinned thrusting in this region. He suggests that the thin-skinned tectonics, extending into the Alpine D3 phase, accommodated the largest amount of shortening (45 km) in the Western Friuli Alps, resulting in the tripling of the sedimentary sequence (fig. 32). This compared to doubling of the stratigraphy in the Eastern area during the D2 phase only, leading to 57 km of shortening (fig. 25). The décollements indicated by Engelen (2016) will also remain active during the subsequent thick-skinned thrusting phases.

Engelen (2016) also mentions NNW-SSE striking normal faults in the west, which were not observed in the east. He associates these small scale faults with the youngest transpressional D5 phase, as they cut trough all other pre-existing structures, just like the strike-slip faults.

Other than these remarks, the deformation histories seemed to be rather similar.
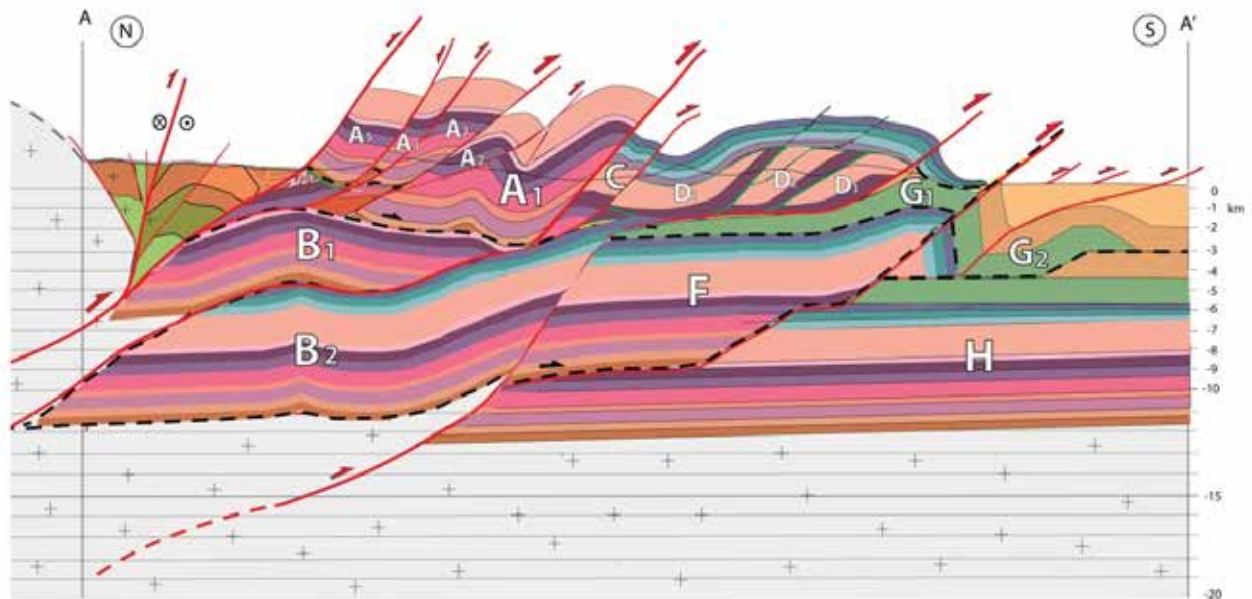
Figure 32. Interpreted cross-section for maximal shortening by Engelen (2016).

In the 2016 report, Engelen proposes in fact two different scenarios for shortening in the Western Friuli Alps: a minimal shortening model that comprises mainly thick-skinned thrusting and a maximal shortening model that involves a phase of thin-skinned thrusting prior to the thick-skinned thrusting. The latter indicates a total of 57.2 km of shortening, a difference of approximately 37 km compared to the minimal shortening model.

The maximal shortening model by Engelen (2016) is preferred as it is more consistent with the 68 km of shortening presented in this study and the approximately 50 km of shortening suggested by Schönborn (1999) and Nussbaum (2009).

The lateral geometrical differences between the Eastern and Western profiles can be explained by the occurrence of complex transverse zones in the central part of the area (Nussbaum, 2002, see fig. 10 for the exact locations). These zones form a discontinuity between the geological structures in the two parts and are able to transfer stresses from one geometrical configuration to another; for example the switch from dextral strike-slip along the Fella-Sava Line (which used to be a north vergent backthrust) in the east to south vergent thrusting in the west (appendix A).

Even though absolute timing of events is not possible in the area due to the absence of Neogene-Quaternary marine deposits, Venturini and Carulli (2002) dated the faults in these zones as Middle to Late Miocene structures, based on geometric and structural comparison with similar tectonic structures in the Dolomites and Southern Alps, that have been dated by for example Castellarin et al. (1992). Venturini and Carulli (2002) also suggest that these faults became reactivated during the Pliocene. It is likely that reactivation was also accommodated along inherited Middle Triassic normal faults (Nussbaum, 2002).

6.4. Regional implications

The 68 km of Paleogene and Neogene shortening in the Friuli Alps implied in this study largely agrees with the ±50 km of shortening estimated by Schmid et al. (1996, for the Western Southern Alps since the beginning of the Oligocene), Schönborn (1999, for the Dolomites since the Late Miocene) and Nussbaum (2002, for the Friuli Alps since the Late Miocene).

The balanced cross-section in figure 27 shows more thin-skinned thrusting than the cross-section by Nussbaum (2002, fig. 11), because no constraints were put on the amount of shortening along the Belleophon and Raibl formations, which lead to the extra kilometres of shortening obtained in this study.

The expectation was that the introduction of more subsurface thin-skinned tectonics would lead to a larger amount of shortening than this extra 18 km (for example a total of 190 km of shortening, as expected by Ustazsewski et al., (2008)). This could only be obtained in the current balanced model when the décollements along the Bellerophon and Raibl formations are interpreted to be longer, which is possible since field constraints are lacking. This option would however require substantial amounts of subduction of the Adriatic derived Southern Alpine units underneath the European plate (fig. 33).

This would be in favour of the polarity switch theory, that is supported by e.g., Lippitsch et al. (2003), Ustazsewski et al. (2008) and Handy et al. (2014). This theory infers that the NE-dipping slab underneath the Eastern Alps that has been observed on tomographic images is derived from the Adriatic plate, implying that the polarity of subduction must have changed, as the European plate subducts towards the south underneath Adria in all other parts of the Alps (fig. 33). Ustazsewski et al., (2008) propose that around 20 Ma, the European slab broke off underneath the Eastern Alps, creating room for the advancing Adriatic plate and thus facilitating a subduction polarity change. The 190 km of shortening, estimated by Ustazsewski et al. (2008) is equivalent to the length of this Adriatic slab.

The NE directed subduction of Adria in the Eastern Alps could also be responsible for the occurrence of the typical north vergent backthrusts in the Eastern Southern Alps, that were not observed more towards the west.

Larger amount of shortening in the Friuli Alps could also be obtained by shallower inclined ramps for the thin-skinned thrust or more ramps that could lead to tripling or even quadrupling of the sediments below the Raibl formation. This last option has however its limitations, due to the existing topography of the area and the thickness of the sediment layers, which cannot exceed the depth at which the basement is expected to be. Schmid et al. (2004) indicate that the retro-wedge below the Southern Alps is at most 10 to 15 km thick.
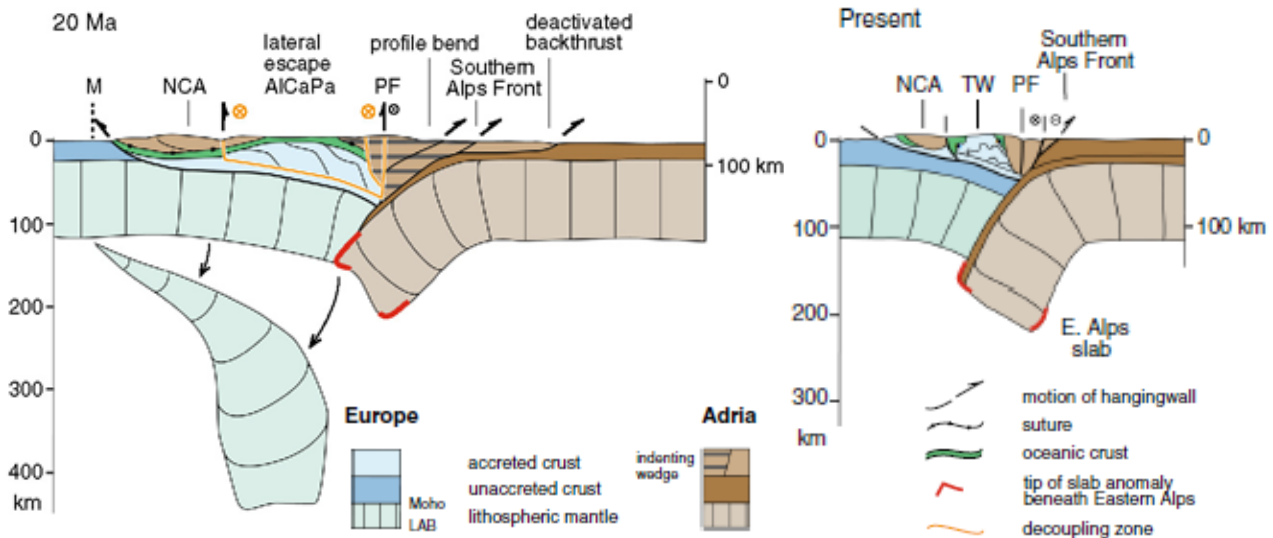
Fig. 33. Larger amounts of shortening could be obtained for the Friuli Alps by longer décollements along the Bellerophon and Raibl formations, during stage 0. This would however require substantial amounts of NE subduction of the Adriatic derived Southern Alpine units underneath the European plate , implying a polarity change in the vicinity of the Eastern Alps combined with slab break off of the European plate, which is suggested by e.g. Handy et al. (2014).

7. Conclusions

The structural evolution in the Friuli Alps consists of 4 deformation stages (see also table 2).

1) N-S extension, creating E-W striking normal faults. Structures are not widespread and likely overprinted by younger faults. No absolute time constraints were observed in the field, but the youngest extensional phase affecting the area was dated as Late Cretaceous.

2) NNE-SSW shortening, characterized by (S)SW vergent thrust faults and NW or SE plunging fold axes, related to the Dinaridic orogeny (60 – 30 Ma). In the subsurface this deformation phase has been accommodated along thin-skinned thrusts along the relatively "soft" Bellerophon and Raibl formations, creating ramp-flat structures. The large amount of deformation that seems to have affected the "soft" formations at the surface suggest that they have also been subjected to thin-skinned thrusting. Their many north and south vergent asymmetric folds imply however that they were overprinted by the next phase.

1) N-S shortening, defined by north and south vergent folds and faults. The faults create large offsets, suggesting thick-skinned tectonics. The phase is interpreted as Alpine (23 Ma) and recent earthquakes along the frontal thrust indicate that the phase is still active.

2) Dextral transpression due to NW-SE shortening along inherited E-W to ENE-WSW oriented thrusts, that were generated during the Alpine phase. Reactivation occurred during the Pliocene (8 Ma) and the phase is still ongoing, as can be inferred from recent seismicity along for example the Fella-Sava Line.

The geology of the Friuli Alps is distinguished by the sequence of thin-skinned thrusting followed by thick-skinned thrusting. The thin-skinned thrusting lead to the biggest amount of shortening: 57 km of a total of 68 km, starting in the Early Paleogene. This is however a minimal amount, as constraints for the amount of shortening were not found in the field. Longer décollements would lead to the subduction of Adria derived material underneath the European plate, which suggest a subduction polarity switch.

The overprinting of Dinaridic structures by Alpine ones and Alpine structures by Pliocene ones, complicated the interpretation. The chosen strike for the balanced cross-section was also not optimal for representing both the Alpine and the Dinaridic features, but still proved to be insightful. As plane strain along strike is assumed, non-

parallel deformation could not be taken into account. A proper assessment of the relationships between the different geological structures could be obtained in a 3D model.

8. Acknowledgements

9. References

Babic, L., Hochuli, P. and Zupanic, J., 2002, The Jurassic ophiolitic mélange in the NE Dinarides, internal structure and geotectonic implications, *Eclogae Geologicae Helvetiae,* 95, pp. 263–275.

Bartel, E., et al., 2014a, States of paleostress north and south of the Periadriatic fault: Comparison of the Drau Range and the Friuli Southalpine wedge, *Tectonophysics*, 637, pp. 305–327.

Bartel. E., et al.. 2014b, A low-temperature ductile shear zone: The gypsum-dominated western extension of the brittle Fella-Sava Fault, Southern Alps, *Journal of Structural Geology,* 69, pp. 18-31.

Benedetti, L., et al., 2000, Growth folding and active thrusting in the Montello region, Veneto, northern Italy, *Journal of Geophysical Research: Solid Earth,* 105, B1, pp. 739-766.

Bosellini, A., 1984, Progradation geometries of carbonate platforms: example from the Triassic of the Dolomites, northern Italy, *Sedimentology*, 31, pp. 1-24.

Bosellini, A. and Doglioni, C., 1986, Inherited structures in the hanging wall of the Valsugana Overthrust (Southern Alps, Northern Italy), *Journal of Structural Geology*, Vol. 8, No. 5, pp. 581-583.

Bressan, G. et al., 1998, Present state of tectonic stress of the Friuli area (eastern Southern Alps), *Tectonophysics,* 292, pp. 211-227.

Bressan, G. and Bragato, P, 2009, Seismic deformation pattern in the Friuli-Venezia Giulia region (north-eastern Italy) and western Slovenia, *Bollettino di Geofisica Teorica ed Applicata*, Vol. 50, n. 3, pp. 255-275.

Carulli, B. et al., 2006, Carta Geologica del Friuli Venezia Giulia, Università degli sturdy di Trieste e Udine.

Casterllarin, A., et al., 1992, Alpine compressional tectonics in the Southern Alps. Relationships with the N-Apennines, *Annales Tectonicae*, 6(1), pp. 62-94.

Castellarin, A. and Cantelli, L., 2010, Geology and evolution of the Northern Adriatic structural triangle between Alps and Apennine, *Rendiconti. Fisiche Accademia Lincei,* 21 (Suppl 1): S3–S14.

Cati, A. et al., 1987b, Carbonate platforms in the subsurface of the northern Adriatic area, *Memorie della Societa Geologica Italiana*, 40, pp. 295-308.

Cousin, M., 1981. Les rapports Alpes-Dinarides, Les confins de l'Italie et de la Yougoslavie*, Société géologique du Nord*, Publ. 5, 1, 1-521, 2, 1-521.

Delvaux, D., 2014, Win_Tensor 5.0.5., Royal Museum for Central Africa, Department of Geology and Mineralogy, Tervuren, Belgium.

Delvaux, D. and Sperner, B., 2003, New aspects of tectonic stress inversion with reference to the TENSOR program, *Geological Society of London, Special Publications*, vol. 212, pp. 75-100.

Doglioni, C., 1985, The overthrusts in the Dolomites: ramp-flat systems, *Eclogae Geologicae Helvetiae*, Vol. 78, Nr. 2, pp. 335-350.

Doglioni, C., 1986, Tectonics of the Dolomites (Southern Alps, Northern Italy), *Journal of Structural Geology*, Vol. 9, No. 2, pp. 181 - 193.

Doglioni, C. and Bosellini, A., 1987, Eoalpine and mesoalpine tectonics in the Southern Alps, *Geologische Rundschau*, 76/3, pp. 735- 754.

Engelen, D., 2016, In press.

Fodor, L. et al., 1998, Miocene-Pliocene tectonic evolution of the Slovenian Periadriatic fault: Implications for Alpine-Carpathian extrusion models, *Tectonics*, Volume 17, No. 5, pp. 690-709.

Fodor, L. et al., 2008, Miocene emplacement and rapid unroofing of the Pohorje pluton at the Alpine-Pannonian-Dinaridic junction, Slovenia, *Swiss Journal of Geosciences*, vol. 101, pp. 255-271.

Fossen, H. 2010, Structural Geology, isbn: 9780521516648.

Frisch, W., Dunkl, I., Kuhlemann, J., 2000, Post-collisional orogen-parallel large-scale extension in the Eastern Alps, *Tectonophysics,* 327, pp. 239-265.

Handy, M., Ustaszewski, K. and Kissling, E., 2014, Reconstructing the Alps–Carpathians–Dinarides as a key to understanding switches in subduction polarity, slab gaps and surface motion, *International Journal of Earth Sciences, Geologische Rundschau,* DOI 10.1007/s00531-014-1060-3.

Hatcher, R., 1995, Structural Geology: Principles, Concepts, and Problems, Prentice Hall.

Horváth, F., et al., 2006, Formation and deformation of the Pannonian Basin: constraints from observational data, *Geological Society London Memoirs*, 32, pp. 191–206.

Janák, M., et al., 2004, First evidence for ultrahigh-pressure metamorphism of eclogites in Pohorje, Slovenia: Tracing deep continental subduction in the Eastern Alps, *Tectonics*, vol. 23, TC5014, doi: 10.1029/2004TC001641.

Kissling, E. et al. 2006, Lithosphere structure and tectonic evolution of the Alpine arc: new evidence from high-resolution teleseismic tomography, *Geological Society London Memoirs,* 32, pp. 129–145.

Lippitsch, R., Kissling, E., Ansorge, J., 2003, Upper mantle structure beneath the Alpine orogen from high-resolution teleseismic tomography, *Journal of Geophysical Research*, Vol. 108, No. B8, 2376, doi:10.1029/2002JB002016.

Luth, S., et al., 2013, Does subduction polarity changes below the Alps? Inferences from analogue modelling, *Tectonophysics,* 582, pp. 140–161.

Mancktelow, N., et al., 2001, The DAV and Periadriatic fault systems in the Eastern Alps south of the Tauern window, *International Journal of Earth Sciences, Geologische Rundschau,* 90, pp. 593–622.

Midland Valley Exploration Ltd, 2014, MOVE: the geologist's toolkit, Glasgow, United Kingdom.

Neubauer, F., Genser, J. and Handler, R., 2000, The Eastern Alps: Result of a two-stage collision process, *Mitteilungen der Österreichischen Geologischen Gesellschaft*, 92, pp. 117-134.

Neubauer, F. and Ilić, A., 2005, Tertiary to recent oblique convergence and wrenching of the Central Dinarides: Constraints from a palaeostress study, *Tectonophysics,* 410, pp. 465–484.

Nussbaum, C., 2002, Neogene Tectonics and Thermal Maturity of Sediments of the Easternmost Southern Alps (Friuli Area, Italy), Institut de Géologie Université de Neuchâtel.

Pamić, J., Gušić, I. and Jelaska, V., 1998, Geodynamic evolution of the Central Dinarides, *Tectonophysics,* 297, pp. 251–268.

Ratschbacher, L., Merle, O., Davy, P., Cobbold, P., 1991, Lateral Extrusion in the Eastern Alps, part 1: boundary conditions and experiments scaled for gravity, *Tectonics,* 10(2), pp. 245–256.

Röller, K. and Trepmann, C., 2007, Stereo32, Ruhr-Universität Bochum, Institut für Geologie, Mineralogie & Geophysik, Germany.

Schmid, S.M. et al., 1996, Geophysical-geological transect and tectonic evolution of the Swiss-Italian Alps, *Tectonics*, Vol. 15, No. 5, pp. 1036-1064.

Schmid , S.M. et al., 2004, Tectonic map and overall architecture of the Alpine orogen, *Eclogae Geologicae Helvetiae,* 97,pp. 93–117.

Schmid, S.M. et al., 2008, The Alpine-Carpathian-Dinaridic orogenic system: correlation and evolution of tectonic units, *Swiss Journal of Geosciences,* 101, pp. 139–183.

Schönborn, G., 1999, Balancing cross sections with kinematic constraints: The Dolomites (northern Italy), *Tectonics*, Vol. 18, No. 3, pp. 527-545.

Tiberi, L. et al., 2012. Ground shaking scenarios for historical earthquakes in the southeastern Alps, *Geophysical Research Abstracts 14*, EGU2012e714214.

Ustaszewski, K. et al., 2008, A map-view restoration of the Alpine–Carpathian–Dinaridic system for the Early Miocene, *Swiss Journal of Geosciences*, 101(1), pp. 273–294.

Venturini, C. and Carulli, B., 2002, Neoalpine structural evolution of the Carnic Alps central core (Mt. Amariana, Mt. Plauris, Mt. San Simeone), *Memorie della Societa Geologica Italiana*., 57, 00-00, 9 ff.

Venzo, S., 1940, Studio geotettonico del Trentino meridionale-orientale tra Borgo Valsugana e M. Coppolo, *Memorie dell'Istituto Geologico dell'Università di Padova*, 14, 1-86.

Viaggi, M. and Venturini, S., 1995, Dati biostratigrafici preliminari sui depositi salmastro-dulcioli neogenici delle Prealpi Veneto-friulane, *Natura Nascosta*, Monfalcone, 13, pp. 32-33.

Viel, G., 1979, Litostratigrafia Ladinica: una revisione. Ricostruzione paleogeographica e paleostrutturale dell'area Dolomitico -Cadorina (Alpi Meridionali); I e II parte, *Rivista Italiana di Paleontologia e Stratigrafia,* 85, pp. 85-125; 85, pp. 297-352.

Willingshofer, E., Neubauer, F. and Cloetingh, S., 1999, The Significance of Gosau-Type Basins for the Late Cretaceous Tectonic History of the Alpine-Carpathian Belt, *Physics and Chemistry of the Earth* (A), Vol. 24, No. 8, pp. 687-695.

10. Appendices

Appendix A: Geological map (modified after Carulli, 2006)

Legend:

Thrust fault	**Subvertical bedding**
Antiform	**Subhorizontal bedding**
Synform	**Steeply inclined bedding (10-45°)**
Strike-slip fault	**Shallowly inclined bedding (45-80°)** *red symbols are for the eastern area, black symbols for the western area

21	Quaternary Cover

Cenozoic sequence

20b	Miocene Molasse
20a	Oligocene Molasse
19b	Eocene Flysch
19a	Paleocene Flysch
18	Calcari a Miliolidi (Paleocene-Eocene)

Mesozoic sequence

17c	Upper Cretaceous carbonate platform
17b	Lower Cretaceous carbonate platform
17a	Scaglia Rossa (Cretaceous-Eocene)
16c	Lower Cretaceous shalow water platform
16b	Biancone (Jurassic-Cretaceous)
16a	Calcari di Polcenigo (Jurassic)
15c	Calcare del Vajont (Jurassic)
15b	Basinal deposits (Triassic-Jurassic)

15a	Calcari Grigi del Friuli (Jurassic)
14	Dachstein (Triassic)
13c	Dolomia Principale (Triassic)
13b	Dolomia di Forni (Triassic)
13a	Monticello (Triassic)
12c	Raibl (Triassic)
12b	Evaporitic lagoon deposits (Triassic)
12a	Dürrenstein (Triassic)
11	Lagoon deposits (Triassic)
10b	Vulcaniti di Riofreddo (Triassic)
10a	Wengen & Livinallongo (Triassic)
9	Schlern (Triassic)
8b	Basinal deposits (Triassic)
8a	Serla (Triassic)
7	Werfen (Triassic)

Post-hercynian Paleozoic sequence

6c	Bellerophon (Permian)
6b	Bellerophon (Permian)
6a	Val Gardena (Permian)
5b	Carbonate platform deposits (Carboniferous-Permian)
5a	Carbonate platform deposits (Carboniferous)

Late Hercynian sequence

4c	Dimòn (Carboniferous)
4b	Dimòn (Carboniferous)
4a	Hochwipfel (Carboniferous)
3b	Basinal deposits (Devonian-Carboniferous)
3a	Carbonate platform margin (Devonian)
2b	Cocco (Silurian)
2a	Uqua (Ordovician)

Metamorphic basement

1	(Ordovician-Devonian)

Appendix B: Formation description*

* Formations and their descriptions are derived from the Geological map of the Friuli Venezia Giulia by Carulli (2006) and Nussbaum (2002). Upper Cretaceous unconformity and the major décollement horizons are indicated in red. Colours correspond to those in the geological map and facies map in appendice A and fig. 7 and those in the tectonostratigraphic column (fig. 8).

| Formation name	Nr. & colour	Age	Description	Depositional Environment
Quaternary	Q	Quaternary	Mostly alluvial and slope deposits.	Alluvial plain
Miocene	20	Miocene	Molasse: calcareous breccias and conglomerates, silt- and sandstones with plant remains.	Deltaic
Flysch	19b	Eocene	Flysch: interbedded shales and sandstones, sometimes with thick carbonate beds.	Basinal (flysch)
Flysch	19a	Paleocene	Flysch: Grey/black calcarenites with breccias beds and sandstone and (reddish) shale intercalations.	Basinal (flysch)
Upper Cretaceous	17c	Upper Cretaceous	Whitish bioclastic limestones, massive with abundant rudists.	Platform
Lower Cretaceous	16c	Lower Cretaceous	Well stratified whitish/grayish and brownish limestones, sometimes with stromatolites.	Platform
Calcare del Vajont	15c	Upper Jurassic	Massive Limestones, with silica nodules and marly interbeds	Slope
Calcari Grigi del Friuli	15a	Lower Jurassic	Alternating grey micritic and stromatolitic limestones; oolitic limestones.	Platform
Dachstein	14	Upper Triassic	Alternating m-thick light grey micritic limestones and dm-thick stromatolitic limestones.	Platform
Dolomia Principale	13c	Upper Triassic	Light grey dolostones in m-thick beds alternating with dm-thick stromatolitic dolostones.	Platform Large, rigid peritidal platform: 1000-1700m thick due to large sediment influx and/or thermal subsidence
Monticello	13a	Upper Triassic	Massive and well stratified grey dolostones with marly intercalations. UCa: Carnian unit.	Slope/ramp
Raibl	12c	Upper Triassic	Dark grey dolostones and fossiliferous limestones. UCa.	Slope/ramp
Wengen & Livinallongo	10a	Upper Triassic	Red, ammonitic-bearing, marly limestones, shales and tuffites; siliceous nodular limestones and piroclastic deposits. UCa.	Basinal
Schlern	9	Upper Triassic	Light grey, massive or well-bedded dolostones or dolomitic limestones. UAL: Anisian- Ladinian unit.	Platform Fast growing. After rifting that broke the area into several basins with different depths.
Calcare di Morbiac	8b	Middle Triassic	Dark grey nodular limestones alternating with marls. UAL.	Basinal
Serla or Gutenstein	8a	Middle Triassic	Whitish dolostones and dolomitic limestones, poorly bedded, often brecciated and vuggy. UAL.	Platform Fast growing
Werfen	7	Lower Triassic	Oolitic limestones; grey, marly limestones in cm-dm-thick beds; yellow well-bedded dolostones and dolomitic limestones; grey and light brown laminated micritic limestones with bivalves and reddish shale	Platform Tidal flats. Climatic shift is the cause between sedimentation changes at PT boundary
Bellerophon	6c	Upper Permian	Dark grey limestones with frequent bioclasts in dm-thick bed, sometimes interbedded with thin marly layers. Lower part of the Bellerophon contains evaporates (gypsum).	Shallow Lagoonal. Transgression prograded westwards.
Basement		Older than Upper Permian		Basement

Appendix C: Dataset by location

Appendix D: Data spreadsheet

Appendix C: Data by location
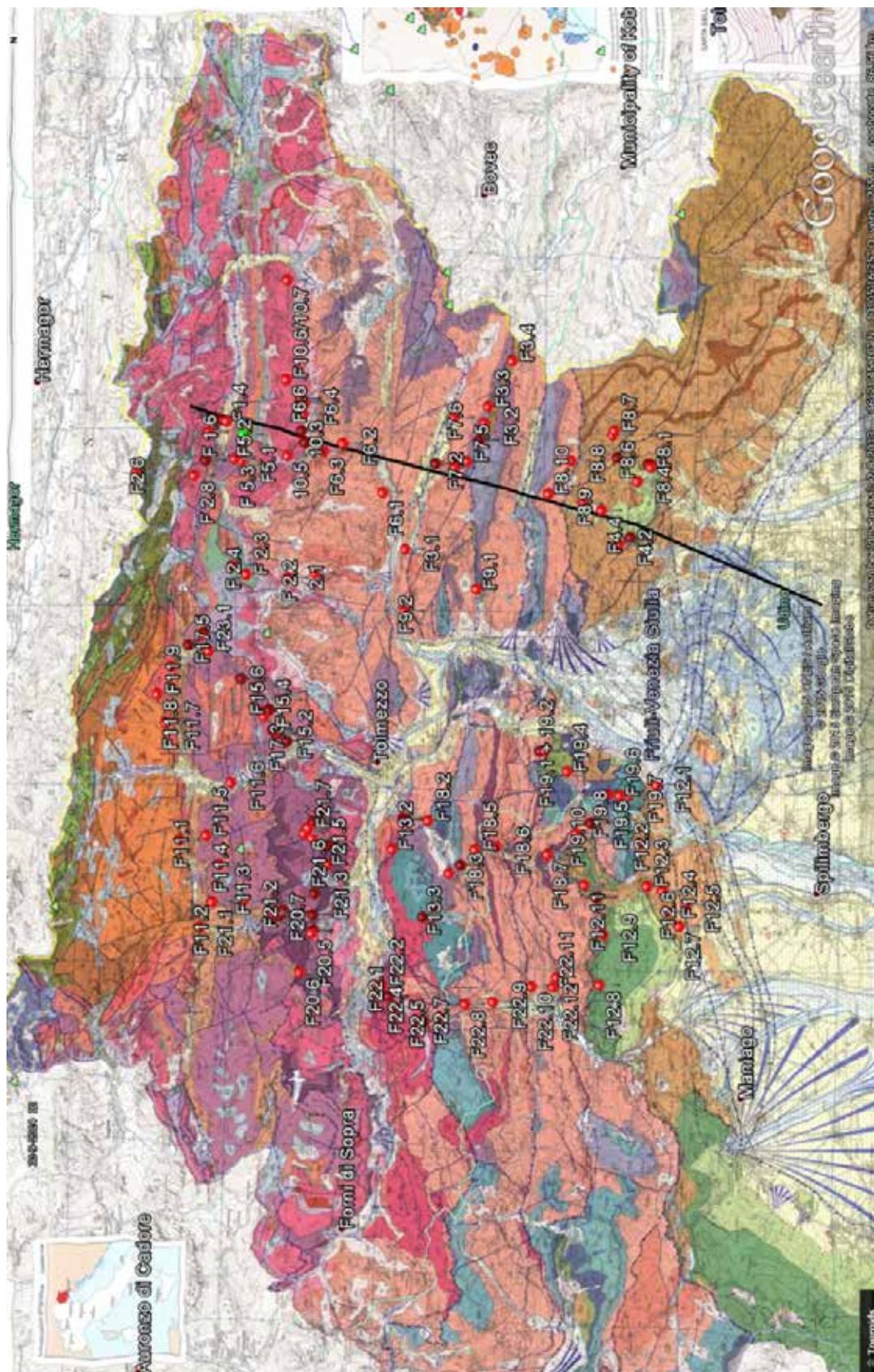
All datapoints collected during this fieldwork, in this appendix D, only the results from the Eastern Friuli Alps will be displayed (near the indicated profile line). For information on the western data points, see Engelen (2015).

1.1: SE of Pontebba

Coordinates: N: 46°50095
                                      E: 13°33748

Rock description: Very fine limestone, dark grey
Gutenstein formation (8a)

Depositional environment: Platform

Formation according to map: Werfen (7)

Measurements:
      Planar structures: Average S1: 18/48

Main sense of movement: -

Structural observations:
      - Cataclasite
      - Fracture cleavages.

Interpretation: -

1.2: SE of Pontebba

Coordinates: N: 46°50180
                                      E: 13°33722

Rock description: Very fine limestone, dark grey
Gutenstein formation (8a)

Depositional environment: Platform

Formation according to map: Werfen (7)

Measurements:
      Planar structures: Average S0: 185/60   S1: 002/30   S2: 272/86

Main sense of movement:
      N/S shortening (intersection of S0 and S1 is parallel to the
      fold axis that caused the cleavage, which is E-W)

Structural observations:
      - Cataclasite
      - 2 Cleavage sets: S2 appears to be straight, while S1 isn't.

Interpretation:
      - S1 has been influenced by S2. N/S shortening indicates
      Alpine process.

Equal angle projection
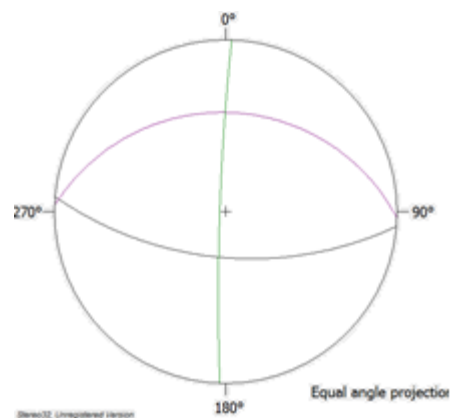
1.2 Gutenstein formation with 2 cleavage sets, S2 is not visible on this picture. S2 is straight, while S1 is not, so S1 must have been influenced by S2.

1.3: SE of Pontebba

Coordinates:	N: 46°49955
	E: 13°33775
Rock description:	Thinly bedded (5-20 cm) sandy limestones
	Gutenstein formation (8a)
Depositional environment:	Platform
Formation according to map:	Werfen (7)

Measurements:
    Planar structures: Average S0: 168/56
    Faults: P: 160/15
                P: 182/65   S: 261/18

N total = 3
n=2 (planar)
● n=1 (linear)

Equal angle projection, lower hemisphere

Stereo32 Unregistered Version

Main sense of movement: Slickenside is dextral
                             Movement along fault:
    NNW (intersection of faultplane/riedel +90 over faultplane)
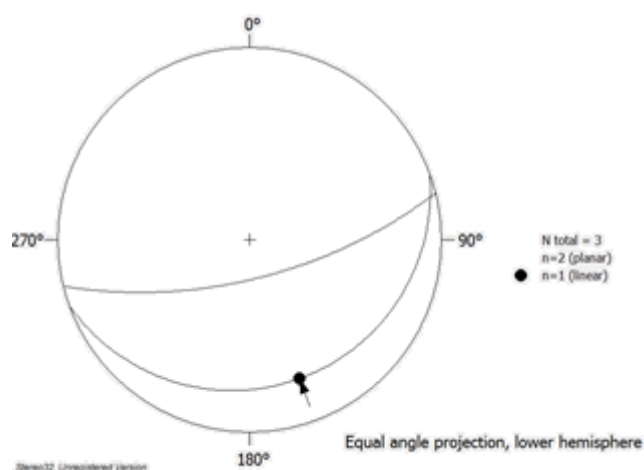
Structural observations:
    - Fault plane intersects plane with slickenslides.
    - Loading structures indicate top is up.

Interpretation:
- The fault must be younger than the slip along the slickenslide-plane.

1.3a. Sandy thinly bedded limestone.

1.3b. Load cast structure, top is up.

1.3b. Slickenside with steps indicating dextral shear.

1.4: SE of Pontebba

Coordinates:	N: 46°49823
	E: 13°33775
Rock description:	Thinly bedded (5-20 cm) sandy limestones
	Gutenstein formation (8a)
Depositional environment:	Platform
Formation according to map:	Werfen (7)

Measurements:
    Planar structures: Average S0: 197/80

Main sense of movement: -

Structural observations: -

Interpretation: -

1.5: SE of Pontebba

Coordinates: N: 46°50317
                   E: 13°33761

Rock description: Limestone
                   Gutenstein formation (8a)

Depositional environment: Platform

Formation according to map: Werfen (7)

Measurements:
    Planar structures: Average S0: 180/60

Main sense of movement: -

Structural observations: -

Interpretation: -

1.6: SE of Pontebba

Coordinates: N: 46°50885
                   E: 13°32516

Rock description: Dark grey limestones with lots of calcite veins.
                   Bellerophon (6c)

Depositional environment: Platform

Formation according to map: Bellerophon (6c)

Measurements:
    Planar structures: Average S0: 000/87 (vertical)
                              S0, 20m to the west : 287/80
    Faults: P: 034/80

P: 218/82	S: 138/10		
P: 026/84	S: 118/18		
P: 004/82	S: 276/05	R:040/86	S:113/20
P: 280/78	S: 012/005 and S:090/28		
P: 184/84	**S: 095/40**		
P: 198/88			
P: 172/85	R: 026/85		
P: 158/85	S: 060/18		

Folds: S0 western limb: 204/86   S1: 283/60

                                            S0 eastern limb: 256/88   S1: 132/40

Main sense of movement: Most faults are dextral, some normal faults also occur.

Structural observations:
- Dextral fault is indicated by 20 cm offset of calcite vein.
- S0 is cut by slickensides.
- Occurrence of stylolites, parallel to bedding.
- Occurrence of bedding parallel faults. Strike-slip is a big scale fault (over 15m, but not entirely visible due to river water.
- Occurrence of tension gashes (280/78).
- 184/84 Fault plane is extremely polished (mirror-plane) and surrounded by breccias, also contains a lot of holes that are related to deformation.
- Fold is open and 10m wide, probably related to big strike-slip fault

Interpretation:
Dextral strike-slip faults and fold might be related to the big dextral Periadriatic strike-slip fault.
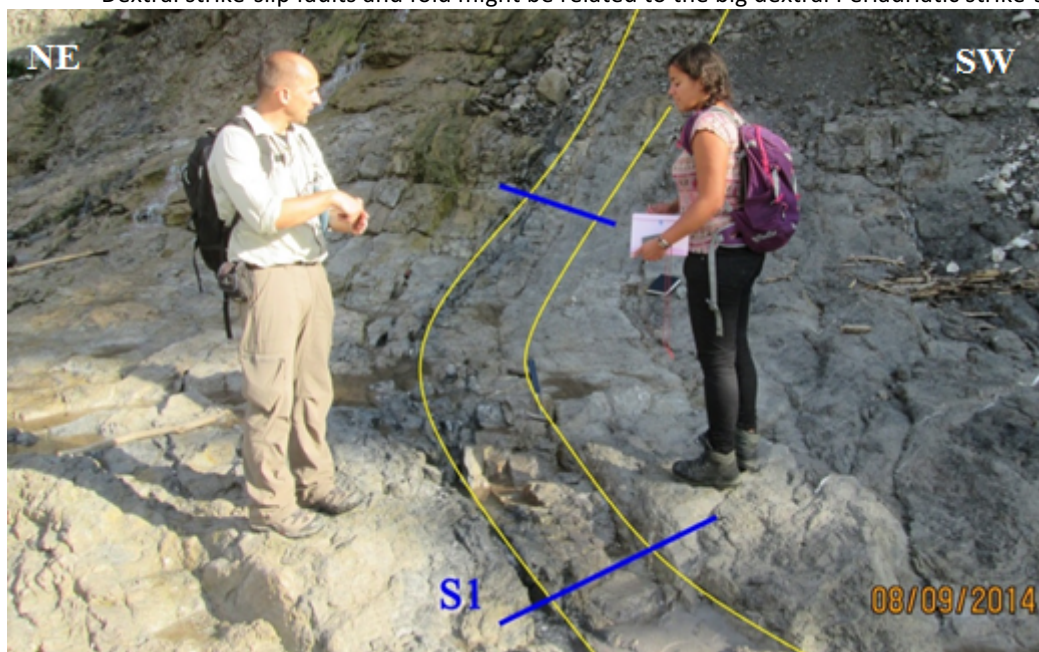
1.6a. 10m Scale open fold with a steep plunge, folding might be related to periadriatic strike-slip fault.
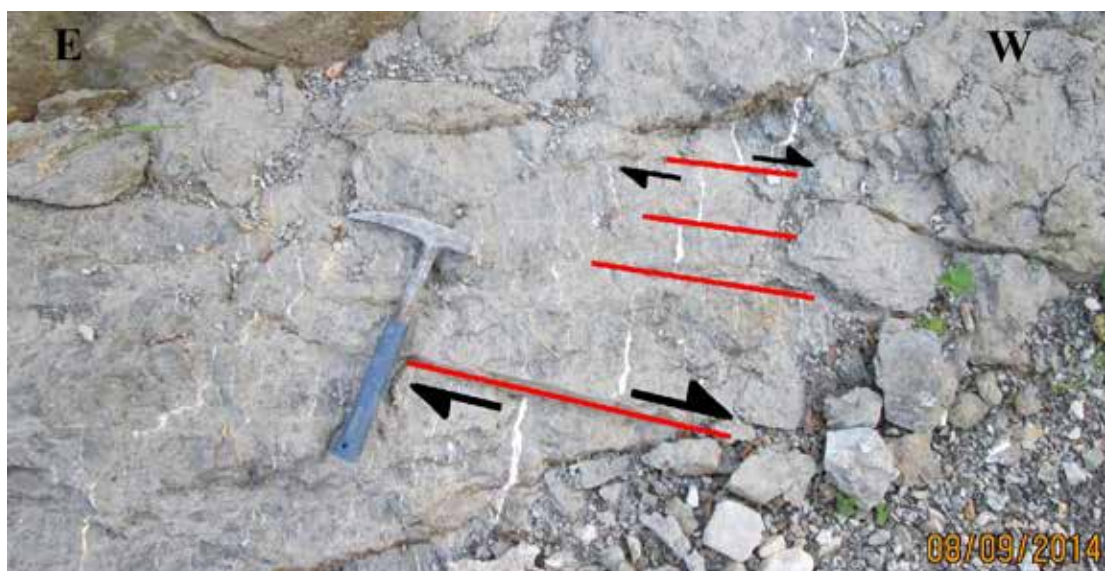
1.6b. Dextral strike-slip faults, offset indicated by calcite veins.

1.6c. 15m strike-slip fault with 2 riedels, indicating dextral shear. Striae have been found on all sliding surfaces. Main faults are along the bedding planes. Dip is almost vertical.

1.6d. Stylolites are indicated by the arrows. Orientation is parallel to bedding plane.

1.6e. Strike-slip fault zone, plane is very smooth (mirror plane) and is surrounded by gauge and breccias.

PBT axes

σ1: 17/140
σ2: 67/276
σ3: 15/045
R: 0,64 AD: 27,9
QRw: D QRt: D

PBT deviation

0 Sum of Weights 8

Schmidt Lower
Weight Mode 2
n/nt: 6/7
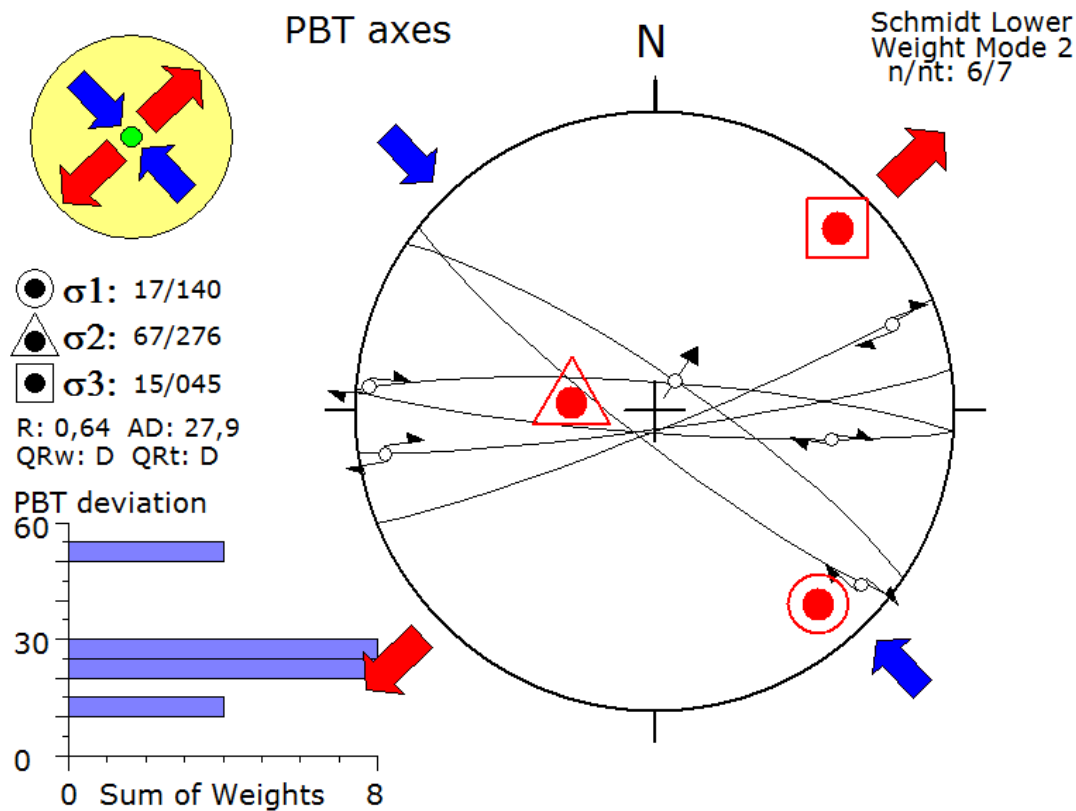
2.1: N of Moggio Udinese

Coordinates:	N: 46°43948
	E: 13°19490

Rock description: Dolomite, with softer marly layers. Brownish, glistening, angular fragmented rock: Monicello (13a)
On top of this: well stratified carbonates/dolostones belonging to the Dolomia Principale (13c) and Dachtstein (14)

Depositional environment: Carbonate ramp

Formation according to map: Monticello (13a)

Measurements:
    Planar structures: Average S0: 180/08

    Faults: P: 124/82   S:082/70

Main sense of movement: Fault is dextral

Structural observations:
    - Fault is probably strike-slip, only 1m vertical displacement, with unknown horizontal component.

Interpretation: -

2.1 Strike slip fault

2.2: N of Moggio Udinese

Coordinates: N: 46°45752
E: 13°18992

Rock description: Well bedded (1-2m
beds), dark grey, blocky dolomite

Depositional environment: Carbonate ramp

Formation according to map: 12c

Measurements:
Planar structures: Average S0: 142/35
S1: 326/61

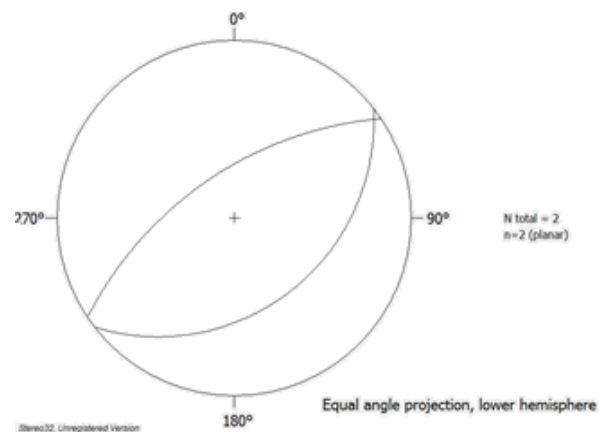**Faults:** multiple: P: 138/40 R:128/18

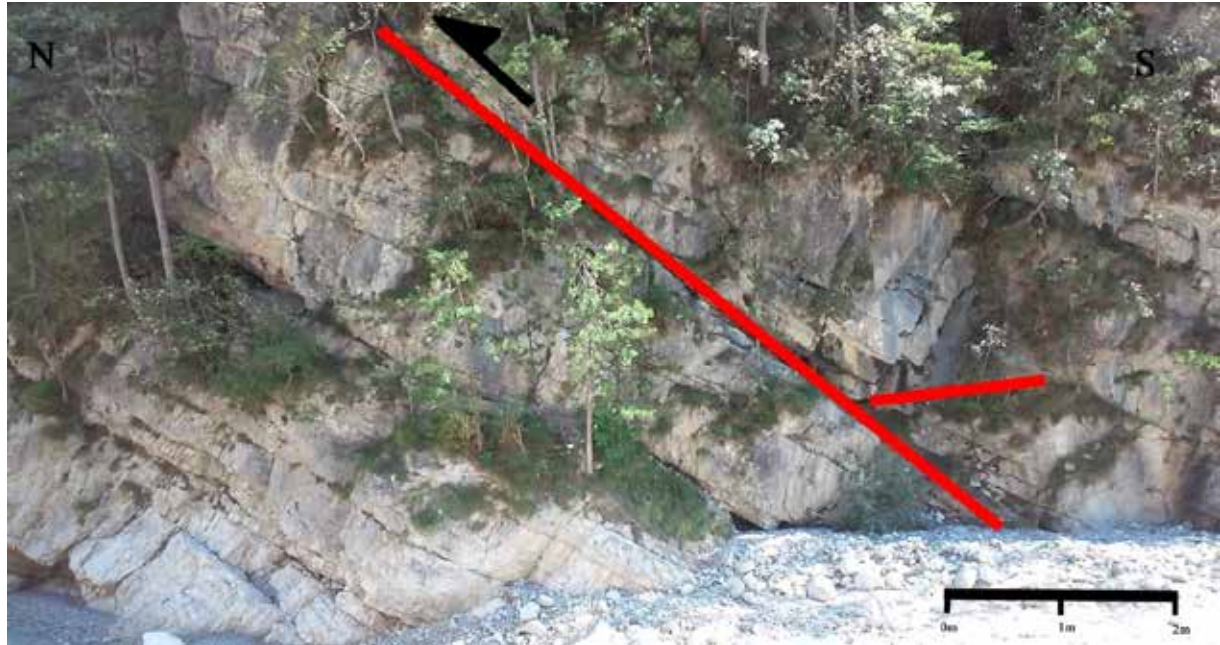**Main sense of movement:** NE plunging fold axis

Structural observations:
- Consistent set of thrust faults.

Interpretation:
Orientation of the thrust faults suits with N-S shortening (Alpine)

2.2. North oriented thrust. Trust is part of a set of multiple similar thrusts.

2.3: N of Moggio Udinese

Coordinates:	N: 48°48388
	E: 13°19218

Rock description: Thinly bedded (0.5-2 cm thick) dark grey limestones with calcite veins, mud and sandy layers. Sandy layers show fining upwards and sedimentary ` nodules. Also contains some volcanic layers with minerals.

Depositional environment: Basinal

Formation according to map: 10a

Measurements:

    Planar structures: Average S0: 152/48

    Faults:

S0	S: 220/32	
P: 106/72	S: 184/26	cross cutting everything else
P: 252/78	S: 316/48	

    Folds: Consistent set of folds (and/or drag due to faulting)

        S0 Limb1: 358/85   S0 Limb2: 135/50

        Measured fold axis: 090/35

Main sense of movement: Steps on S0 striae indicate sinistral movement (towards 220°).
Steps on 106/72 plane indicate dextral movement (N?)

Structural observations:
- Layers have a wavy surface (3-4m interval).
- Bedding parallel movements indicated by striae with steps
- 106/72 fault crosscuts every other structure, so it must be the youngest.

Interpretation:
- Fining upwards of the quartz grains within the sandy layers probably represents turbidites.

- Measured (and calculated) fold axis indicate N-S shortening (Alpine).
- Wavy surface (folds) might be caused by folding or drag due to faulting, although drag cannot be correlated to observed striae. A shearing component towards the south must have present in the case of folding, in order to obtain the asymmetrical shape of the folds. When a fault was the cause of these structures, it must have ran parallel to the steep limbs of the folds.
- At least 3 phases can be recognised:
  1. S0 was tilted towards the south + bedding parallel slip
  2. asymmetrical folding or faults with drag
  3. younger fault

2.3a. Overview of the outcrop. Wavy surface is repeated several times and cross-cutted by a younger fault. Wavy surface is probably caused by tight folding, or maybe by drag due to faulting.
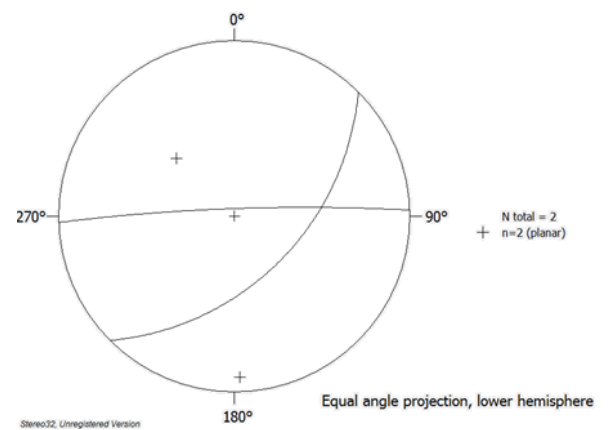
2.3b. Young fault that crosscuts every other structure.

2.3c. In green: fold axis that could have caused the wavy surface of the outcrop. A shearing component to the south must have been present in order to get the asymmetrical shape. Another cause might be drag along a fault that ran parallel to the steep limbs of the folds.

2.4: N of Moggio Udinese

Coordinates:	N: 46°49294
	E: 13°28954

Rock description: Thinly bedded grey marls, very fine.
Few sandy blue grey limestones, fining upwards (10-20cm thick).

Depositional environment: Basinal

Formation according to map: 8b

Measurements:
    Planar structures: Average S0 in the North: 166/86 (vertical)
Average S0 in the South: 161/61
(Measured 50m apart from one another)
    Faults: S0   S: 107/20
    Folds: Refolded fold: 2nd generation limbs:
S0 limb1: 160/42   S0 limb2: 161/79   E-W fold axis
Steep beds and shallower beds in the north vs. the south might also be part of a fold: S0 limbN: 166/86   S0 limbS: 161/61

Main sense of movement: E-W Fold axis belongs to N-S shortening.
Striae is dextral

Structural observations:
- Is topped by thickly bedded carbonate platforms. According to map: unconformity in-between them (fault).
- Asymmetrical fold, to the north the layers are steeper than to the south.
- Refolded fold.

Interpretation:
- These thinly bedded, basinal sediments (also stop 2.3) are better recorders of deformation than the thicker/massive carbonate platforms.
- N-S shortening indicates Alpine movements.

- Asymetrical (refolded) folds indicate a north vergent fold-system. However, the southern Alps are a south vergent thrust system.

2.4 Left side of a 30-40m big refolded fold. The green line represents the youngest fold axis.

2.5: W of Pontebba

Coordinates: N: 46°51093
                          E: 13°29983

Rock description: Red/grey limestone with nodules.
                          Werfen (7)

Depositional environment: Platform

Formation according to map: Werfen (7)

Measurements:
    Planar structures: Average S0: 168/75
                          S0: 128/65   S1: 128/80
    Folds: Refolded fold: 2nd generation limbs:
                          S0 limbN: 134/55   S0 limbS: 032/40
                          Calculated axis: 071/32

Main sense of movement: Fold is north vergent
                          S0/S1 relation also shows north vergence (intersection gives foldaxis →
                          40/50°, so NW/SE compression)

Structural observations:
    - N vergent folds are parasitic folds, belonging to a bigger scale north vergence.

Interpretation:

    - S1 is steeper than S0, so the section is not overturned. Younging direction towards the SE.

2.5 N-vergent parasitic fold.

2.6: Almost in Nassfeld, Austria

Coordinates: N: 46°55443
                                     E: 13°27933

Rock description: Quartz rich, fine grained limestone, with conglomerate layers of 5cm thick.
                                     No micas.

Depositional environment: Platform (Basement on the facies map; Paleozoicum)

Formation according to map: Gruppo di Pramollo (5a)

Measurements:
    Planar structures: Average S0: 030/40

Main sense of movement: -

Structural observations:
    - Cleavage set observed, however not measured.

Interpretation: -

2.7: On the road from Pontebba to Nassfeld

Coordinates: N: 46°53580
                          E: 13°29116

Rock description: Massive brown/greyish limestone

Depositional environment: Platform

Formation according to map: Bellerophon (6c)

Measurements:
   Planar structures: S0: 220/52
                            S0: 056/75
   Faults: P: 044/55   (almost layer parallel)

Main sense of movement: -

Structural observations:
   - Cleavage set observed, however not measured.

Interpretation: -

2.8: W of Pontebba

Coordinates: N: 46°51823
                          E: 13°28481

Rock description: Carbonates

Depositional environment: Platform

Formation according to map: Bellerophon (6c)

Measurements:
   Planar structures: S0a: 314/25
                            S0b: 148/5

Main sense of movement: -

Structural observations:
   - Different S0's, caused by folding or faulting. Outcrop from a distance (70m scale), so unsure.

Interpretation: -

2.8 Different S0's

3.1: W of Resiutta

Coordinates:	N: 46°38218
	E: 13°21806

Rock description: Dolomites, often brecciated and faulted, with smooth mirror planes. Fault zone is located on 'ground level', on top of this (mostly in the SW) lie relatively undisturbed carbonate beds. Dolomia principale (13c)

Depositional environment: Platform

Formation according to map: Dolomia Principale (13c) or Monticello (13a)

Measurements:

Planar structures: S0: 164/65

S0 50m further to the W: 196/36   S1: 324/62

Faults:

P: 160/62		
P: 154/62		
P: 359/58	R: 026/45	dextral
P: 272/40		
P: 135/40		
P: 155/52		
P: 185/30	R: 344/45	dextral
P: 180/58	R: 192/45 with S: 305/00	dextral (W)
P: 322/60	R: 338/75	dextral
P: 255/23	R: 345/40	dextral
P: 295/78	R: 252/70 with S: 358/22	sinistral (S?)

or	P: 340/38	R: 314/50 with S: 290/50	dextral	
	P: 174/50			
	P: 148/45	*S: 146/20*	*thrust*	
	P: 210/65	*S: 126/28*	*dextral*	
	P: 136/32	*S: 170/25*	*thrust*	
	P: 010/62	*R: 010/40*	*thrust*	
	P: 196/32	*R: 190/48*	*R': 250/35*	*sinistral*
	P: 208/75	*S: 120/25*	*dextral*	
	P: 180/58	*R: 192/45 with S: 300/05*		
	P: 284/82	*S: 208/70*	*thrust*	
	P: 178/52	***R: 210/30***	***dextral (picture)***	
	P: 218/50	*R: 258/40*	*dextral*	
	P: 170/48	*R: 206/45*	*thrust*	
	P: 186/85	*S: 186/85*	*thrust*	
	P: 280/58	*S: 320/50*	*thrust*	
	P: 166/55			
	P: 185/54	R: 248/54	dextral (NW)	
	P: 022/50			
	P: 203/46	S: 125/18		
	P: 211/60	S: 140/34	NW-SE strike	
	P: 147/35			
	P: 300/80	R: 009/15		
	P: 332/58	S: 290/54	WNW-ESE strike	
	P: 346/35	S: 336/34		

Equal angle projection, lower hemisphere

N total = 34
n=11 (planar)
n=23 (planar)

Stereo32, Unregistered Version

PBT axes

Schmidt Lower
Weight Mode 2
n/nt: 20/24

⊙ σ1
△ σ2
▣ σ3
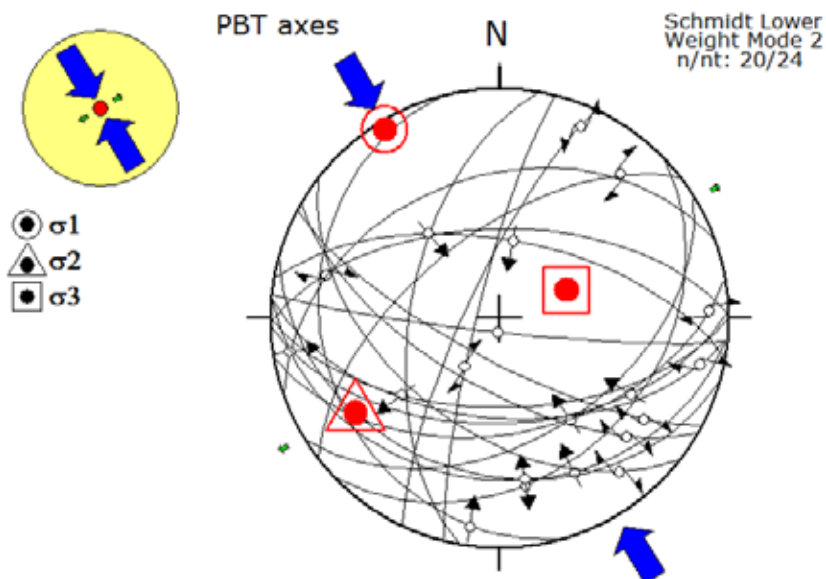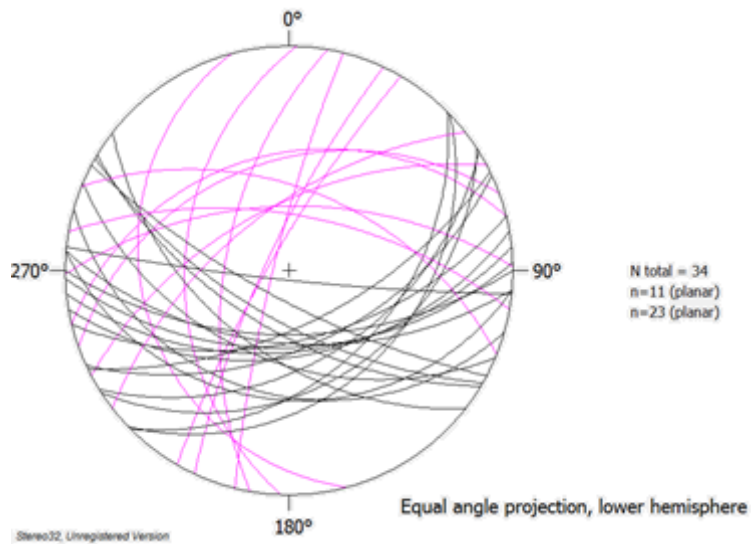
Main sense of movement: -

Structural observations:
- Lots of breccias, gouges and mirror fault planes, so there must have been quite some deformation.
  Among the breccias, organic material was also found.
- Usually, there is one sharp mirror plane, surrounded by a zone of smaller faults, breccias and gouge.
- South-west dipping, bedding parallel fault planes seem dominant.
- Fault found by Ernst is young, as it is not crosscutted by any other structure.

Interpretation:
- 2 Different sets of deformation stresses See wintensor/stereonet
- Very strong cataclastic deformation must have caused these breccias and mirror fault planes.
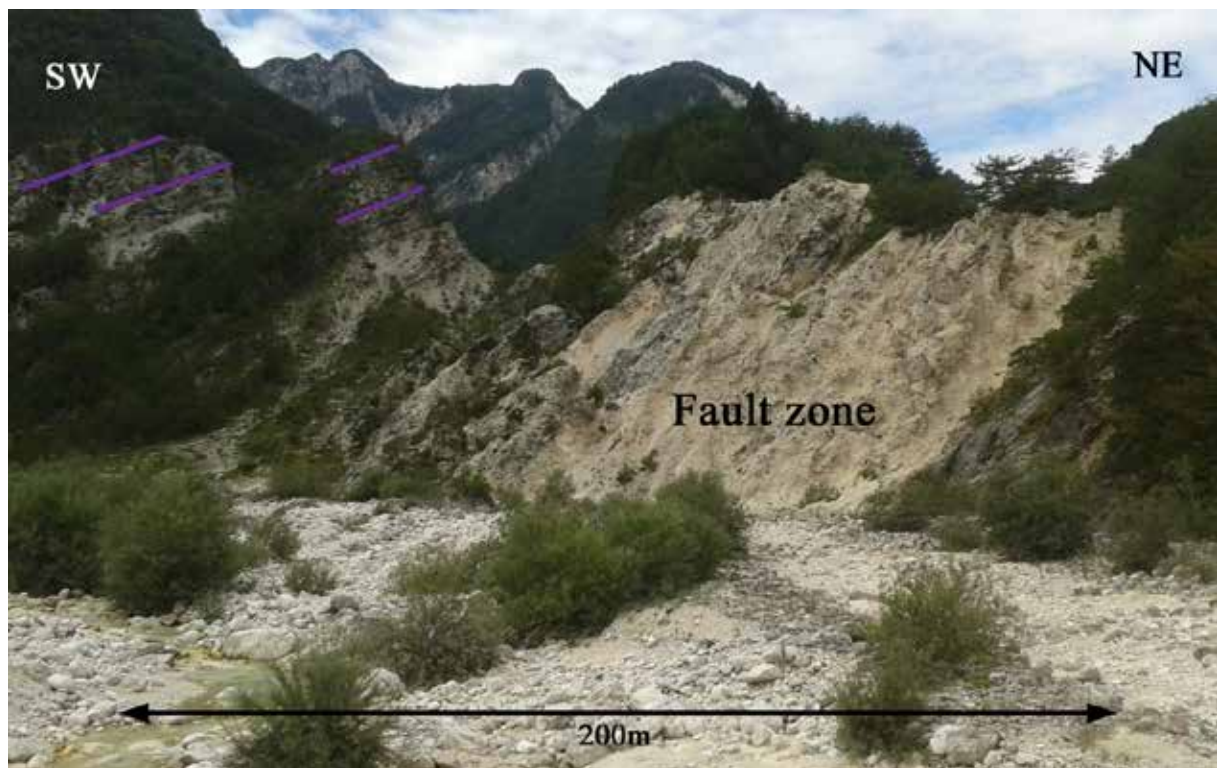- This outcrop represents the hanging wall of the big thrust in this valley.

Figure 3.1a. Overview of the outcrop

Figure 3.1b mirrorplane

Figure 3.1c. Striae on mirrorplane

Figure 3.1d Dextral fault with riedel

3.2: Along the road east from Resiutta

Coordinates: N: 46°33303
                                     E: 13°33576

Rock description: Alteration of brownish very thin (1-2cm) and greyish thicker (5-10cm)
                                     limestones. Thin layers are sometimes sandy and contain calcite veins.
                                     Thicker limestones are also sandy sometimes, have slickensides and contains
                                     shell fragments. The coarser shell fragments seem to be replaced by the
                                     finer sandy limestone within the thicker limestones; indicating a fining
                                     upwards. Younging upwards (towards the north) Inbetween these well
                                     stratified layers is red mud, which looks very chaotic (base of the turbidite).

Depositional environment: Basinal: flysch

Formation according to map: Flysch (19a)

Measurements:
    Planar structures: S0: 344/32
                                     S1: 334/45
                                     S on calcite vein: 275/28
    Faults: P: 251/64   S: 322/25   dextral
                                     P: 217/85   S: 124/24   sinistral
                                     P: 314/40   S: 335/32   dextral

Main sense of movement: -

Structural observations:
    - Cleavage is steeper than bedding, so formation is not overturned (to the North).

Interpretation:
    - The fining upwards within the thicker limestones can be interpreted as a mass flow mechanism, such
     as a turbidite. Turbidites create the flysch depositis.
    - Flysch is a deep marine facies, originating in the foreland basin of a developing orogen, during the
     early stage of the orogenesis. (Followed by the deposition of molasses).
    - Flysch is a young formation, but lies in a valley. While surrounding mountain tops are older
     carbonates. There must be a big thrust here.

Figure 3.2a. Flysch, mass flow, flysch

Figure 3.2b. Transition of shell breccia zone to calcarenit

Figure 3.2c. Sinistral slickensides

3.3: Along the road East from Resiutta

Coordinates:	N: 46°32994
	E: 13°35200

Rock description: More flysch, but mostly thinly bedded (1-2cm), containing lenses of more calcareous rock. Series of small and big (20m) scale faults. S0 is steeper here than at 3.2.

Depositional environment: Basinal: flysch

Formation according to map: Flysch (19a)

Measurements:

    Planar structures: S0: 356/76
                                    S1: 338/84

    Faults: P: 332/18   drag
                          P: 028/80   S: 305/10
                          P: 008/35

    Folds: Axis of kinkbands: 247/10

Main sense of movement: Kinkbands: top to SSE
                                                              Fault with drag: SSE
                                                              Vergence to the south

Structural observations:
    - Biggest offset by the thrust faults is about 35-40cm.

Interpretation:
    - The fining upwards within the thicker limestones can be interpreted as a mass flow mechanism, such as a turbidite. Turbidites create the flysch depositis.
    - Flysch is a deep marine facies, originating in the foreland basin of a developing orogen, during the

early stage of the orogenesis. (Followed by the deposition of molasses).
- Flysch is a young formation, but lies in a valley. While surrounding mountain tops are older carbonates. There must be a big thrust here.
- 1. Development of cleavage and large scale folds
  2. Development of kinkbads (SSE)
  3. Big scale (20m) faults (SSE)
  All Alpine.

Figure 3.3a. Cleavage, kinkbands, big scale faults

Figure 3.3b. Kinkbands in flysch (dextral SSE)

Figure 3.3c. Offset 332/18 plane

3.4: Along the road east from Resiutta

Coordinates:	N: 46°31401
	E: 13°39428
Rock description:	Dolostones
Depositional environment:	Platform
Formation according to map:	Dolomia Principale (13c)
Measurements:	
Planar structures:	S0: 152/30
Main sense of movement:	-
Structural observations:	-
Interpretation:	-

4.1: North of Tarcento

Coordinates:	N: 46°23694
	E: 13°22933
Rock description:	Flysch containing layers of conglomerate and sandier beds up to 10 cm thick. Layers are practically vertical, burrows indicate that layers are overturned. Younging direction towards the South.
Depositional environment:	Basinal: flysch
Formation according to map:	Flysch (19b)

Measurements:

Planar structures:	S0: 034/83			
	S1: 192/80			
Faults:	P: 221/60	with drag		
	P: 030/85	S: 055/80	normal (beddingparallel)	
	P: 000/16	S: 094/60	S0: 216/75	normal
	P: 218/40	*S: 210/35*	*thrust*	
	P: 322/30	S: 228/02	thrust	
Fold:	Axis kinkband: 290/05			
	Limb1: 330/15	Limb2: 210/38		
	Fold axis: 285/12			
Main sense of movement:	Fault with drag shows top to NE movement. All top to NE.			
	Cleavage indicates S vergence			

Structural observations: -

Interpretation:

   - Top to NE, indicates Dinaric influences.

Figure 4.1a. Flysch with conglomerate layer

4.2: North of Tarcento

Coordinates: N: 46°24401
           E: 13°22538

Rock description: Thick limestone bed within flysch

Depositional environment: Basinal : flysch

Formation according to map: Flysch (19b)

Measurements:
      Planar structures: S0: 245/48

Main sense of movement: -

Structural observations: -

Interpretation: -

4.3: North of Tarcento

Coordinates: N: 46°23640
           E: 13°23165

Rock description: Light grey, fossil rich limestone (with rudists).

Depositional environment: Platform

Formation according to map: Upper Cretaceous (17a)

Measurements:
      Planar structures: S0: 220/50
                             S1: 086/58
      Faults: P: 220/50 (bedding parallel)
                             P: 228/30   R: 200/56   dextral
                             P: 094/44

Main sense of movement: -

Structural observations: -

Interpretation: -

4.4: North of Tarcento

Coordinates: N: 46°25529
           E: 13°25642

Rock description: Light grey, fossil rich limestone (with rudists).

Depositional environment: Platform
Formation according to map: Lower Cretaceous (16c)

Measurements:
    Planar structures: S0: 055/40

Main sense of movement: -

Structural observations: -

Interpretation:
     This stop is more towards the North than stop 4.3, which means that the S0 has changed from SW dipping in the South to NE dipping in the North, due to an anticline, which might have been caused by Dinaric processes.

5.1: South of Pontebba

Coordinates: N: 46°48801
     E: 13°29916

Rock description: Dark grey, quite massive dolomite. On the other side of the valley the bedding is more prominent (10-50cm thick beds).

Depositional environment: Shallow platform

Formation according to map: Dolomia del Popera (8a)/Schlern (9)

Measurements:
    Planar structures: S0 W: 168/70
     S0 E: 190/69

Main sense of movement: -

Structural observations:
     - Some folding seems to going on, with N/S shortening.

Interpretation: -

Figure 5.1. Picture of the south dipping strata on the other side of the road

5.2: SE of Pontebba

Coordinates:	N: 46°48647 E: 13°32298
Rock description:	Estimated from a distance: Folded thinner beds on top of more massive limestones.
Depositional environment:	Basinal
Formation according to map:	8b and/or 10a
Measurements: **Planar structures:**	S0 N: 175/45 estimated S0 S: 167/30 estimated
Main sense of movement:	-
Structural observations:	-
Interpretation:	-

Figure 5.2. Thinly bedded, basinal deposits in the top of the hill

5.3: SE of Pontebba

Coordinates:	N: 46°49251
	E: 13°30136

Rock description: Thinly bedded (1-10 cm), very fine clayish yellow greyish and red layers with some calcite veins. The red beds are marly and contain micas.
Probably 8b or 10a. Bedding is almost vertical at most places, the red layers are most heavily folded (on the western bank of the river).

Depositional environment: Basinal

Formation according to map: Quaternary. Further eastwards, 8b/10a are mapped along this strike. So maybe this location is an extension.

Measurements:

Planar structures:	S0 E: 187/80	
	S0 W: 195/65	
Faults:	P: 038/44	sinistral normal
	P: 178/88	sinistral thrust
	P: 108/26	sinistral strike slip
Folds:	Axis: 285/20	
	Axis: 272/20	
	Axis: 265/20	
	Axis: 270/35	Chevron + hinge collapse
	Axis: 283/07	Chevron + hinge collapse

Main sense of movement: The asymmetric folds, have their long limb on the South side and their short limb pointing towards the North, indicating a main movement towards the North.

Structural observations:
- Burrows and wave ripples indicate that the top is up (towards the S).
- The first fault has an offset by the second one. The third fold terminates on the second fold.
- Folds (up to 0.5m big) were mainly found on the Western bank of the river, most were asymmetric and some were chevron shaped (with hinge collapse).
- Kink bands seem to be a weaker continuation of the asymmetrical folds.

Interpretation:
- The folding matches with N-S Alpine shortening, with main sense of movement towards the North.
- The folds seem to be a miniature version of the folds seen in stop 2.3.
- Hinge collapse in the chevron faults indicate severe folding.
- Chevron folding preferentially occurs when the bedding regularly alternates between contrasting competences.
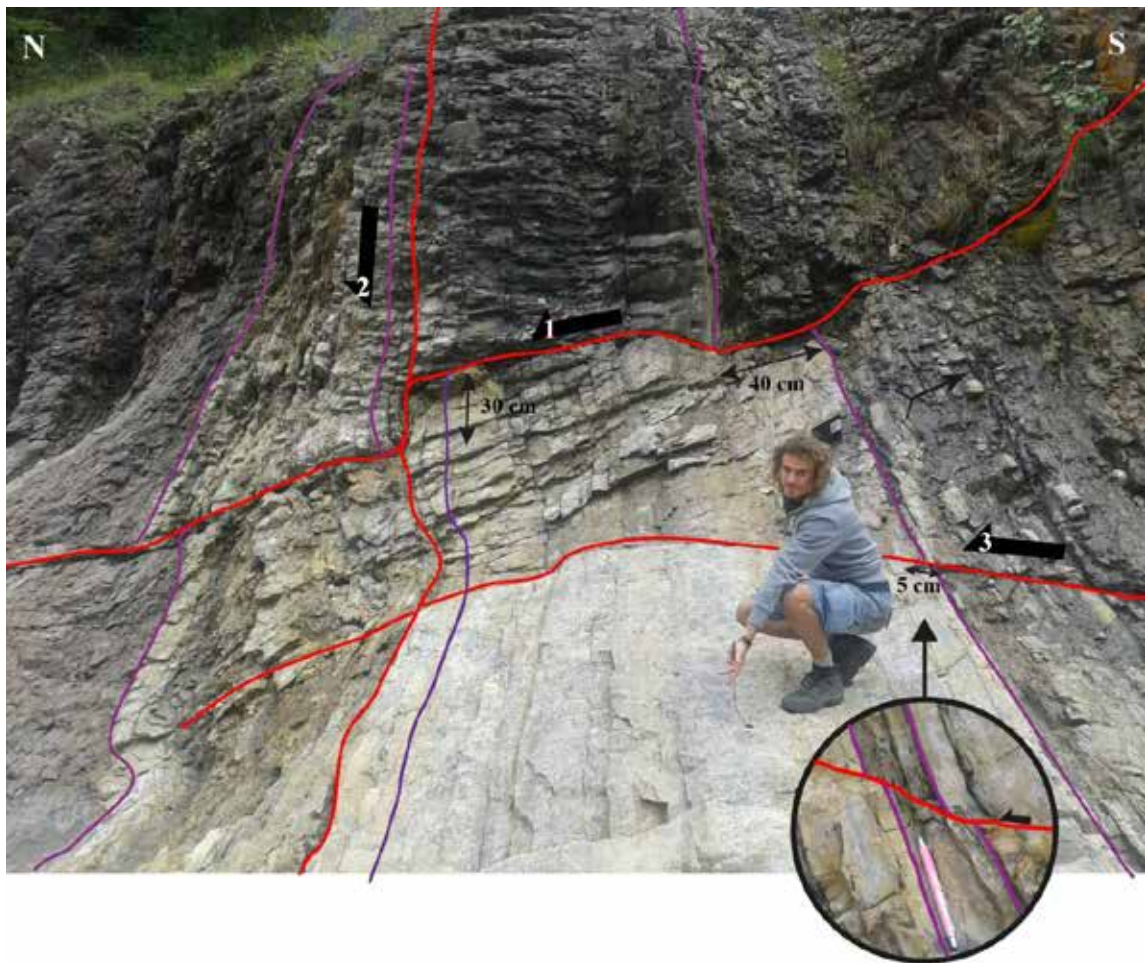

Figure 5.3a. Overview of the fault set

Figure 5.3b. Wave ripples at the bottom of the bed (N)

Figure 5.3c. Wave ripples at the top of the bed (S)

Figure 5.3d. Structures on the eastern bank of the river, seems to indicate S-vergence?

Figure 5.3e. Structures on the western bank of the river

Figure 5.3f to i (clockwise, starting with the upper left: asymmetrical folds; S limb is longest; vergence to the north. Some folds are almost chevron style folds.

5.4: South of Pontebba

Coordinates:	N: 46°44715
	E: 13°31706
Rock description:	Alteration of grey/brown dolo/limestone (5-30cm) and marls (0.5-5cm).
Depositional environment:	Carbonate ramp
Formation according to map:	Fm. di Rio del Lago (12c)

Measurements:
Planar structures: S0: 181/55
Faults: P: 089/82   with foldaxis of drag: 180/12   sinistral
P: 185/65   S: 172/75   R: 180/58   sinistral

Main sense of movement: Thrust towards the North plot
Also plot drag + faultplane → move point 90 deg along line

Structural observations:
     - Riedels are parallel to the bedding.

Interpretation:
     Fault with riedel fits within a N/S shortening (Alpine) event.
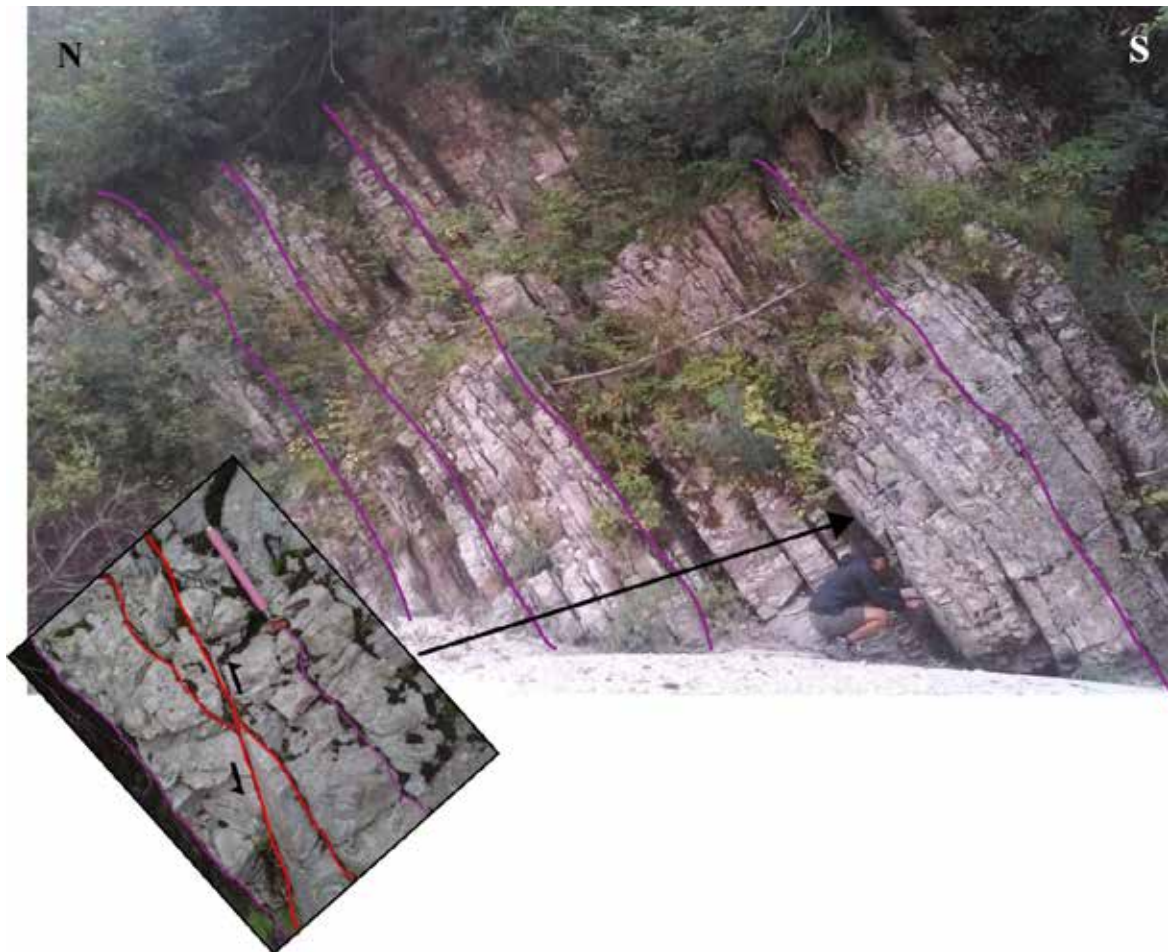

Figure 5.4. Formation 12c, detail of the sinistral fault with riedels parallel to the bedding

6.1: On the road from Resiutta to Pontebba

Coordinates: N: 46°39632
                                              E: 13°27062

Rock description: Brownish dolomite, not much weathering (0.1 – 1.5m beds) with dark grey
                                              organic rich layers and stromatolites.

Depositional environment: Carbonate platform

Formation according to map: Dolomia Principale (13c)

Measurements:
    Planar structures: S0: 116/12
    Faults: P: 238/70   (fold axis of drag: *294/12*)   sinistral
                                                        S:174/60   *down*   *And a possible riedel*
                                              P: 184/60   dextral
Main sense of movement: south

Structural observations:
- Big fault (10's of meters) has a very smooth surface, surrounded by a narrow band of breccia. Might have been an eroded mirror plane → normal fault.
- Other fault seems to be a continuation of the first fault, but has different angle (also a normal fault).
- Both have their hangingwall to the S(W)

Interpretation:
Faults are Alpine (N/S)

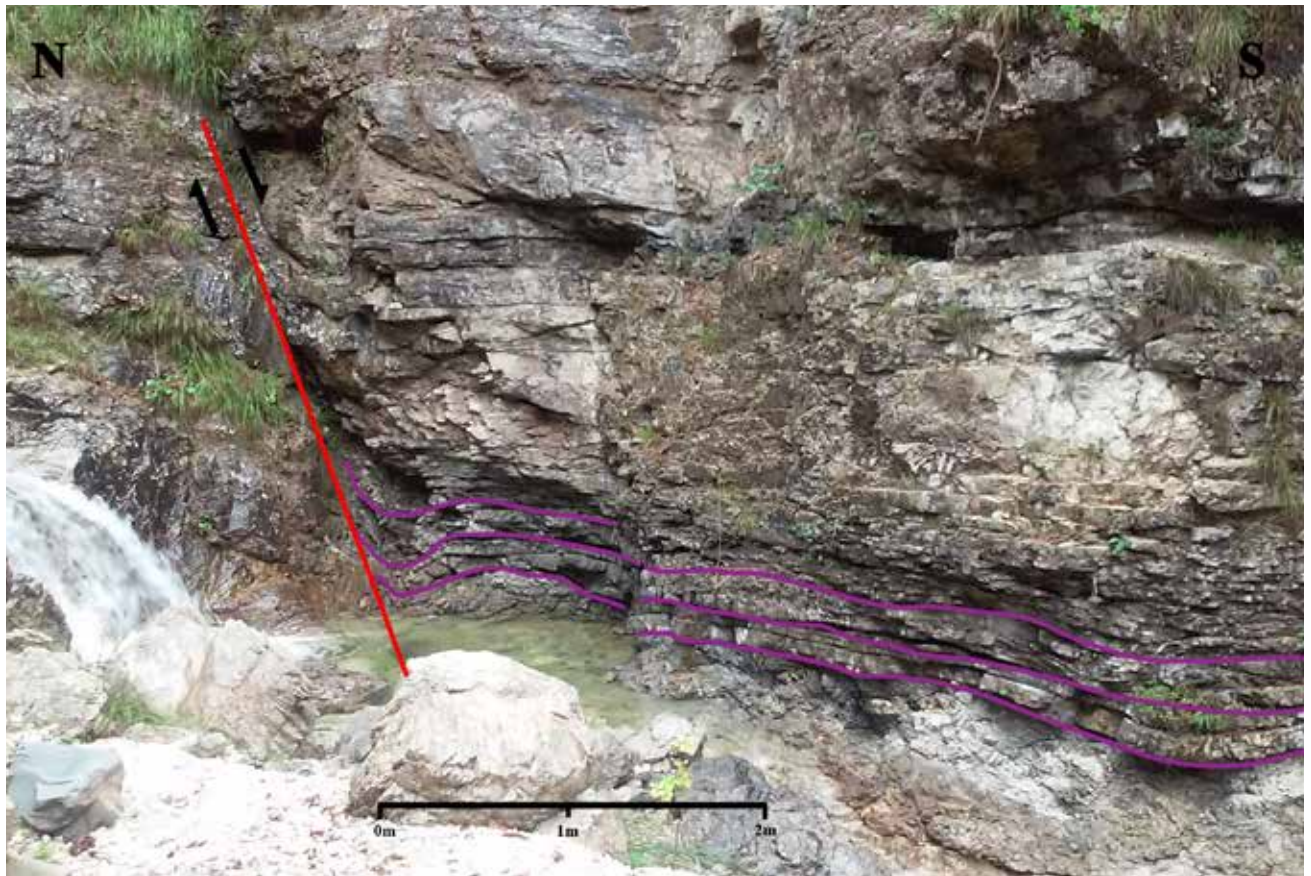Figure 6.1a. Normal fault with drag fold, plane 238-70, striae 174-60,

Figure 6.1b. Possible continuation of the fault in figure 6.1a, on the other side of the valley

6.2: In the strike-slip zone above Chiusaforte

Coordinates:	N: 46°42254
	E: 13°31701

Rock description: Dolomite , little to invisible bedding. Many smooth fault planes (also mirror planes). Bedding was estimated to be almost horizontal in the opposite side of the valley.

Depositional environment: Carbonate platform

Formation according to map: Dolomia Principale (13c)

Measurements:
   Planar structures: S0: 096/10 and 247/05
   Faults: P: 105/28
   P: 056/70   S: 135/20

Main sense of movement: plot

Structural observations:
   - So many faults that the entire area is more like one big mess.

Interpretation:
   Faults might fit in a big strike-slip zone, which this area is according to the map.
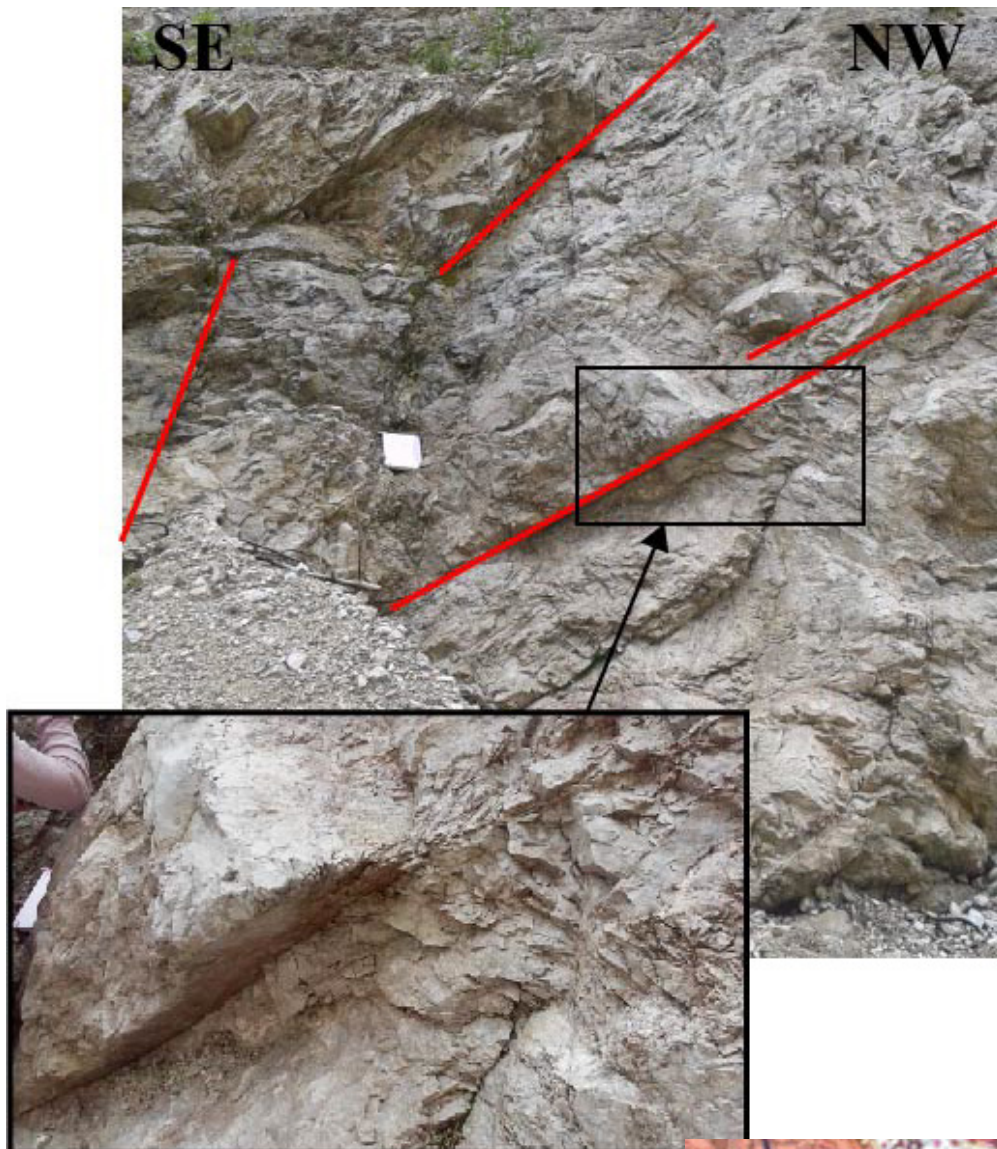
Figuur 26.2 grote breuk in dal=strike slip
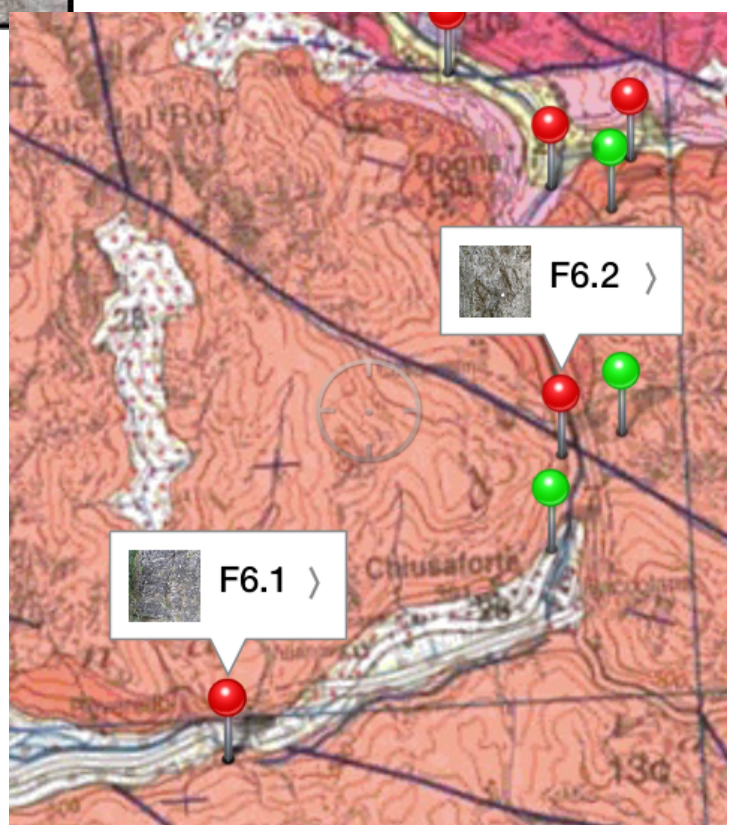
6.3: South of Pontebba

Coordinates: N: 46°43490
                                        E: 13°30885

Rock description: Dolomite (1-20cm beds) with marly layers.

Depositional environment: Carbonate platform

Formation according to map: Dolomia Principale (13c)

Measurements:
       Planar structures: Average S0: 169/16
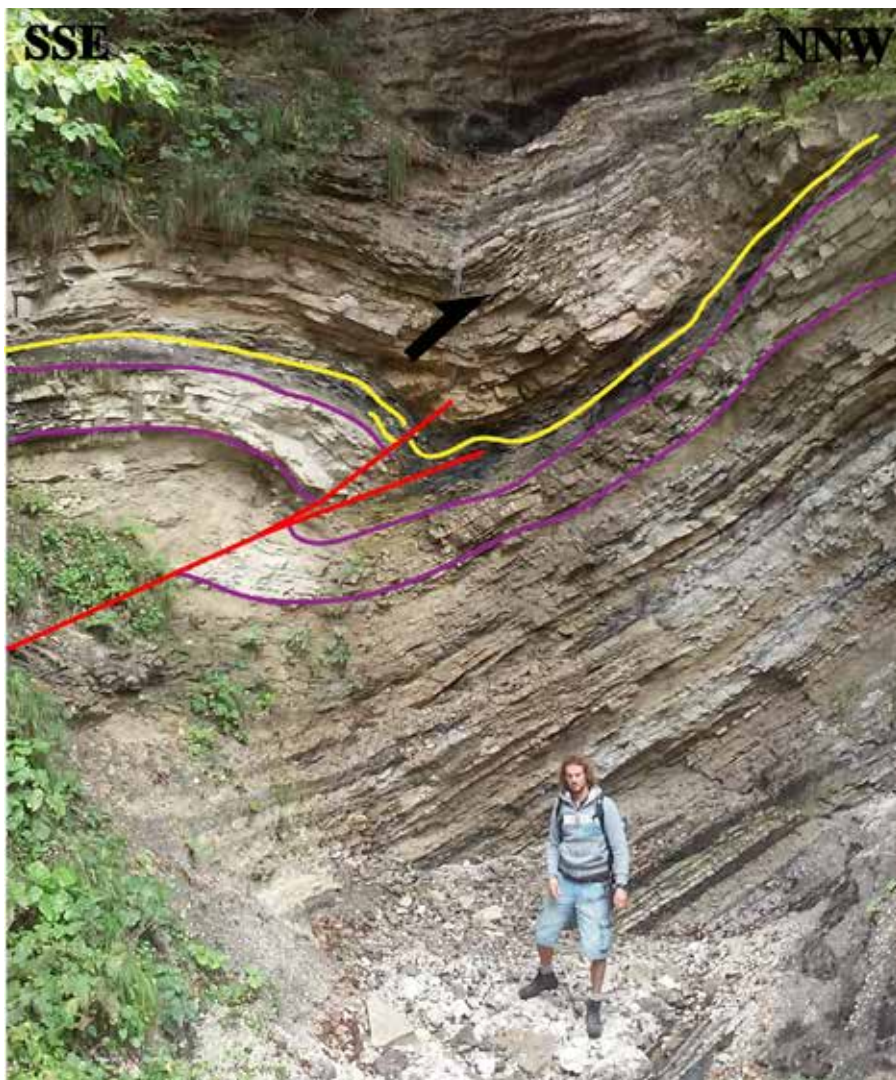   **Faults:**   P: 216/18   with foldaxis of drag: 094/10   dextral

Main sense of movement: plot

Structural observations:
      - Thrust
      - 50m towards the south is another, similar thrust.

Interpretation:
      Fold axis (and thrust motions) indicate Alpine movements.

6.4: East of Dogna

Coordinates: N: 46°44745
                            E: 13°35329

Rock description: Thick (1m) limestone beds.

Depositional environment: Carbonate platform

Formation according to map: Dolomia Principale (13c)

Measurements:
    Planar structures: Average S0: 180/33
                            S1: 178/48

Main sense of movement: Vergence to the North

Structural observations: -

Interpretation: -

6.5: East of Dogna (also 10.1)

Coordinates: N: 46°45019
                            E: 13°35722

Rock description: Very steep to almost vertical bedding. Mix of marly mudstone (5-30 cm thick) and lime/dolostone (5-50 cm). Limestones are fossiliferous and contain what appear to be burrows. Many small scale faults with steps, all indicating different senses of movement.

Depositional environment: Slope (with events)
                            However, not continuous: shedding, so near basinal environment.

Formation according to map: Fm. di Raibl (12c)

Measurements:
    Planar structures: S0 varies from 318/50 in the WSW, to 322/75 in the middle and 329/88 or 150/82 in the ENE

    Faults:

P	S		
P: 180/60	S: 150/48	top to NW	hanging wall up
P: 148/82	S: 101/85	top to WNW	hanging wall up
P: 354/70	S: 290/70	to NW	hanging wall down
P: 310/70	S: 310/70	to 310	hanging wall down
P: 315/78	S: 230/15	to 230	hanging wall down
P: 134/85	S: 125/80	to 305	hanging wall up dextral
P: 196/60	S: 145/50		
P: 170/80	S: 214/78	to 214	down
P: 166/78	S: 146/75		
P: 176/83	S: 192/80	to 192	down
P: 165/52	S: 148/49		
P: 230/50	S: 258/50		
P: 330/90	S: 270/65		
P: 328/85	S: 230/15	to 230	down
P: 254/68	S: 266/71		

Main sense of movement: Different senses of movement: plot
To the South?? (Things moved over the Raible to the S?) Looks more like its moving to the (W)NW (from the thrusts) At least Alpine compression.

Structural observations:

- The beds in the northern part of the outcrop have a much shallower inclination than in the southern part.
- Along the road, towards the south, the same beds have a different S0: 170/48
  → fold axis: 242/17 (NW/SE compression).
- In the picture: A: thinly bedded black/grey marls.
  B: Limestone with medium sized nodules, shell fragments: mass flow deposit. Lots of shearbeds and small faults with striations and steps.
  C: Nodular beds: might also be mass flows, and not burrows (nodules are too big: 10x10cm), also shell fragments, striated fault planes and very calcareous.
- Younging direction towards the SSE (fining upwards).

Interpretation:

In a bigger context: N: More massive limestone beds (Schlern: 9)
Gliding beds (Raibl: 12c) → steep
Less steep (Monticello: 13a)
(Dolomia Principale: 13c)
        S: (Dachstein 14)

So the big carbonate platforms are 'less deformed' than the Raibl, which might have acted as a gliding bed.

5b. Mass flow event, indicated by the yellowbrown load structure in the calc bed. Younging direction is to the (SSE). Since layers
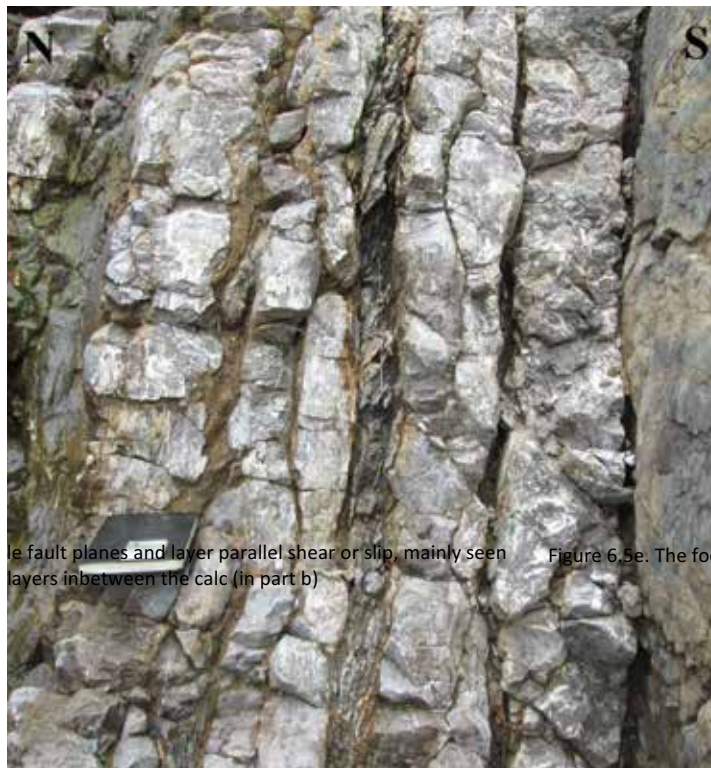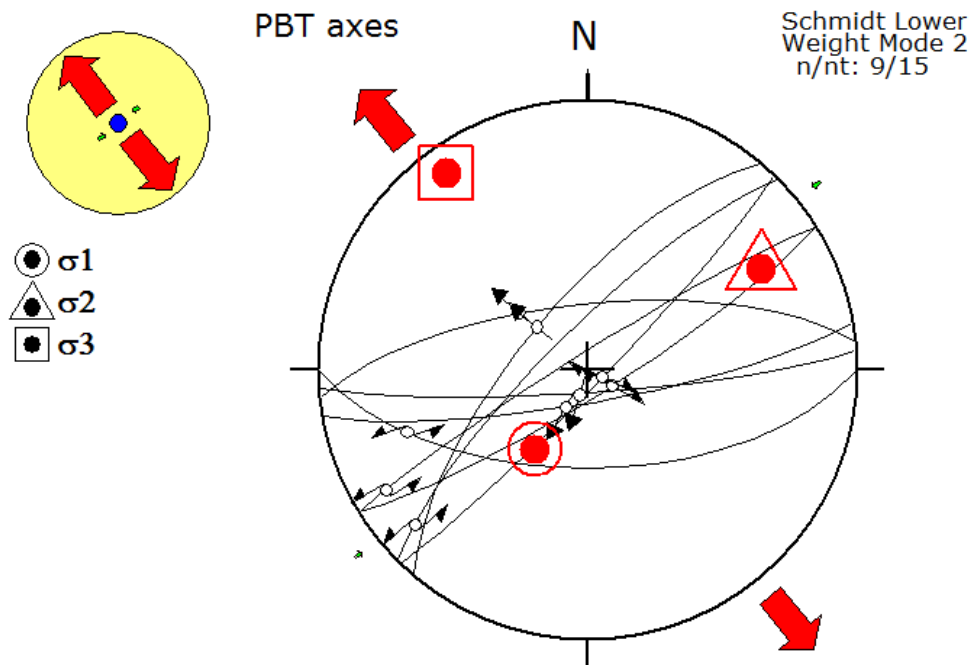ically vertical, sometimes they are overkipt, and sometimes not. (In part b)

le fault planes and layer parallel shear or slip, mainly seen
layers inbetween the calc (in part b)

Figure 6.5e. The footwall that goes down

PBT axes

Schmidt Lower
Weight Mode 2
n/nt: 9/15

σ1
σ2
σ3

6.6: East of Dogna

Coordinates:	N: 46°45905
	E: 13°37500

Rock description: Whitish to light grey limestone. Seems to be part of a large fault zone (10-20 m wide).

Depositional environment: Carbonate platform

Formation according to map: Schlern (9)

Measurements:

Planar structures: S0: 294/60, S0: 318/40, S0: 145/82, S0: 340/76, S0: 328/70??? S0: 170/52

Faults: P: 233/44 big fault   R: 163/45   normal fault, sinistral to SE
P: 175/28   R: indicates normal fault to the S?

Main sense of movement: S(E)

Structural observations:
Big fault, contains a lot of fault gouge.
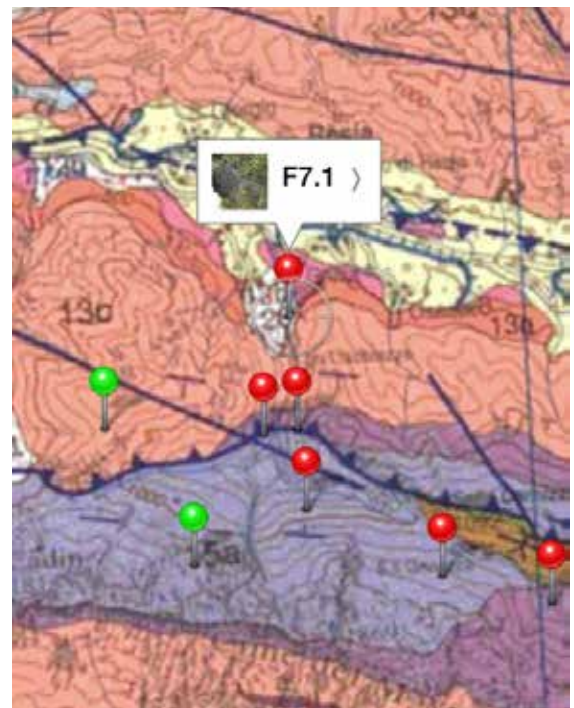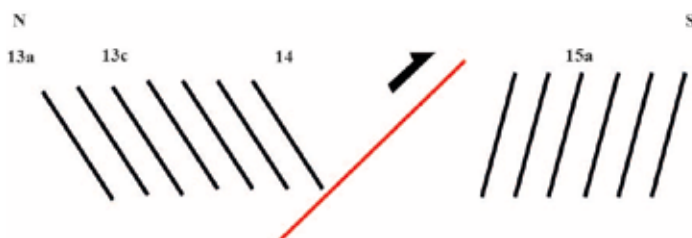
Interpretation: -

fault gouge

7.1: Along the road east from Resiutta

Coordinates: N: 46°36285
E: 13°29811

Rock description: Dolorite/limestone, 5-30cm thick beds.

Depositional environment: Carbonate platform

Formation according to map: Monticello (13a)

Measurements:
    Planar structures: Estimated S0: 198/48

Main sense of movement: -

Structural observations: -

Interpretation:
According to the map, this area is dominated by a big North
dipping thrust. On the Northern side of the thrust the beds are
dipping to the South and on the Southern side of the thrust the
beds are dipping to the North, with a much steeper angle (see
drawing).

7.2: Further along the road East from Resiutta

Coordinates: N: 46°35089
           E: 13°29316

Rock description: Dolorite/limestone

Depositional environment: Carbonate platform

Formation according to map: Dolomia Principale (13c)/ Dachstein (14)

Measurements:
  Planar structures: Estimated S0: 204/34

Main sense of movement: -

Structural observations: -

Interpretation: **-**

7.3: Further along the road East from Resiutta

Coordinates: N: 46°34703
           E: 13°29502

Rock description: Dolomite with some marls

Depositional environment: Carbonate platform

Formation according to map: 15a

Measurements:
  Planar structures: S0 on NW side: 234/50
          S0 on SE side: 358/90
          S0 more to the W (not in the picture): 186/42
  Faults   P: 136/82   S: 168/80
          P: 024/82   big plane (more than 20x20m) with some mirror patches,
          but heavily eroded
          P: 70/60   S: 336/30   *hanging wall down*
          P: 232/90   S: 305/25
          P: 050/65   S: 340/50   hanging wall down
Main sense of movement: -

Structural observations:
  - Two different sets of S0: separated by a fault/fold?
  - Vertical layers seem to have experienced a certain amount of drag
  - Rocks near 'fault' seem to be a little brecciated

Interpretation:

7.3b. Detail of the mirror patches on the big fault plane

7.4: Further along the road East from Resiutta

Coordinates: N: 46°33720
                                   E: 13°31731

Rock description: Whitish limestone, heavily eroded bedding

Depositional environment: Carbonate platform

Formation according to map: 15a

Measurements:
        Planar structures: S0: 025/60

Main sense of movement: -

Structural observations: -

Interpretation:

7.5: Further along the road East from Resiutta

Coordinates: N: 46°34190
                                   E: 13°29757

Rock description: Dark grey/brownish oolitic dolomite

Depositional environment: Carbonate platform

Formation according to map: 15a

Measurements:
        Planar structures: S0: 012/40
                                     S0 estimated 500m to SW: 000/44
                                     S0 estimated in the 'hanging wall'of the thrust (big distance): 222/24
                                     (The green pins in figure?)

Main sense of movement: -

Structural observations: -

Interpretation: The North dipping bedding of formation 15a extends over quite a big area.

E   W

North dipping strata

7.6: Further along the road East from Resiutta

Coordinates:	N: 46°33237
	E: 13°33824
Rock description:	Flysch
Depositional environment:	Flysch: basinal
Formation according to map:	19a

Measurements:

Planar structures:	S0: 026/58		
	S1: 020/77		
Fault:	P: 026/58 (bedding parallel)	S: 084/62	hanging wall down

Main sense of movement:	Vergence to 200
Structural observations:	-
Interpretation:	**-**

8.1: East of Tarcento

Coordinates:	N: 46°22366
	E: 13°29726
Rock description:	Flysch with thick limestone beds, also contains conglomerate layers.

Depositional environment:	Flysch: basinal

| **Formation according to map:** | Transition zone between Cretaceous limestones (17a) and flysch (19b) |

Measurements:

Planar structures:	S0: 165/59		
Fault:	P: 172/50	S: 070/80	hanging wall to W

Main sense of movement:	-

Structural observations:	-

Interpretation:

8.2: East of Tarcento

Coordinates:	N: 46°22480
	E: 13°29951

Rock description:	Flysch with distinct bedding: 1-50cm thick.

Depositional environment:	Flysch: basinal

Formation according to map:	Transition zone between Cretaceous limestones (17a) and flysch (19b)

Measurements:

Planar structures:	S0: 172/58
Main sense of movement:	-

Structural observations:	-

Interpretation:	**-**

8.3: East of Tarcento

Coordinates:	N: 46°22577
	E: 13°29945

Rock description: Flysch with burrows and layers of conglomerate.

Depositional environment: Flysch: basinal

Formation according to map: Transition zone between Cretaceous limestones (17a) and flysch (19b)

Measurements:
Planar structures: S0: 150/50
S1: 190/70

Main sense of movement: -

Structural observations:
Figure 8.3. Burrows - overkipt
- Burrows are found at the upper part of the bedding, so it must be overturned. Younging direction to
the NE.

Interpretation:
Based on the younging direction and vergence: the next antiform should be towards the NE.

8.4: NE of Tarcento

Coordinates:	N: 46°23227
	E: 13°28404

Rock description: Thickly bedded limestones (0.5-2m).

Depositional environment: Carbonate platform

Formation according to map: Calcare del Cellina (16c)

Measurements:
     Planar structures: S0: 174/45
     Faults: P: 170/80   S: 076/15

Main sense of movement: -

Structural observations:
     - Multiple faults like the one described above, all more or less parallel to the bedding

Interpretation: -

Figure **8.4. Fault, parallel to bedding, with striae**

8.5: NE of Tarcento

Coordinates: N: 46°24573
                              E: 13°30563

Rock description: Limestones with no distinct bedding

Depositional environment: Carbonate platform

Formation according to map: Calcare del Cellina (16c)

Measurements:
        Planar structures: S0: 154/48

Main sense of movement: -

Structural observations: -

Interpretation: -

8.6: NE of Tarcento

Coordinates: N: 46°24573
                E: 13°30563

Rock description: Flysch with limestone beds. Limestone beds can be as thick as 30m, or the
                flysch is very calcareous.

Depositional environment: Flysch: basinal

Formation according to map: Flysch (19b)

Measurements:
        Planar structures: S0: 082/23

Main sense of movement: -

Structural observations: -

Interpretation: -

8.7: NE of Tarcento

Coordinates: N: 46°24815
                E: 13°33096

Rock description: Flysch with on top of it a thick limestone bed (>10m).

Depositional environment: Flysch: basinal

Formation according to map: Flysch (19b)

Measurements:
        Planar structures: S0: 065/30

Main sense of movement: -

Structural observations:
        - Bioturbation on the bottom part of the flysch layers, so not overturned.

Interpretation:
        Younging direction to the ENE

thick limestone bed/ calcareous flysch

thinly bedded flysch
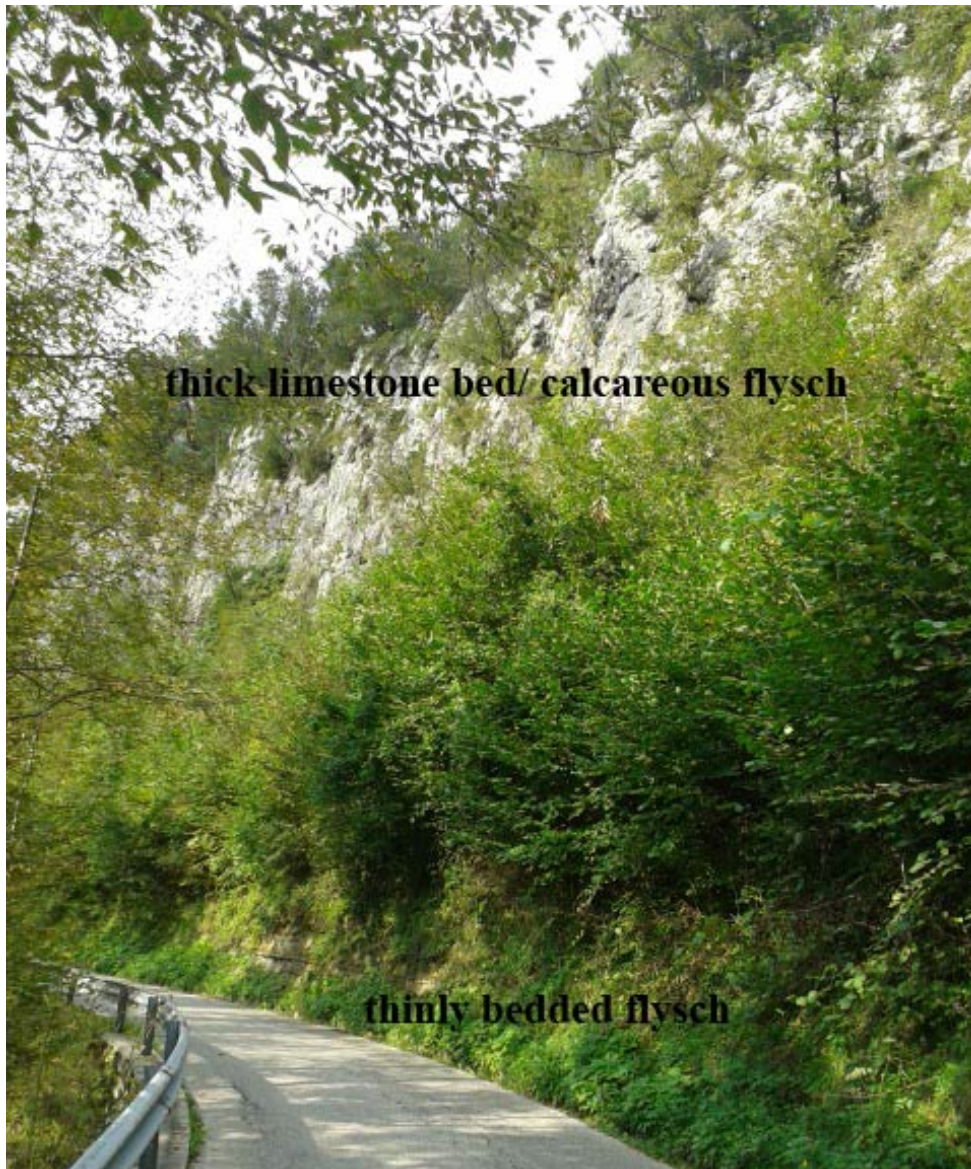
8.8: NE of Tarcento

Coordinates:	N: 46°27578
	E: 13°30179
Rock description:	Flysch with limestone beds (0.5-1m thick) and conglobeds (up to 0.5m thick). Clasts in the conlgo layer are up to 5x10cm big.
Depositional environment:	Flysch: basinal
Formation according to map:	Flysch (19b)
Measurements:	
Planar structures:	S0: 022/40
Main sense of movement:	-

Structural observations:
- Fining upwards, burrows and the bottom print of wave ripples indicate that the outcrop is not overturned.

Interpretation:
Younging to the NNE

8.9: NE of Tarcento

Coordinates:	N: 46°26738
	E: 13°26233
Rock description:	Flysch with burrows at the top.
Depositional environment:	Flysch: basinal
Formation according to map:	Flysch (19b)
Measurements:	
Planar structures:	S0: 312/26
Main sense of movement:	-
Structural observations:	Not overturned.

Interpretation: S0 compared to stop 8.1 (165/59) indicates an antiform with Alpine (late phase) strike. Or compared to stop 8.3 (150/50).

8.10: NE of Tarcento

Coordinates:	N: 46°26738
	E: 13°26233
Rock description:	Thick limestones
Depositional environment:	Carbonate platform
Formation according to map:	Dolomia Principale (13c)
Measurements:	

Planar structures: S0: 008/38

Main sense of movement: -

Structural observations:
- Valley where the S0 is very visible, no other clear structural observations, fault planes are absent, but the location of the river/valley is remarkable: it cuts through the S0.

Interpretation:
Valley could be a big fault (parallel to the thrust south of the location.) Or simply a weaker layer that eroded more easily.
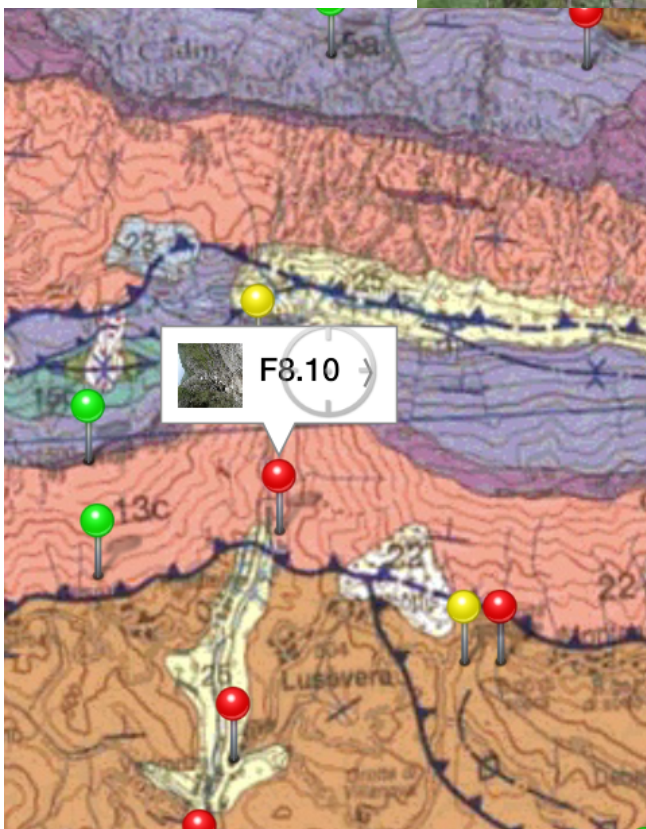
9.1: E of Venzone

Coordinates: N: 46°33566
E: 13°18156

Rock description: Thick limestones/dolomites, quite massive and no clear bedding. Mm-scale lamination visible.

Depositional environment: Carbonate platform

Formation according to map: Dolomia Principale (13c)

Measurements:
    Planar structures: S0: - (S0 is 'formed' by parallel cleavages which are 2m apart).
                       S1: 345/50
    Faults: Faults are mainly bedding (S1) parallel

P: 354/58	thrust	thrust: top to the S
P: 355/58	thrust	thrust: top to the S, mirror plane
R: 320/58		
P: 265/88	strike slip	S: 000/00
P: 296/72	strike slip	S: 025/10 to NE
P: 345/50		
P: 355/59		
P: 075/50	S: 068/52	

Main sense of movement: -

Structural observations:
    - Strike slip fault cuts the 'bedding parallel' faults, so is younger, also contains fault gouge.
    - Towards the SE, the outcrop becomes more brecciated/cataclastic.

Interpretation:
    The thrust match with Alpine ('layer parallel) shortening, apparently the strike slip also??
    (Related to Tarminto? strike slip zone).
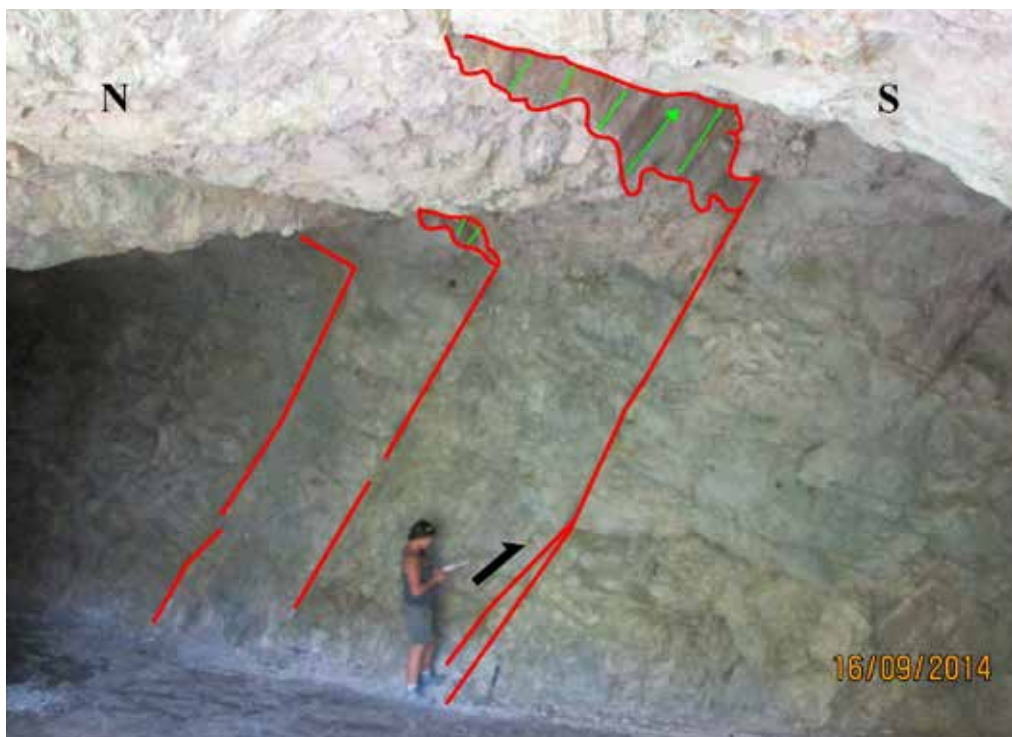
9.2: W of Resiutta

Coordinates:	N: 46°38217
	E: 13°16022

Rock description: Brecciated limestones/dolomite, with lamination. Heavily brecciated. with very well developed cleavage planes.

Depositional environment: Carbonate platform

Formation according to map: Monticello or Dolomia Principale (13a or c)

Measurements:

    Planar structures: S0: 175/52

                           S1: 250/66

    Faults: P: 232/86   S: 324/18   dextral to NW

                         P: 175/52

    Folds: Eastern limb: 123/49   Western limb: 200/50   Axis: 154/55

Main sense of movement: Vergence to the W

Structural observations:
- S0 indicated by occurrence of lamination.
- The m-scale 'S0 beds', are due to layer parallel shortening and not to sedimentation. (Alpine)
- Also fault gouge has been found along these planes.
- When bedding (158/50) and cleavage (252/40) relation is calculated (218/32), it does not really matches with the measured fold axis → but these axes vary, as they might have been affected by later deformation phases. (Other intersection (169/53) is more like it.).

Interpretation:
- Extended area of the large thrust fault south of Resiutta.
- Layer parallel shortening has taken place here.
- The S0 (layer parallel shortening) is most prominent, so it must be the youngest: Alpine
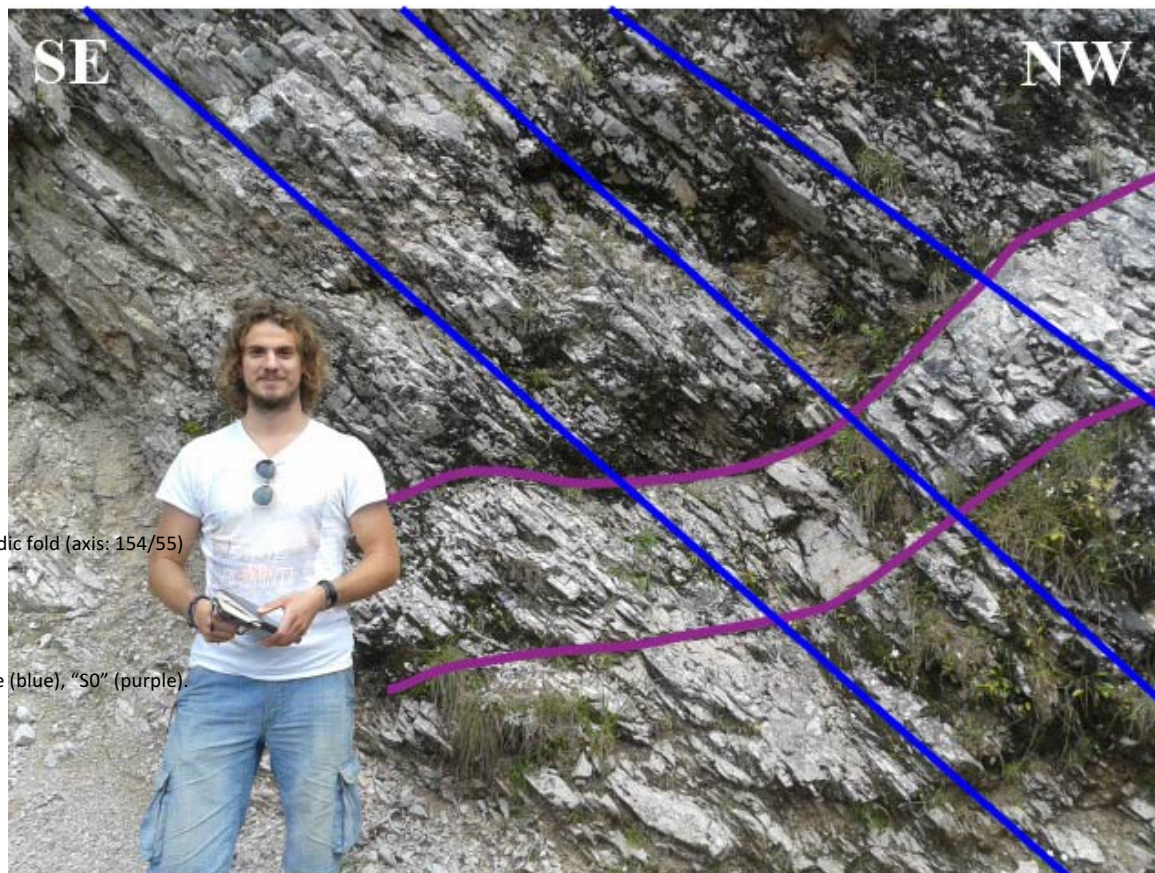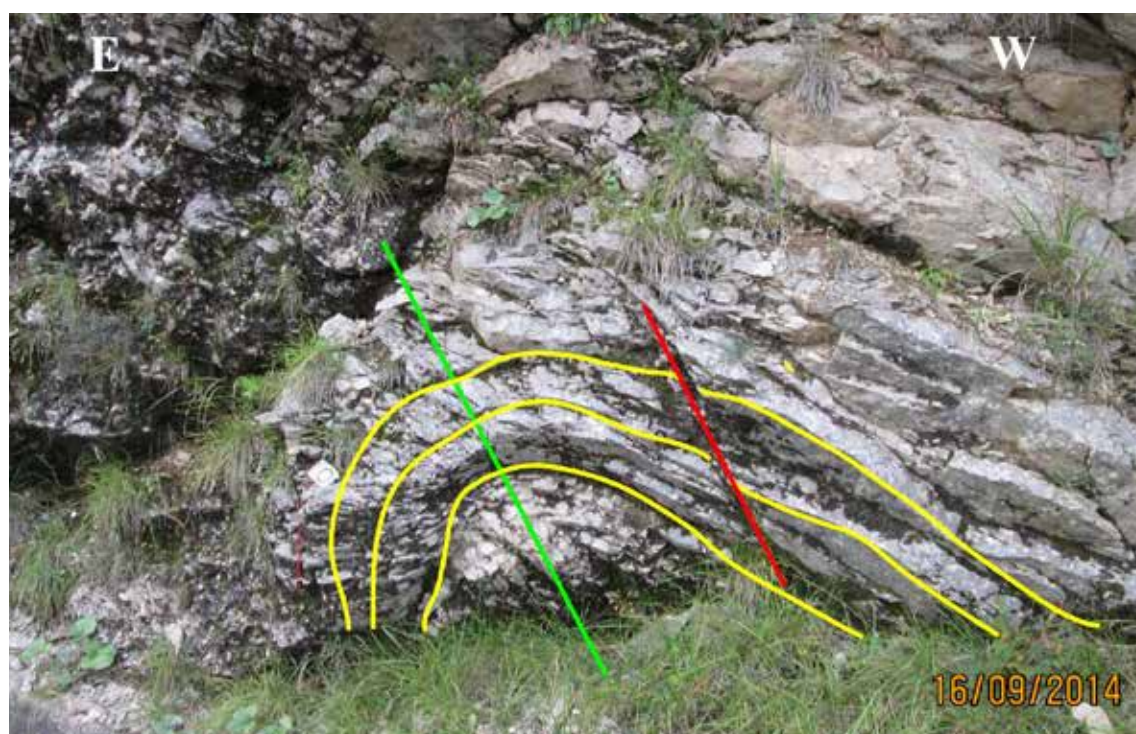- The cleavage and fold less prominent, so older: Dinaric

Figure 9.2c. Dinaridic fold (axis: 154/55)

Figure 9.2b. Cleavage (blue), "S0" (purple).

10.1: E of Dogna, see 6.5

10.2: E of Dogna

Coordinates: N: 46°44891
                             E: 13°35445

Rock description: Quite massive limestone, that becomes more massive towards the North, no
                             fossils. To the south: the Raibl formation (thinly bedded, alternating marls
                             and calcareous turbiditc events + fossils).

Depositional environment: Carbonate platform (perhaps border between slope and platform)

Formation according to map: Schlern (9) and Raibl (12c)
                             And Monticello (13a)

Measurements:
  Planar structures: S0: 148/60
  Folds: Limb1: 328/76   Limb 2: 148/60   Calculated axis: 075/10

igure 10.2a. Load casts and bioturbation, indicating youging direction to the left (S -SSW) So here, it's overkint
                             Axis of drag along thrust stack: 082/20 to N

Main sense of movement: From the Raibl: towards the south??
                             From the Schlern? (drag): towards the north.

Structural observations:
   - Loading structures indicate younging direction is still SSE.
   - The calculated fold axis in the Raibl corresponds to N/S (Alpine) compression.
   - Drag in the Schlern (might already be Monticello?) also fits N/S compression.

Interpretation:
   The Raibl inbetween the Schlern and the Monticello/Dolomia Principale is not only more sensitive to
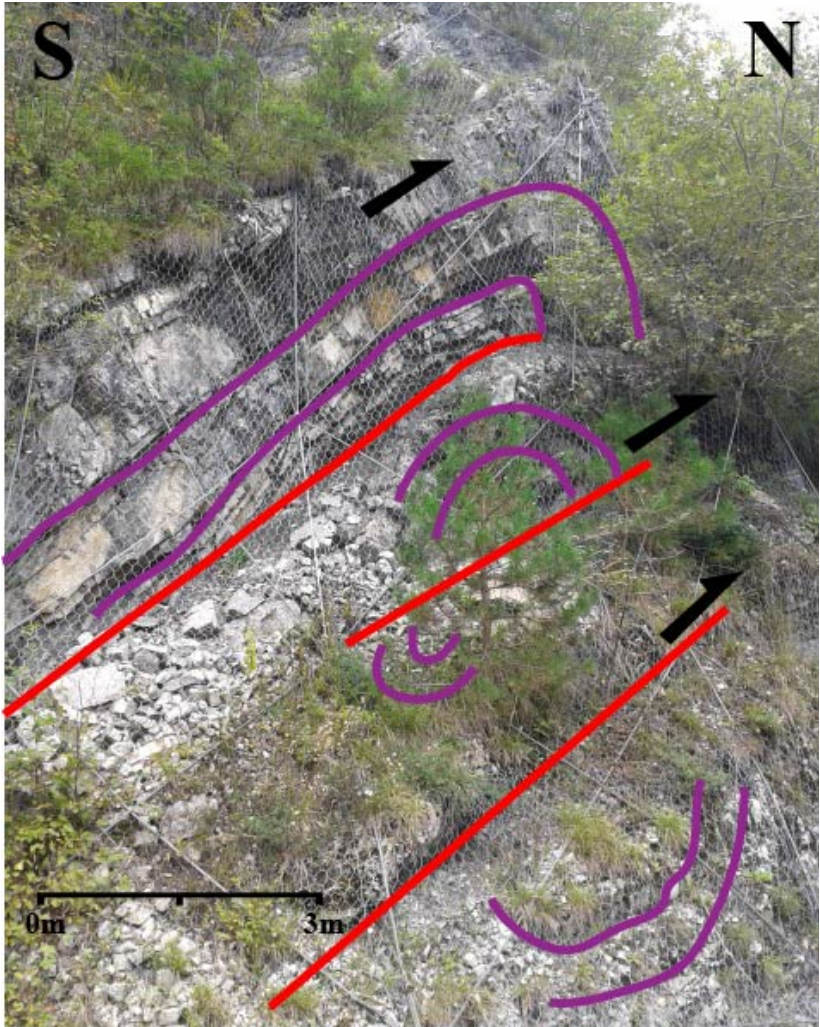   deformation but also to later collapse, caused by gravity.

10.2b. Overview of Raibl folds. Vergence to the south, but slope is also really unstable.

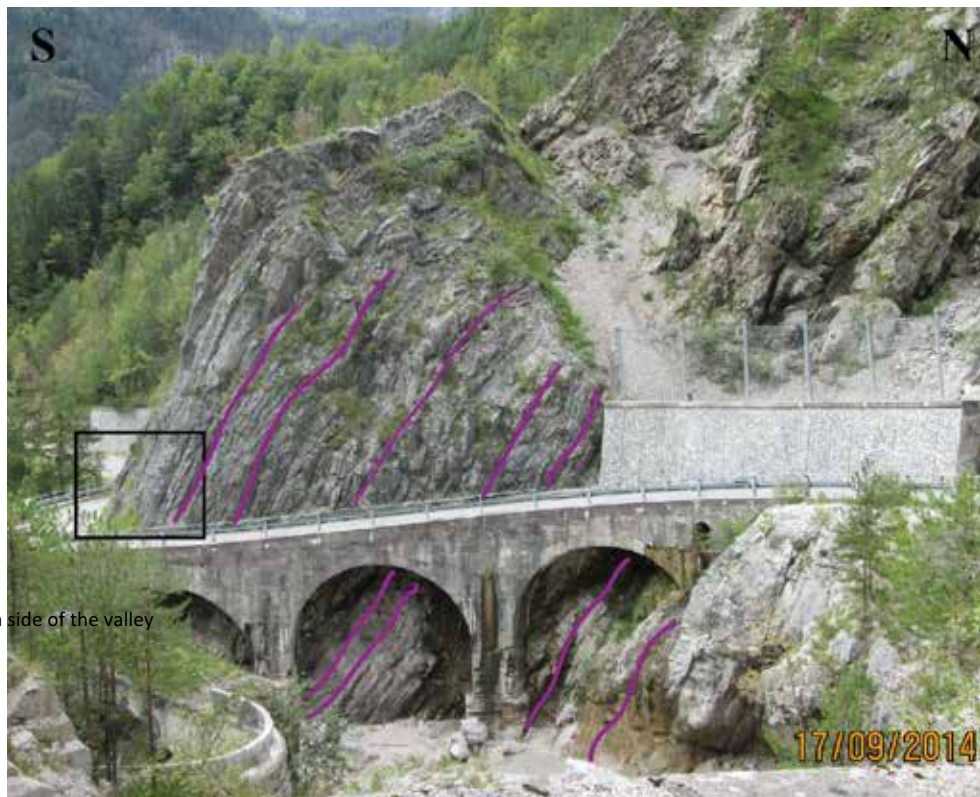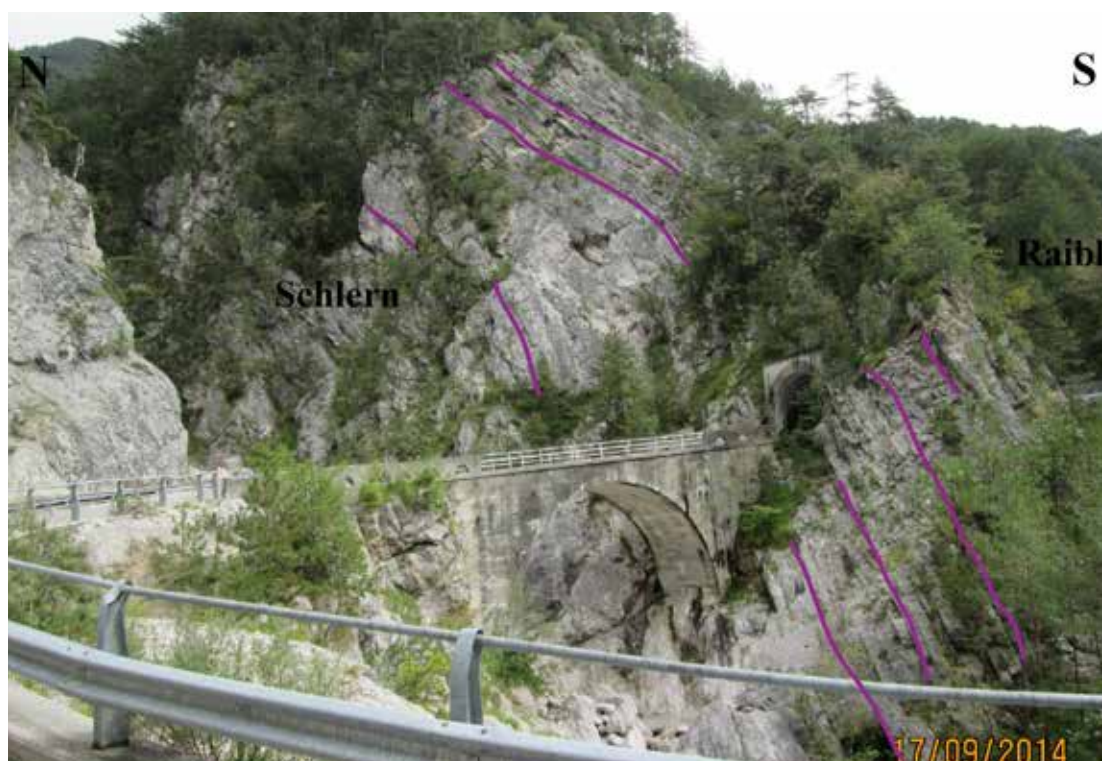Figure 10.2e. Eastern side of the valley

10.3: E of Dogna

Coordinates: N: 46°44835

                                        E: 13°34327

Rock description: Massive dolostone beds, with marly intercalations.

Depositional environment: Carbonate platform

Formation according to map: Monticello (13a)

Measurements:
        Planar structures: S0: 184/30

Main sense of movement: -

Structural observations: **-**

Interpretation: **-**

10.4: E of Dogna

Coordinates: N: 46°44937

                                        E: 13°32816

Rock description: Marls alternating with events (shell fragments).

Depositional environment: Slope

Formation according to map: Raibl (12c)

Measurements:

Planar structures:	S0 steep: 192/85		
	S0 shallow: 012/40		
Faults:	P:040/70	dextral shear plane photo	
	P: 044/25	S: 348/15	top to 168 (SSW) photo
Folds:	Axis: 118/15		
	Axis: 090/20		
	Axis: 122/20		
	Axis: 115/10		
	Axis: 086/15	photo	
	Limb 1: 062/45	Limb2: 358/39	(small:1m fold)

Main sense of movement: From the Raibl: towards the south.

Structural observations:
- A lot of layer parallel slip.
- A lot of folds, more or less the same orientation (to the S), some open, some even almost isoclinal: long limb to the N/short limb to the S.
- Towards the S, the deformation becomes more intense.
- Raibl is less nodular and marly than at 6.5/10.1: less events??
- Offset along the shear plane has been 10 cm, top to SE. Crosscuts all other folds, so must be a younger phase.
- Mircofolds (2-20 cm) in the softer marl beds.

- At least 2 folds seemed almost cut by a north dipping fault (see picture/drawing), or was it just an isoclinals fold? S0: 032/50 OR drag?

Interpretation:

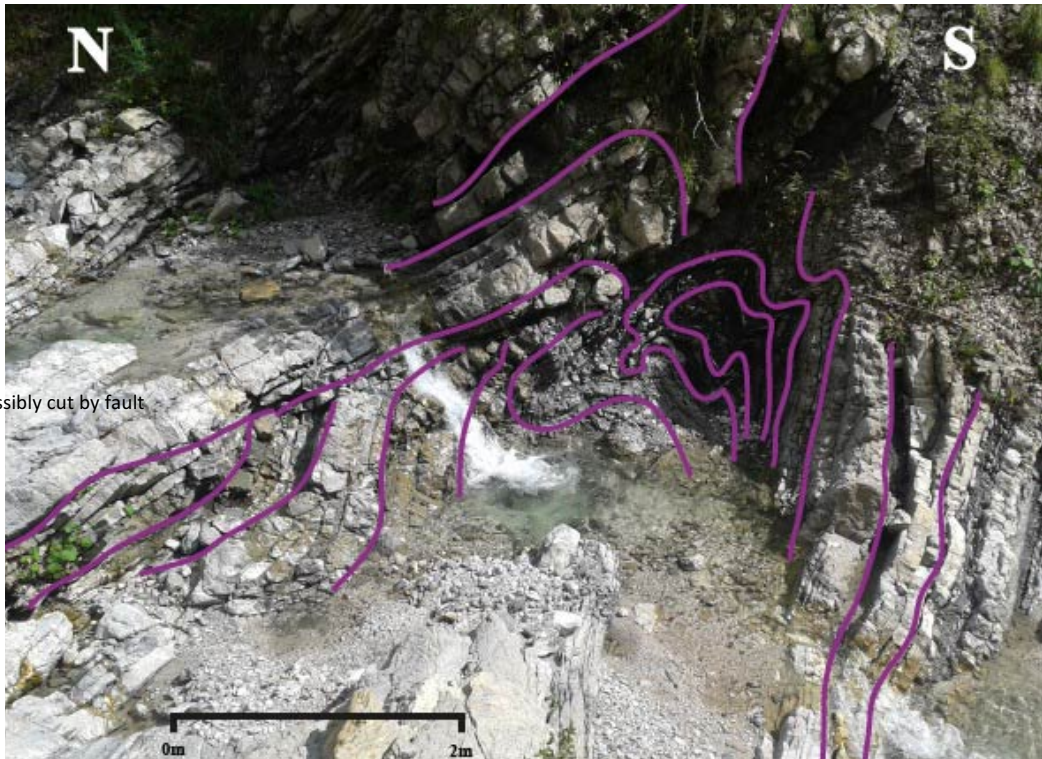Because of the intensification (of deformation and steepness) towards the South: platforms might have been surfing towards the South here?
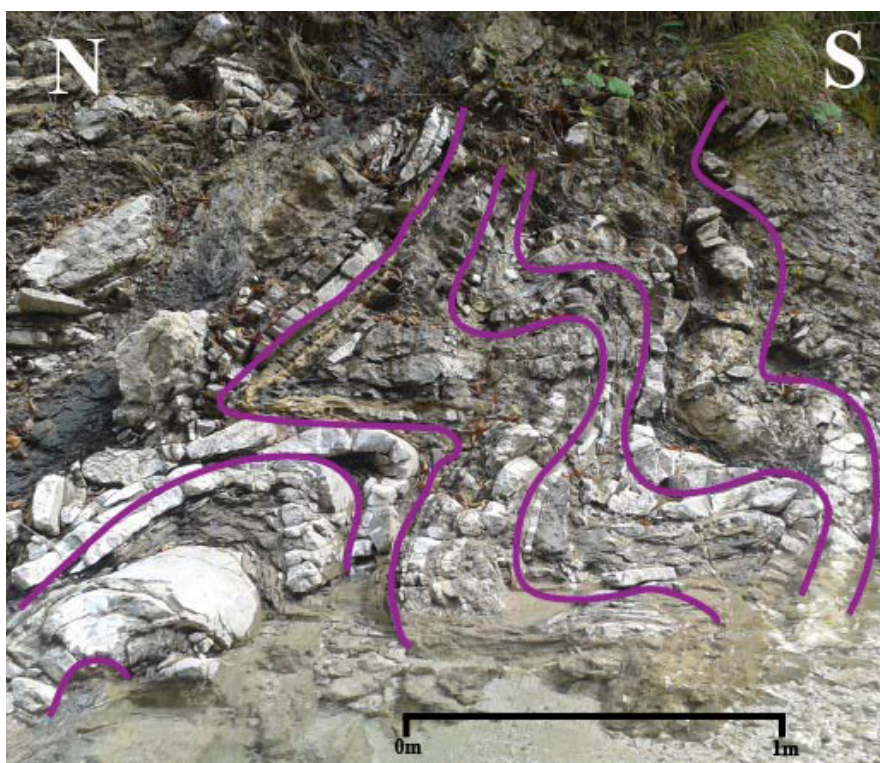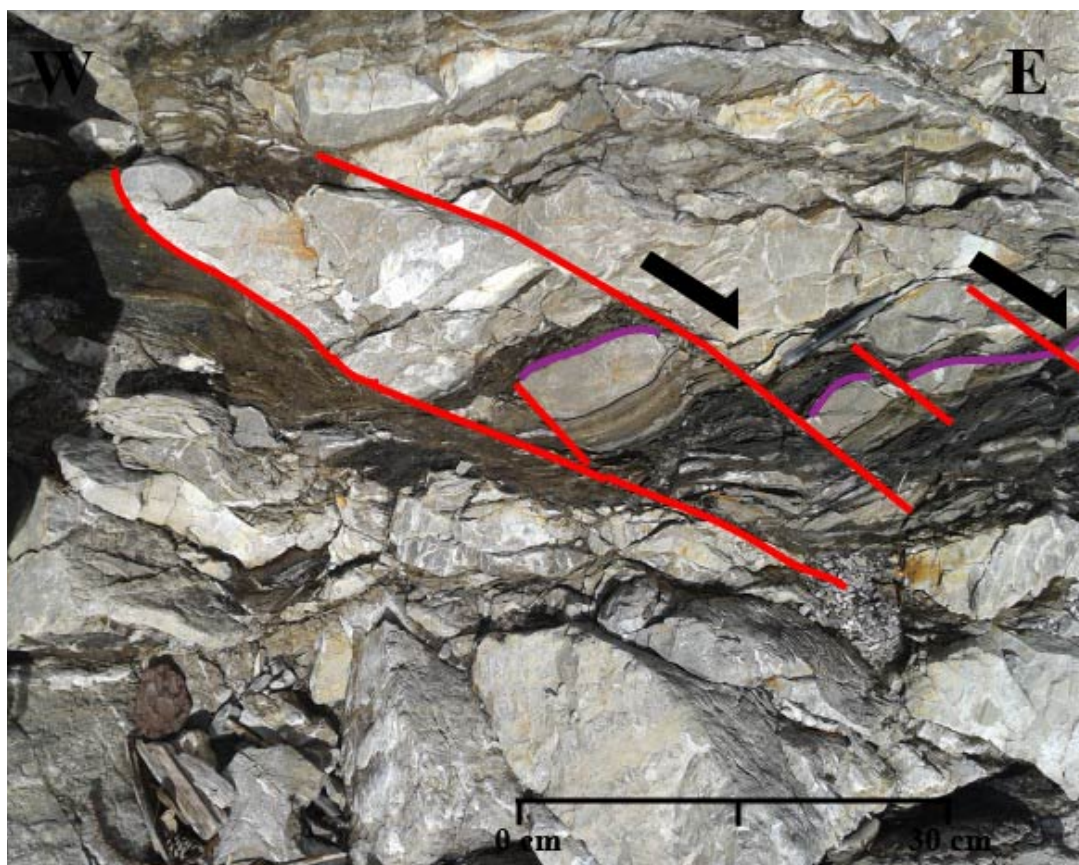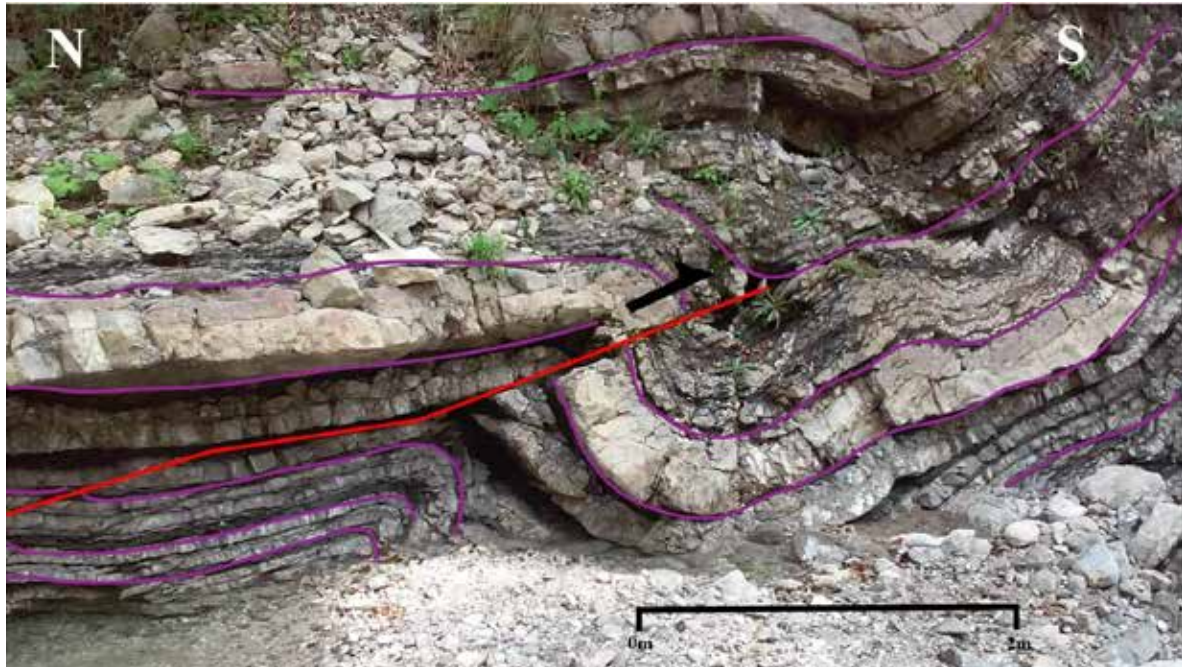

Figure 10.4a fold, possibly cut by fault
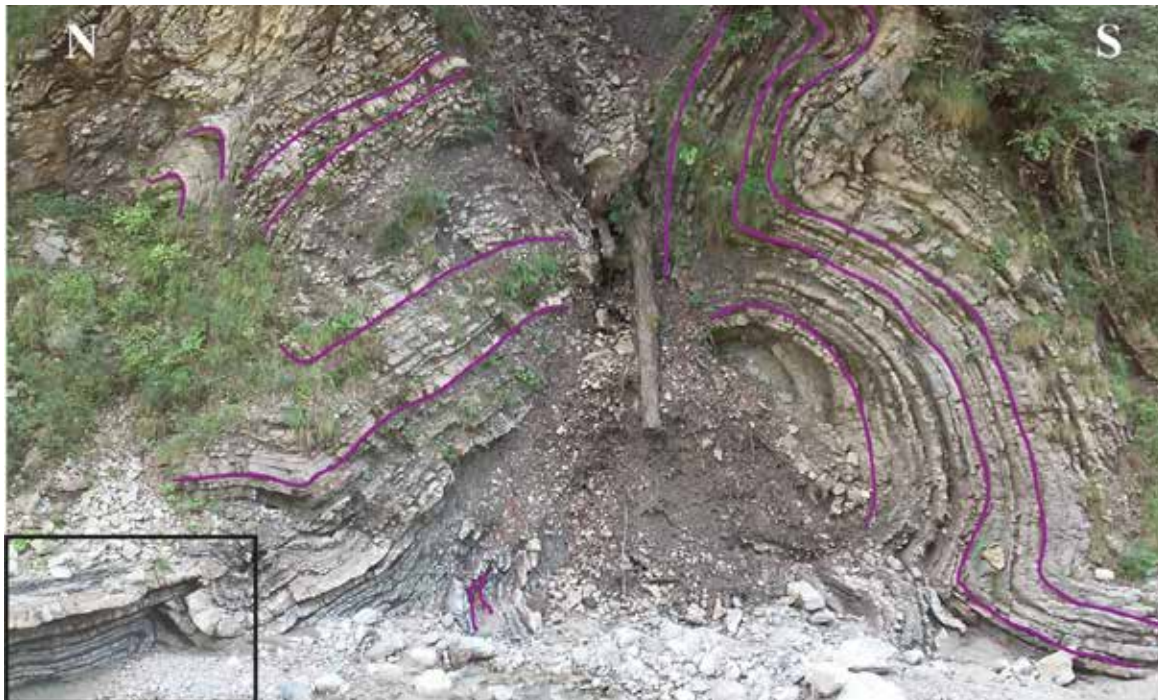
Figure 10.4e. Thrust fault with drag folds, plane 44-25, striae 348-15 top to 168 (SSE). Detail of figure 10.4f

10.5: N of Dogna

Coordinates:	N: 46°45827 E: 13°30459
Rock description:	Very nodular muddy limestone with shell fragments.
Depositional environment:	Carbonate platform
Formation according to map:	Schlern (9)?

Measurements:
      Planar structures: S0: 178/40

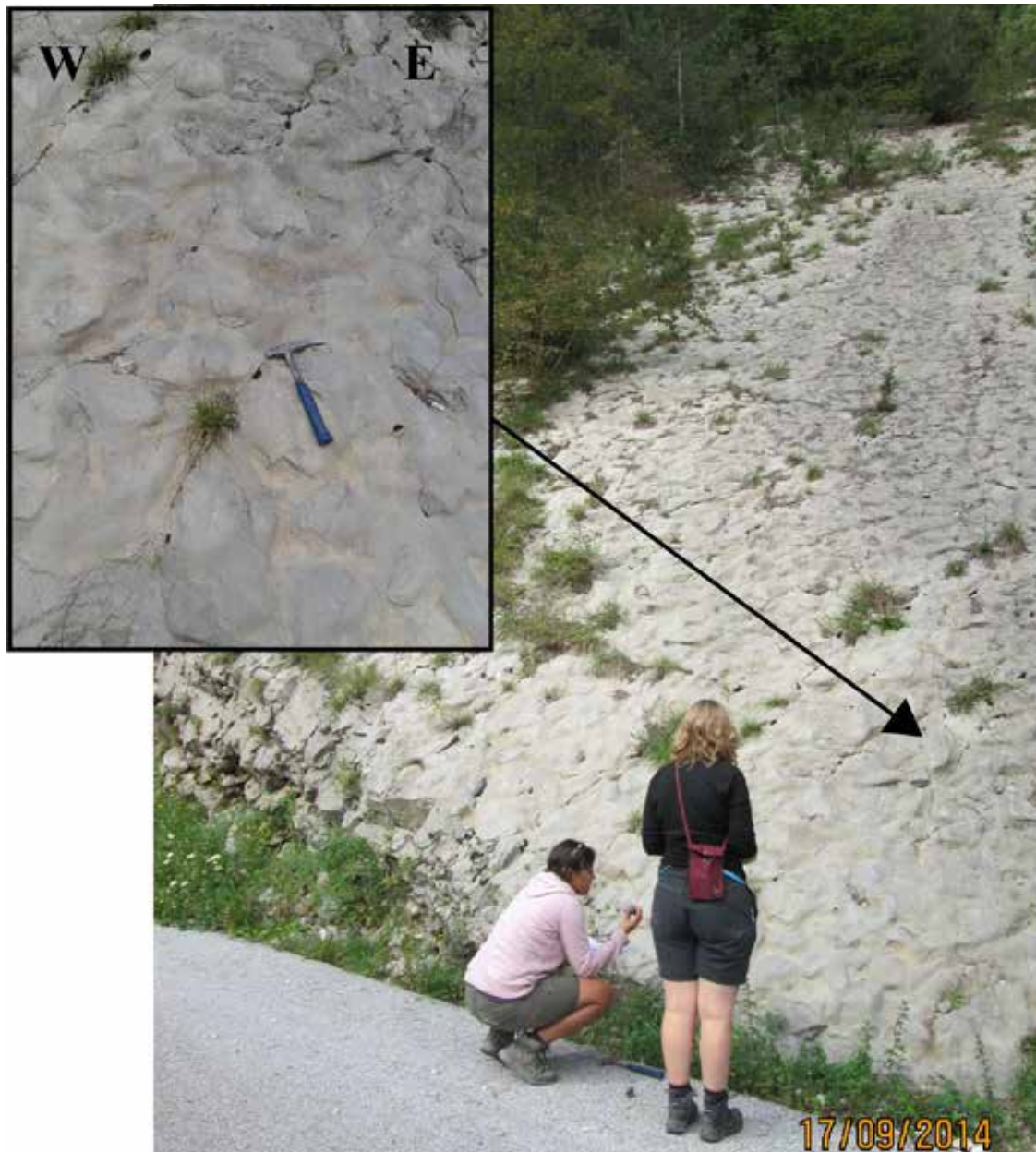**Main sense of movement:**   -

Structural observations:
      - Strange nodules, if they are load structures, than: top is up. Not overturned.

Interpretation: -

10.6: SW of Valbruna

Coordinates: N: 46°45855
      E: 13°46674

Rock description: Massive 1m thick dolomite beds → Monticello (13a)

Depositional environment: Carbonate platform

Formation according to map: Raibl (wrong)

Measurements:
    Planar structures: S0: 154/67
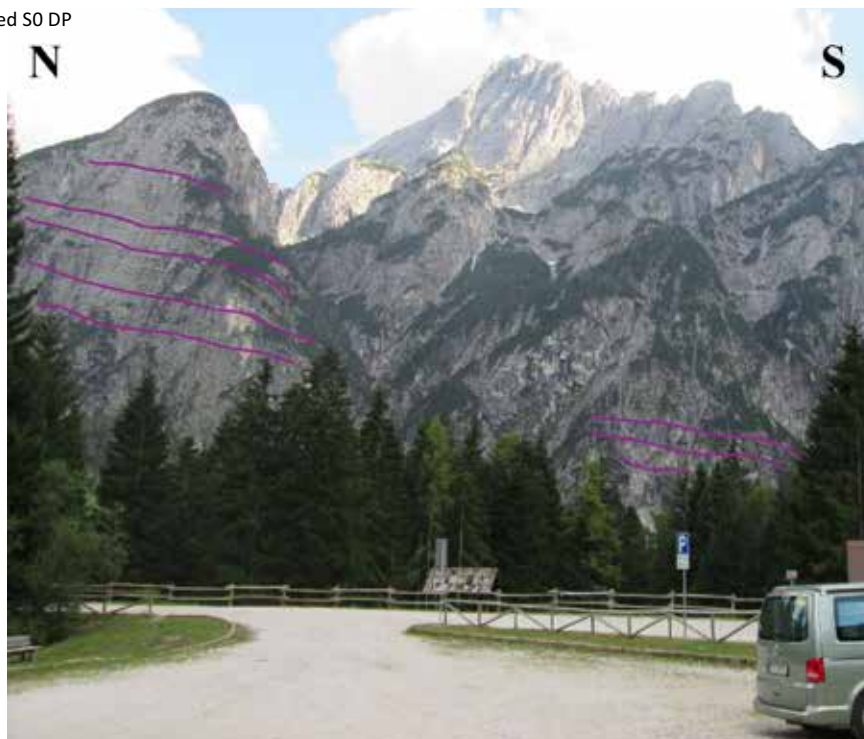   Estimated S0 other side of the valley (DP): 180/16

Main sense of movement: -

Structural observations:
    - Nodular on bottom side, not overturned. Younging to the S.

Interpretation:

iur 310.6 estimated S0 DP

10.7: 100m W of 10.6

Coordinates: N: 46°45855
                                  E: 13°46674

Rock description: Cataclastic limestone with lots or mirror plane faults → Still Monticello
                                  (13a). Also patches where there are lots of calcite veins with 'breccia clasts'
                                  (spider web structure).

Depositional environment: Carbonate platform

Formation according to map: Raibl (wrong)

Measurements:

| **Planar structures:**	Average S0: 174/55		
Faults:	P: 102/90	S: 190/15	
	P: 152/80	S: 140/85	sinistral
	P: 165/70	S: 251/40	dextral with fault gouge

Main sense of movement: -

Structural observations:
- The affected 'zone' with many faults: the fault zone: is about 20-30m high. The formation on top of that is more or less still intact.

Interpretation:
Just like the thrust fault seen in stop 3.1, near Resiutta, the faults are relatively shallow. Leaving the ` formations on top of them quite undisturbed.
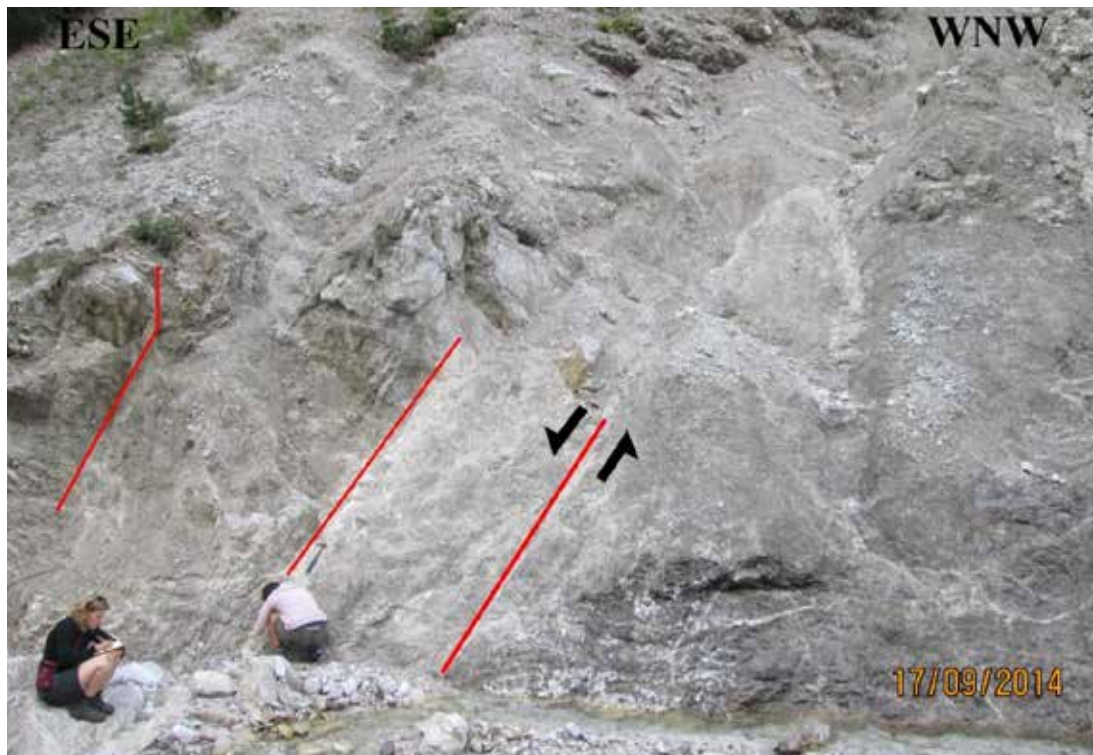
Abbreviations used:

S0= bedding plane
S1, 2, 3= cleavage sets
P= fault plane
P= mirror fault plane
S=slickenside or striae